

## BACHELOR THESIS

<b>Title of the project:</b>	<b>Date:</b> 26.05.2023
<b>Mooring design, dynamic analysis, and testing for an autonomous ocean sampling profiler.</b>	<b>Number of pages including attachments:</b> 118
<b>Students:</b> Louis Robert Crosbie, Emma Josefine Junge, Jill Nikki Jeciel Lirio and Jakop Haugan Holden	<b>Supervisors:</b> Rafael Borrajo-Pelaez, Alex Alcocer and Ivar Saksvik

**Project Partner:** OsloMet Oceanlab

### Summary:

This report concerns a mooring system for an ocean sampling profiler and includes a literature review of the fundamentals of mooring and its applications, a study of the design process along with dynamic simulations, a walkthrough of the software OrcaFlex, CFD analysis, model testing and recommendations for the final mooring system.

### Three keywords:

Mooring  
OrcaFlex  
Profiler

## Preface

This bachelor's thesis represents the results of our studies and reflects our hard work and dedication to our chosen field. The goal was to investigate and analyse mooring system design for an autonomous ocean sampling profiler and contribute to the existing knowledge in this area. This thesis summarises our results from our efforts and the knowledge we gained along the way.

We would like to take this opportunity to thank our thesis supervisors, Rafael Borrajo-Pelaez from OsloMet, Alex Alcocer, and Ivar Saksvik from OsloMet Oceanlab, for their guidance and support and valuable feedback which helped us shape our research and findings. We would also like to thank our families and friends for their support and encouragement throughout the duration of our studies.

We hope this thesis contributes to the existing knowledge and inspires more research in offshore system design. Our hope is to contribute to discussions and encourage future scholars to explore this exciting area of knowledge and research.

Louis Robert Crosbie, Emma Josefine Junge, Jill Nikki Jeciel Lirio and Jakop Haugan Holden

OsloMet – Oslo Metropolitan University

26.05.2023

## Table of contents

<b>Preface</b> .....	2
<b>Table of contents</b> .....	3
<b>Abstract</b> .....	6
<b>Symbol List</b> .....	7
<b>Terminology List</b> .....	10
<b>Table List</b> .....	11
<b>Figure List</b> .....	12
<b>Equation List</b> .....	13
<b>1. Introduction</b> .....	14
1.1 Background and issues .....	14
1.2 Project goals and limitations .....	16
1.3 Quality assurance .....	16
<b>2. Mooring system theory</b> .....	17
2.1 Mooring system.....	17
2.2 Mooring design considerations.....	18
2.3 Types of mooring system .....	18
2.3.1 Spread versus single-point mooring.....	19
2.4 Mooring system components (Components and component materials).....	21
2.4.1 Chain .....	21
2.4.2 Wire rope .....	21
2.4.3 Polyester rope.....	22
2.4.4 Other synthetic ropes .....	22
2.5 Buoys .....	23
2.6 Clump weight .....	24
2.7 Scope of a mooring system .....	24
2.8 Failure conditions .....	24
2.8.1 Cyclic loading .....	24

2.8.2 Chafe-zone .....	24
2.8.3 Human interference/fish-bite .....	25
2.9 Mathematical Theory .....	25
2.9.1 Line mechanics .....	25
2.9.2 Internal Forces .....	25
2.9.3 External Forces .....	26
2.9.4 Morison's equation.....	27
2.9.5 Buoyancy, Archimedes principle .....	28
2.9.6 Drag.....	28
2.9.7 Mass moment of inertia .....	29
2.9.8 Dry length .....	29
<b>3. Literature Review .....</b>	<b>30</b>
<b>4. Methodology .....</b>	<b>34</b>
4.1 Task requirements and assumptions .....	34
4.1.1 Task assumptions and parameters.....	35
4.2 Concept discussion .....	36
4.3 Forming and design .....	37
4.4 Choice of solution.....	42
4.5 OrcaFlex guide.....	43
4.5.1 The objects .....	43
4.5.2 6D buoys .....	43
4.5.3 Lines.....	46
4.5.4 Clumps .....	46
4.5.5 Object states and connections .....	46
4.5.6 Control bar.....	47
4.5.7 The help tab.....	51
4.5.8 Basic controls.....	52
4.5.9 Setting up a model.....	53
4.5.10 Running a simulation .....	63
4.5.11 Post simulation .....	65

4.6 Preliminary simulations.....	67
4.6.1 First iteration .....	70
4.6.2 Second iteration .....	75
4.6.3 Third iteration.....	85
<b>5. Results.....</b>	<b>90</b>
5.1 Final design.....	90
5.2 Scale model .....	101
<b>6. Discussion .....</b>	<b>108</b>
6.1 Consequences of line length .....	108
6.2 System mass .....	109
6.3 Effects of subsurface buoys.....	110
6.4 Line diameter .....	110
6.5 Line length vs SSB volume .....	111
6.6 Current resistance .....	111
6.7 Stability due to tension .....	112
6.8 Recommendations for future research.....	113
<b>7. Conclusion .....</b>	<b>114</b>
<b>8. Reference List .....</b>	<b>116</b>
<b>9. Appendix.....</b>	<b>118</b>

## Abstract

The mooring system is an essential component of floating systems to keep it on station consisting of a mooring line, anchor, and connectors. This paper provides a mooring design system for an autonomous profiler to keep it on station and to ensure it remains on the surface while considering varying waves, current, wind and water depth. In addition to these factors, the mooring system should not come into contact with the seabed to ensure negligible impact on the local marine ecosystem. The chosen mooring system for the project is a catenary single-point mooring system that consists of a profiler, mooring line, buoy, sub-surface buoy and anchor. The properties of the line and sub-surface buoy were determined after extensive research, a thorough design process and simulations carried out in Orcina's OrcaFlex software, which provided graphical dynamic simulations based on the chosen real-life parameters. The simulation results show how increasing subsurface buoy volume and the line length, increases the system's ability to withstand more aggressive metocean conditions, essential for use in real-life applications.

## Symbol List

$F$	Forces acting on the line
$l_s$	Segment length
$T_1$ and $T_2$	Tensions in the given directions
$T_t$	Total tension
$F_t$	Tension
$P_f$	Fluid pressure
$A_l$ and $A_f$	Cross-sectional area of the line
$F_1$	Force due to weight and buoyancy
$F_2$	Force due to added mass forces
$F_3$	Force due to fluid flow
$\rho_f$	Density of the fluid
$g$	Gravitational force
$w$	Submerged weight of the line per unit length
$b$	Buoyancy
$F_b$	Total buoyancy of the system
$f$	Fluid force per unit length on the body
$\Delta$	Mass of fluid displaced by the body
$a_f$	Fluid acceleration relative to earth
$C_a$	Added mass coefficient for the body
$\mathbf{a}_r$	Fluid acceleration relative to the body
$\rho$ and $\rho_w$	Water density
$C_d$	Drag coefficient for the body
$A$	Drag area
$v_r$	Fluid velocity relative to earth
$V$	Volume of the body submerged under the fluid

$F_d$	Drag force
$v$	Flow velocity relative to the body
$A$	Reference area
$m$	Mass
$r$	Radius
$h$	Height
$r_1$	Inner radius
$r_2$	Outer radius
$L_d$	Dry length
$L$	Length
$V_{above}$	Cylinder volume above the surface
$V_{under}$	Cylinder volume under the surface
$V_{tot}$	Total volume of the cylinder
$\lambda_d$	Wavelength
$T$	Wave period
$D_o$	Ocean depth
$\eta$	Kinematic viscosity
$t$	Ocean temperature
$v_c$	Ocean current (direction)
$v_w$	Wind speed (direction)
$T_{sim}$	Time period
$f_m$	Morison's force
$G$	Total force of gravity
$d$	Diameter
$I_{xy}$ and $I_z$	Mass moment of inertia
$L_t$	Total length of the line
$y$	Depth of the water column
$x$	Profiler's horizontal displacement from the origin



$F_u$	Drag force due to current
$\Delta F_t$	Change in tension
$\beta$	Angle

## Terminology List

ULS	Ultimate Limit State
ALS	Accidental Limit State
FLS	Fatigue Limit State
SPM	Single-point Mooring
CALM	Catenary Anchor Leg Mooring
PET	Polyethylene Terephthalate
HMPE	High Modulus Polyethylene
MODU	Mobile Offshore Drilling Unit
2D	Two-dimensional
3D	Three-dimensional
WEC	Wave Energy Converter
FWT	Floating Wind Turbine
6D	Six-dimensional
SSB	Subsurface Buoy
PLA	Polylactic Acid Filament

## Table List

Table 1: Standard environmental conditions .....	36
Table 2: An overview over degrees of freedom with description and position. ....	44
Table 3: Dimensions of the hollow cylinder .....	71
Table 4: Dimensions of the solid cylinder .....	71
Table 5: Default line dimensions .....	72
Table 6: Metocean conditios .....	76
Table 7: Nylon dimensions.....	76
Table 8: Buoyancy and weight values.....	78
Table 9: Tabulated maximum morisons force and tensile stress .....	84
Table 10: Metocean conditions for third iteration .....	87
Table 11: Buoyancy and weight .....	88
Table 12: Tabulated maximum Morison's force and tensile stress .....	89
Table 13: Constant parameters for the three sets of simulations .....	91
Table 14: Relevant parameters for figure 53 .....	92
Table 15: Relevant parameters for figure 54 .....	93
Table 16: Relevant parameters for figure 55 .....	94
Table 17: Wet weights and breaking forces .....	95
Table 18: Weight and buoyancy .....	98
Table 19: Morisons force and tensile stress .....	98
Table 20: Simulation and model volumes .....	101

## Figure List

Figure 1: Autonomous vertical profiler. Source: Adapted from [4] .....	15
Figure 2: Internal forces tension.....	26
Figure 3: Free body diagram of weight and buoyancy acting on each component.....	27
Figure 4: Solid cylinder mass moment of inertia .....	29
Figure 5: Hollow cylinder mass moment of inertia.....	29
Figure 6: Definition of dry length graphically .....	30
Figure 7: Dry length illustration .....	34
Figure 8: Cylinder declanation .....	35
Figure 9: Design 1 .....	38
Figure 10: Design 2 .....	39
Figure 11: Design 3 .....	40
Figure 12: Design 4 .....	41
Figure 13: A 6D spar buoy consisting of multiple cylinders with different diameters, along with local axis and six degrees of freedom. ....	44
Figure 14: from left to right, Lumped buoy, spar buoy and towed fish .....	45
Figure 15: OrcaFlex opening window with two-dimensional view.....	47
Figure 16: 3D view Ocean view in OrcaFlex.....	48
Figure 17: General tab with user-definable settings .....	49
Figure 18: Environment control window .....	50
Figure 19: Variable data control .....	51
Figure 20: OrcaFlex help window .....	52
Figure 21: Component tool bar location.....	53
Figure 22: First line position .....	54
Figure 23: Location of Line1.....	55
Figure 24: Line Editing .....	56
Figure 25: First Line anchored .....	57
Figure 26: Profiler properties .....	58
Figure 27: System with buoy .....	59
Figure 28: Buoy zoomed .....	60
Figure 29: Clump window .....	61
Figure 30: Attachment tab.....	62
Figure 31: Model with SSB added.....	63
Figure 32: Run simulation button .....	64
Figure 33: System after running simulation .....	65
Figure 34: Results window.....	66
Figure 35: Graph showing tension plotted against time .....	67
Figure 36: Point P on the cylinder.....	68
Figure 37: Process of running the simulations .....	69
Figure 38: illustration of the 6D spar buoy with a hollow section .....	71
Figure 39: Centre of gravity in the hollow and solid cylinder respectively.....	72
Figure 40: System setup for the first iteration .....	73
Figure 41: a comparison in the difference in dry length between a hollow and solid cylinder.....	74
Figure 42: Illustration of the difference in dry length. ....	75
Figure 43: System setup in 2D view, to the right is SSB 1 and to the left is SSB 2 .....	77

Figure 44: System setup in 3D view, to the right is SSB 1 and to the left is SSB 2 .....	77
Figure 45: Average dry length.....	78
Figure 46: Average declination .....	79
Figure 47: Motion pattern XZ-plane .....	79
Figure 48: Motion pattern XY – plane for test 1 .....	80
Figure 49: Motion pattern XY – plane for test 2 .....	81
Figure 50: Motion pattern XY – plane for test 3 .....	81
Figure 51: Test comparisons .....	83
Figure 52: Dimensions of the final profiler .....	87
Figure 53: Final design .....	90
Figure 54: Current resistance due to SSB volume .....	92
Figure 55: Current resistance due to slack .....	93
Figure 56: Current resistance due to line type .....	94
Figure 57: Average declination .....	96
Figure 58: Motion pattern XZ-plane .....	97
Figure 59: Motion pattern XY-plane .....	97
Figure 60: Combination of a larger volumed SSB and a longer line .....	100
Figure 61: Preview of the 3D cylinder.....	102
Figure 62: 3D printer cylinders with masses.....	102
Figure 63: Profiler floating in the same manner as in the simulations.....	103
Figure 64: Dry length of model profiler .....	104
Figure 65: Working model of a 30L system .....	105
Figure 66: Model of 15L system in tank.....	106
Figure 67: Failed 15L system model .....	107
Figure 68: SSB free body diagram.....	112

## Equation List

(Equation 1) .....	25
(Equation 2) .....	26
(Equation 3) .....	27
(Equation 4) .....	27
(Equation 5) .....	28
(Equation 6) .....	28
(Equation 7) .....	28
(Equation 8) .....	29
(Equation 9) .....	29
(Equation 10) .....	29
(Equation 11) .....	29
(Equation 12) .....	30
(Equation 13) .....	30
(Equation 14) .....	83
(Equation 15) .....	87
(Equation 16) .....	112
(Equation 17) .....	113

## 1. Introduction

OsloMet Oceanlab is a collaboration between the Department of Mechanical, Electronic, and Chemical Engineering (MEK) and Makerspace at the Faculty of Technology, Art, and Design (TKD) that coordinates research, innovation, and public outreach activities related to ocean technology and sustainability. The lab's main objective is to contribute to developing innovative technologies and projects that positively impact the ocean and contribute to the more sustainable development of ocean-related activities [1].

Collecting ocean data is essential for understanding the ocean, monitoring climate change, managing fisheries, assessing natural hazards, and supporting marine industries. Various methods and technologies are used to collect ocean data, ranging from ship-based measurements and autonomous underwater vehicles to buoys, floats, satellites, and citizen science [2]. The mooring design plays a crucial role in the ocean, enabling the safe and effective operation of various offshore structures and instruments.

The crucial requirement for a mooring system is its ability to keep a floating structure on the station under specific environmental conditions to allow various operations such as drilling, production, offloading, and wind power generation to be safely conducted. Mooring systems can be designed for multiple conditions, from a harsh environment like the North Sea to a calm atmosphere like the Gulf of Thailand or Offshore West Africa. In addition, they can also be designed for a wide range of water depths from a few meters to over 3000 m [3].

### 1.1 Background and issues

The oceans have been recognized as one of humanity's most critical natural resources and a vital component of Earth's ecosystem, providing numerous ecological, economic, and social benefits. However, human activities such as overfishing, pollution, and climate change have significantly affected the ocean's health and sustainability. For this reason, developing innovative technologies that promote sustainable activities has become increasingly essential [2].



FIGURE 1: AUTONOMOUS VERTICAL PROFILER. SOURCE: ADAPTED FROM [4]

OsloMet Oceanlab is working on commercialising a moored autonomous vertical profiler to collect ocean environmental data where a mooring has to be designed such that the profiler can consistently communicate via satellite in the presence of different parameters in a given location in open water [1]. The thesis will focus on designing a mooring system to keep the profiler in place and ensure consistent satellite communication. In addition to this, the solution will be designed such that one person can practically handle the design solution in the field.

The research conducted during the thesis will focus on various parameters and environments in order to attain an accurate and dynamic analysis overview on how various mooring designs behave in such conditions, before ultimately determining a final system. This research will be

aided by OrcaFlex, a software that provides professional dynamic analysis of offshore marine systems, particularly useful for research within engineering applications [5].

The thesis's outcome will contribute to developing sustainable ocean technologies. The mooring system's design solution will enable the consistent collection of precise ocean environmental data, promoting sustainable ocean-related activities.

## 1.2 Project goals and limitations

The project goal is to design a mooring system that will allow the autonomous vertical profiler to be in place and ensure consistent satellite communication. The research will analyse various parameters and environments to gain an accurate and dynamic overview of how different mooring designs behave under those conditions. Orcaflex, a software developed and commissioned by Orcina LTD, will aid this research by providing professional dynamic analysis of the systems.

The limitations of this project include the need to balance the length of the mooring line, as a too-short line may prevent the profiler from reaching the surface, while a too-long line may increase the risk of entanglement. Different oceanic regions may also have specific weather patterns and environmental conditions that can affect the profiler's performance and should be considered during the design stage. Another area for improvement is understanding the effect of different parameters on the mooring, which may require preliminary simulations or model-scale experiments. Additionally, the simulations or experiments may need to be repeated or refined as new information is gathered or design changes are made.

## 1.3 Quality assurance

Quality assurance focuses on providing confidence that quality requirements are fulfilled. It includes all the planned and systematic actions established to ensure that the trial is performed and the data are generated, documented, and reported are in compliance with the requirements [6].



The quality assurance aspect of this project would involve ensuring that the final product meets the required standards for functionality, reliability, safety, and performance. To achieve this, quality assurance measures would need to be implemented throughout the project's lifecycle, including [6]:

1. Defining and documenting the goals, requirements, and objectives for the mooring system and ensuring they are documented and understood by the project team at all levels.
2. Ensuring that appropriate processes are implemented to fully satisfy the needs, expectations, and objectives of the OsloMet Oceanlab.
3. Conducting thorough testing and validation where it should undergo extensive testing to verify that it performs as intended under a range of operating conditions.
4. Documenting all activities related to the project including design, testing and validation to ensure traceability and accountability.
5. Implementing a quality management system ensures that quality assurance processes are consistently applied throughout the project's lifecycle.
6. Deciding on actions for continual quality improvement of the project.

## 2. Mooring system theory

### 2.1 Mooring system

A mooring system is a collection of components and equipment that are used to secure a vessel, such as a ship or an offshore platform, to a fixed point in the water. The system typically includes one or more anchor points and is conventionally connected to a vessel or object via chains, cables or ropes. The system is then secured using an anchor in one or more locations [3]. Mooring systems are designed to withstand the forces of waves, wind, and currents, and to keep the vessel or object in a fixed position relative to the anchor point. Mooring systems are commonly used in offshore oil and gas exploration, marine transportation, and in the construction and maintenance of marine structures [3].

## 2.2 Mooring design considerations

The design for mooring structures must consider design loads, design criteria, design life, maintenance, and operation. The requirements of the design are identified concerning limit states by Offshore design standards, which are the ultimate limit state (ULS), accidental limit state (ALS), and fatigue limit state (FLS). The ULS must ensure that mooring cables have sufficient strength to survive the load impacts caused by environmental behaviour. The ALS assures that a mooring mechanism can tolerate the collapse of one mooring cable. The FLS ensures that the mooring cables can survive cyclic loading [7]. The evaluation used for the mooring structure was carried out by the three types of limit states and consisted of two categorisations of the environmental conditions: the maximum operational and maximum design conditions.

The maximum design condition is determined by the relation of wind, current, and waves for the design of mooring structures. This condition is described as an intense conjunction of the waves, wind, and currents that cause extreme loads within the design environment. The environmental loads include wave height, wave period, wave spectrum, wind direction, wind speed, the function of wind spectrum, current direction, the current direction, the current speed of the surface, and current profile over the depth. While the maximum operational condition is defined as a relation of wind, currents, and waves under which the device is capable of continuous operation, for example, drilling, offloading, or sustaining a gangway connection, this condition does not surpass the overall specification limit [7].

## 2.3 Types of mooring system

Offshore moorings are essential to the station-keeping systems developed for exploring and producing offshore oil and gas resources. Depending on the profiles and configurations, mooring systems can be classified into catenary and taut leg mooring systems [3].

The catenary mooring system has a line profile with a segment of the mooring line resting on the seabed in a static equilibrium position. Due to the mass of the mooring line, the mooring leg forms a catenary shape, generating the necessary compliance to cope with the floater's static offset and dynamic motion. The catenary mooring system is widely used in shallow to medium-depth waters [3].

The taut leg mooring system has no excess line lying on the seabed. Instead, the mooring lines are taut from the anchor at the seabed to the fairlead (a device used to guide a cable, rope, or chain and prevent catching or fraying) on the floater. Thus, the anchor footprint is much smaller, and the system uses less physical material than a catenary mooring system. Although the lines are taut, the compliance to floater offset and dynamic response is mainly from the line tensile stretch. Therefore, a taut leg system in shallow waters is typically too stiff and can raise the line tension excessively, hence why it is more suitable for deep or ultradeep water applications [3].

### 2.3.1 Spread versus single-point mooring

According to the mooring system's requirement to restrict the floater's heading, mooring systems can be divided into spread and single-point mooring (SPM) systems.

A spread mooring system has multiple mooring lines distributed around the floating structure, restricting the floater's offset, and heading to ensure operation in the designated location. In designing the layout of a spread mooring system, the preferred heading is decided by the local environmental conditions. A spread mooring system is a simple and economical system that does not require the use of complicated rotational mechanical systems. Once the anchors are deployed, the position and direction of the floating vessel are efficiently restricted, and risers and umbilical systems can be installed and operated as required [3]. Most mobile offshore drilling units (MODU) and a handful of floating production systems utilise the spread mooring system for station-keeping purposes.

A SPM system has one or multiple mooring lines connecting the floater's centre of rotation to the seabed. It thus allows the floater to weathervane about this centre of rotation to head into the prevailing environment to minimize environmental loading. SPM systems are adaptable to work in different environmental conditions, although they are technically challenging and expensive to build. Companies with state-of-the-art SPM system technology include SBM Offshore, SOFEC, Bluewater, and NOV APL [3]. Typically, the SPM system has two functions, the first for station-keeping and the other for transferring liquid and power.

The most common types of mooring profiles used for production systems are [3]:

1. Catenary system with an all-chain setup, which is best for shallow waters.
2. Catenary system with a chain-wire-chain setup.
3. Taut or semi taut leg system with a chain-wire-chain setup.
4. Taut or semi taut leg system with a chain-polyester-chain setup, which is best for ultradeep waters.

Selecting a technically feasible and cost-effective mooring system type primarily depends on water depth and environment. Additional factors to be taken into account are vessel offset restrictions imposed by risers and umbilicals. Further guidance for selecting a mooring profile is listed below [3]:

- For water depth less than 500 m – Catenary systems are the most cost-effective choice where both all-chain- and chain-wire-chain should be considered. In addition to this, the latter may be more cost-effective for depths larger than 300 m.
- For water depth between 500 and 1000 m – All four choices may be considered and offset constraints by riser type or vicinity to other structures may govern selection.
- For water depth between 1000 and 2000 m – Taut leg systems are the most cost-effective choices where both chain-polyester-chain and chain-wire-chain should be considered.
- For water depth greater than 2000 m – Taut leg system with polyester rope is likely the most cost-effective choice, mostly for harsh environments. A chain-wire-chain system can still be acknowledged, but it gets heavier as the water depth increases.

The selection of mooring system profiles may involve comparing two or more types of system. Catenary systems generally require a larger anchor radius to water depth ratio (RD ratio) than taut leg systems. Catenary systems are more costly at more significant water depths (more than 1000 m) as the mooring lines are longer. Taut leg systems can be more expensive in shallow waters because of their high stiffness, as shorter lines lead to high tensions, meaning the system requires larger components [3].

## 2.4 Mooring system components (Components and component materials)

### 2.4.1 Chain

The most common component in a mooring system is a chain, available in different diameters and grades. Offshore mooring chains are typically large, with bar diameters ranging from 70 to 200 mm [3]. Primarily, there are two different chain designs that are used frequently, studlink and studless.

The studlink chain is mainly used for temporary moorings that must be deployed and retrieved numerous times during their lifetime. An excellent example of this is the chain used for drilling semisubmersibles. Whereas studless chain is often used for permanent moorings, such as those for S(P)SOs, catenary anchor leg mooring (CALM) buoys, spars, and production semisubmersibles. These floating production facilities are designed to stay at the site for 20-30 years, and their mooring lines are not meant to be retrieved once installed [3].

### 2.4.2 Wire rope

Wire ropes have less mass and a higher elasticity than a chain of the same breaking load, so engineers use them in the make-up of mooring lines when all-chain designs become too heavy in deeper water. Typical wire ropes used in offshore mooring lines are six-strand, eight-strand, and spiral-strand. Six-strand and eight-strand ropes are typically easier to handle due to their flexibility to bend on sheaves and are used more in temporary moorings. While the spiral strand is torque neutral, and can have a protective polyurethane sheath, meaning it is therefore more suitable for permanent moorings [3].

### 2.4.3 Polyester rope

A polyester rope has become the choice of line type for deepwater permanent mooring applications due to its lightweight and high elasticity. The elasticity of polyester ropes has enabled the use of taut systems in deep and ultradeep water conditions, without catenary compliance to limit dynamic tensions, mostly excited by vessel motions due to waves. It has been broadly used in permanent moorings in deep water where mooring analysis studies showed that polyester rope has desirable elasticity and stretch characteristics for mooring systems in the 1000 – 3000 m water depth range. Furthermore, a polyester mooring system can maintain a smaller vessel offset to better effect than a steel chain-wire-chain system in deep waters [3].

Additional benefits of using polyester moorings include reducing hull structural costs due to smaller vertical loads and reducing the extreme line dynamic tension due to lower stiffness [3]. In summary, polyester rope reduced vessel offset, has a smaller mooring footprint, improved vessel payload capacity, and possesses excellent fatigue properties.

### 2.4.4 Other synthetic ropes

Polyester [polyethylene terephthalate (PET)] is not the only fibre material used to make mooring ropes. Several fibre materials can be considered for use in permanent or temporary moorings, which include nylon (polyamide), high modulus polyethylene (HMPE), aramid (aromatic polyamide), and others.

Nylon is highly elastic compared to other materials used for moorings. For decades, nylon rope has been extensively used for mooring lines for vessels alongside piers, towing hawsers, and CALM buoy hawsers. It is used wherever high elasticity is a required property where these hawsers can also be inspected often and replaced. In addition to this, when it comes to shallow water locations, a length of nylon rope can be inserted in the mooring line to absorb the energy from vessel dynamics [3].

HMPE has properties superior to other fibre materials, such as excellent abrasion resistance, higher strength, and less specific gravity than seawater. HMPE ropes (used in Dyneema and Spectra brands) have been used in mobile offshore drilling unit (MODU) moorings, which are lighter, easier to handle, and have a smaller diameter than comparable polyester ropes of the same breaking strength; though, they may not be as cost-effective as polyester ropes in most mooring applications. Also, the conventional grades of HMPE maybe more susceptible to creep (a time-dependent strain that occurs under load at elevated temperature) and creep rupture stress (a stress at which a test piece made from material fractures when held for a specified time at a defined temperature) [3].

Aramid used in Kevlar and Twaron brands is a rope with strength and stiffness comparable to steel wire rope. It is occasionally used for offshore moorings because axial compression fatigue has a failure mode, which can cause the rope to fail if fibres are subjected to compression [3]. However, axial compression can be avoided or minimized by sound rope design and sound termination techniques that ensure that tension is maintained, and the fibres do not experience compression.

## 2.5 Buoys

Surface or subsurface buoys can be connected to a mooring line to increase the vertical clearance between the mooring line and any subsea equipment, such as pipelines or mooring lines from another floater near the system. Buoys can also improve mooring performance (reduced vessel offset) and reduce the weight of mooring lines that the vessel hull must support. However, because of the extra connections, integrity issues can arise throughout the system[3]. These issues can quickly outweigh the benefits, so engineers usually avoid them in permanent moorings unless necessary.

## 2.6 Clump weight

Clump weights are sometimes fitted on ground chains to improve mooring performance, especially in reducing vessel offset. The additional weight from these cast steel structures can increase the restoring force of the mooring system, as the vessel would have to lift this mass before it can offset further. The structures are typically added to a short segment of the ground chain near the touch down point to increase the restoring force of a mooring leg. Note that clump weights have integrity issues if they are not designed carefully, where they tend to break loose, or, eventually mechanically deteriorate as a result of many years beating up and down in the touch down zone [3].

## 2.7 Scope of a mooring system

The scope of a mooring system is often expressed as a number and refers to the ratio of mooring line to water depth in a system. For example, in taut mooring systems this value is conventionally less than one [8].

## 2.8 Failure conditions

### 2.8.1 Cyclic loading

Cyclic loading is the rapid consistent loading and unloading on a material and often causes failures in materials. Common for all the designs we have investigated is deterioration over time due to cyclic loading. While this is an issue that cannot be completely resolved, it can be mitigated by decreasing the total load in the mooring system [9].

### 2.8.2 Chafe-zone

This only applies to designs with an anchor chain. The “Chafe-zone” is where the mooring line or anchor-chain scrapes across the seafloor. This “chafing” erodes the mooring decreasing longevity [9]. This issue can be completely solved by using a design where no part of the mooring touches the seafloor.



### 2.8.3 Human interference/fish-bite

Only about 10% of all failures can be attributed to this category. Common issues are fishing lines or nets becoming entangled with the mooring system, vandalism and in some climates “fish-bites” [9].

Little can be done to solve the issues of human interference apart from education but if “fish-bite” is found to be an issue, some reinforcement of the top 500m of line can be applied. A rapport released by the woods Hole Oceanographic institute in 1981 concluded that instances of fish bite decrease as the water depth increases and tend to trail off completely at depths of around 500m [10].

## 2.9 Mathematical Theory

### 2.9.1 Line mechanics

The longest component and perhaps the component with the most effect on stability of the system is the line itself. At varying depths, the line length will increase and decrease to suit the active working environment and therefore the mechanics of the line must be able to support the system in varying depths. In general, the forces acting on the line can be expressed as

(EQUATION 1)

$$F = \Sigma \text{External forces} + \Sigma \text{Internal forces}$$

### 2.9.2 Internal Forces

The internal fundamental force in the line is tension, as the line chosen is elastic, we can assume that this is the only internal force we need to account for as the torsional forces are negligible. As Balzola [11] describes, the internal forces generally act in the same direction as the line itself and will be very comparable to a non-submersed line in tension. The line weight

will be affected by damping due to the fluid it is submersed in, here, water. Below is a graphical representation in both 2D and 3D of the tension per unit of length along the line.

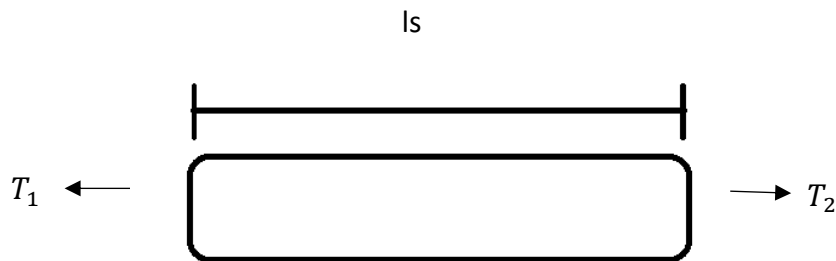


FIGURE 2: INTERNAL FORCES TENSION

Where,  $l_s$  is the segment length and  $T_1$  and  $T_2$  are the tensions in the given directions.

And tension is thereafter calculated by:

(EQUATION 2)

$$T_t = F_t + P_f + A_l$$

Where;  $T_t$  is the total tension,  $F_t$  is the given tension,  $P_f$  is the fluid pressure and  $A_l$  is the cross-sectional area of the line.

### 2.9.3 External Forces

External forces are the forces in the system considered to act on the line which otherwise would have no effect on the line if not connected. There are three main forces which we will consider individually [11]. These forces are as follows:

$F_1$  = Force due to weight and buoyancy

$F_2$  = Force due to added mass forces

$F_3$  = Force due to fluid flow

Line weight and buoyancy forces are calculated as follows:

(EQUATION 3)

$$F_1 = \rho_f A_l g - w$$

Where;  $\rho_f$  is the density of the fluid,  $A_l$  is the cross-sectional area of the line,  $g$  is the gravitational force and  $w$  is the submerged weight of the line per unit length.

The added mass components can be calculated and added to the above equation to solve for the whole system weight and buoyancy. The equation is as follows:

(EQUATION 4)

$$F_2 = \sum w + b$$

This part of the equation can be visually represented as a free-body diagram as shown below:



**FIGURE 3: FREE BODY DIAGRAM OF WEIGHT AND BUOYANCY ACTING ON EACH COMPONENT**

Finally, the force due to fluid flow is calculated by Morison's equation, as shown in section 2.9.4.

#### 2.9.4 Morison's equation

Morison's equations is defined as the following

(EQUATION 5)

$$\mathbf{f} = (\Delta \mathbf{a}_f + C_a \Delta \mathbf{a}_r) + \frac{1}{2} \rho C_d A |\mathbf{v}_r| \mathbf{v}_r$$

Where  $\mathbf{f}$  is the fluid force per unit length on the body,  $\Delta$  is the mass of fluid displaced by the body,  $\mathbf{a}_f$  is the fluid acceleration relative to earth,  $C_a$  is the added mass coefficient for the body,  $\mathbf{a}_r$  is the fluid acceleration relative to the body,  $\rho$  is the water density,  $C_d$  is the drag coefficient for the body,  $A$  is the drag area and  $\mathbf{v}_r$  is the fluid velocity relative to earth [12].

Hydrodynamic loads are calculated by an extension of Morisons equation by having two components of force, fluid inertia force and drag force per unit length [12].

#### 2.9.5 Buoyancy, Archimedes principle

Buoyancy was determined through the following equation:

(EQUATION 6)

$$F_b = \rho g V$$

Where  $F_b$  is the buoyancy,  $\rho$  is the density of the fluid,  $g$  is the acceleration of gravity (9.81 m/s<sup>2</sup>) and  $V$  is the volume of the body submerged under the fluid.

#### 2.9.6 Drag

A mooring system will always experience some type of drag force. The two main components that are subject to drag are the buoys and the line itself [13]. Drag is calculated by:

(EQUATION 7)

$$F_d = \frac{1}{2} \rho v^2 C_d A$$

Where  $F_d$  is the drag force,  $\rho$  is the mass density of the fluid,  $v$  is the flow velocity relative to the body,  $C_d$  is the drag coefficient and  $A$  is the reference area.

2.9.7 Mass moment of inertia

For a solid cylinder the following applies

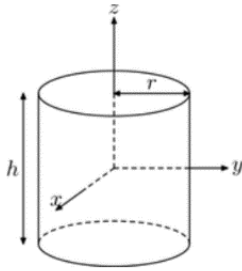


FIGURE 4: SOLID  
CYLINDER MASS  
MOMENT OF INERTIA

$$I_z = \frac{1}{2} m r^2$$

(EQUATION 8)

(EQUATION 9)

$$I_x = I_y = \frac{1}{2} m (3r^2 + h^2)$$

Where  $m$  is the mass,  $r$  is the radius and  $h$  is the height.

For a hollow cylinder the following applies:

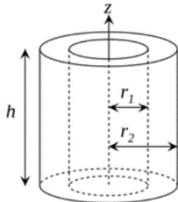


FIGURE 5:  
HOLLOW  
CYLINDER MASS  
MOMENT OF  
INERTIA

$$I_z = \frac{1}{2} m (r_2^2 + r_1^2)$$

(EQUATION 10)

(EQUATION 11)

$$I_x = I_y = \frac{1}{12} m [ 3 (r_2^2 + r_1^2) + h^2 ]$$

Where  $m$  is the mass,  $r_1$  is the inner radius,  $r_2$  is the outer radius and  $h$  is the height.

2.9.8 Dry length

Dry length refers to the amount of material of the profiler that is not submerged when in an active mooring system. This length can be expressed as its absolute value or as a percentage of the entire component. OrcaFlex calculates dry length,  $L_d$  using the following equation:

(EQUATION 12)

$$L_d = \frac{L V_{above}}{V_{tot}}$$

Where  $L_d$  is the dry length,  $L$  is the cylinder length,  $V_{above}$  is the cylinder volume above the surface and  $V_{tot}$  is the total volume of the cylinder.

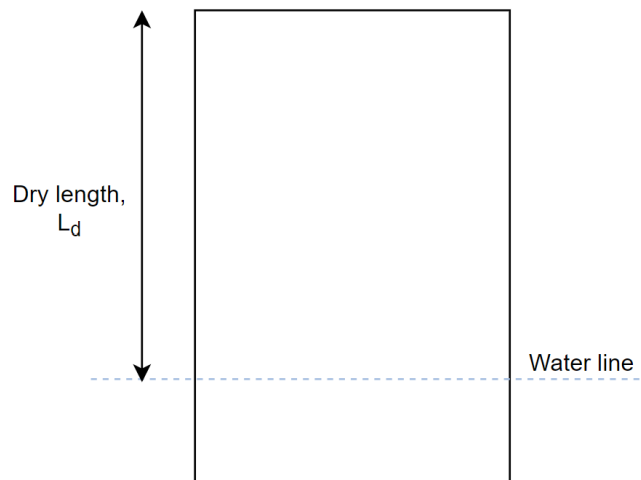


FIGURE 6: DEFINITION OF DRY LENGTH GRAPHICALLY

Wavelength/period

(EQUATION 13)

$$\lambda_d = \frac{gT^2}{2\pi}$$

Where  $\lambda_d$  is the wavelength,  $g$  is the gravitational acceleration and  $T$  is the wave period.

### 3. Literature Review

Mooring systems are essential components of maritime infrastructure, used to secure vessels, offshore structures, and floating wind turbines in place. They play a critical role in ensuring safety, stability, and efficiency in structures in often very challenging conditions at sea. The design, selection, and installation of mooring systems are complex processes that require delicate consideration of various factors, including water depth, wave and current conditions

and load capacity. As such, a significant amount of research has been conducted on mooring systems, with a particular focus on improving their reliability, performance, and cost-effectiveness. This literature review aims to provide a comprehensive overview of the current state of research on mooring systems, highlighting key findings and challenges in existing systems to assist the design process based on the task brief.

Martini et al [14] describe that the design of a mooring solution is driven by only three parameters: water depth; wave weight and current speed. The trio also derived that a successful mooring system moored at a significant depth that would be subjected to high current speeds would almost certainly require a subsurface flotation device, or subsurface buoy [14]. This study is reinforced by a study by Feng et al [15], where the motion of the object on the surface is a superposition of the static displacement of the mentioned forces and the wave motion pattern.

Ghafari's [16] study into catenary mooring systems describes them as simple yet effective, and highlights that they are highly reliable. The use of a heavy anchor chain significantly reduces the vertical load on the anchor, reducing the risk of the anchor becoming dislodged. This lower section of the system is also the main source of the system's compliance, as described by Taft [9] in a study into low load mooring systems.

However, this particular system invokes some negative aspects. Luff et al [17] discovered that as the buoy deviates slightly, the chain section located on the seabed considerably disturbed the sea life also located here. With the anchor as the midpoint, the chain created a circular area, whose radius was equal to the chain length, in which the chain dragged and disturbed the seabed. This resulted in a considerable decrease in the length and density of the seagrass at this location, and was proven on several occasions [17]. Additionally, the consistent scraping of the chained section along the seabed was found to lower the lifespan of the system. The increase in wear and tear was found to be a common source of failure within this mooring system type, also known as chafing [9].

The semi-taut mooring system was found to be an effective setup in resolving the disturbance of the seabed. A semi-taut mooring system typically does not have any line in contact with

the seabed. A study presented by Yu et al derived that this particular type of mooring system also eliminated the chafing failure condition [18]. The research describes two methods of achieving this. The first method relies on a highly elastic line with a scope lower than one, ensuring the line is under constant strain. The second method uses a subsurface flotation device situated at approximately  $4/5^{\text{th}}$  of the depth of the water column in which a system is deployed [18].

The drawback of these systems is that they are conventionally less suitable for rougher ocean conditions, due to the elasticity of the mooring line. The elasticity presents more flexibility in the line and when subjected to rougher conditions, the longevity of the system was compromised [9].

Taft and Teng's research also spanned to a system known as the inverse catenary mooring. This system type appears to be somewhat of a middle ground between a catenary and semi-taut system. This system offers high durability, compliance and adaptability in the field and does not employ the use of an anchor chain. The research accounted mostly for systems deployed in depths of greater than 500m, but found that with minimal adjustments that the system was also able to efficiently cope with water depths of as low as 30m [9].

A typical inverse catenary mooring setup is usually divided into two sections. The primary section comprises of the anchor and lower subsurface flotation device. The secondary section consists of the surface buoy and a subsurface buoy. The lower subsurface flotation device is used to ensure that no line is in contact with the seabed, and is in some instances replaced by buoyant line [9]. This section usually spans to half the depth of the water column. The secondary section consists of the surface buoy and subsurface buoy and have a general scope value of 1.75. The slack located along the primary line ensures mechanical compliance in this type of mooring [9]. The two sections are joined by line of length also defined by the scope. This type of mooring design theoretically encounters the lowest load on the system as they derive most of their compliance from the slack in the system [9].

Thorough research has also been conducted into the different materials used in mooring lines. A study by Ding et al revealed that chain was extremely effective for use in catenary systems



but often incurred high costs due to its metal structure and mass. However, chain systems in deepwater environments have encountered considerable issues with both deployment and maintenance, as chain is often buried in the seabed. An article by Reimer [19] demonstrates the use of autonomous remote control subsurface vehicles to tackle this issue. This solution also contributes to the high price of chain-based solutions.

Synthetic lines are receiving increased attention in the offshore field. A study by Xu et al [20] concluded that nylon and polyester are suitable for use in mooring systems due to their excellent fatigue performance, high flexibility and ability to tackle high loads. Further research conducted by, Xu et al [20], deduced that such lines have a distinct advantage in applications involving significant wave movement, such as Wave Energy Converters (WECs), due to their ability to withstand fatigue whilst maintaining their ability to be highly flexible. Nylon in particular outperformed wire and polyester lines in research conducted by the same trio, where the dynamic characteristics of polyester and wire were virtually inseparable, but nylon performed significantly better across all categories tested [21]. On the contrary, nylon suffered significantly higher fatigue damage than its counterparts [21].

Further research into nylon lines concluded that nylon reduced mooring line lengths and contributed to a stronger overall system. This information is based on the modelling and analysis of chain-nylon-chain and chain-polyester-chain mooring system designs [22]. The effects of cyclic loading also reinforce the advantages of nylon. The consistent lifting of the heavy chain anchor from the seafloor increases the load on the system and therefore further discourages the use of a heavy anchor chain, making nylon an attractive alternative solution [9]. The research does highlight doubts about the fatigue characteristics of nylon, but also mentions that new techniques such as coating nylon lines appear to approve nylon's fatigue characteristics [22].

To conclude, the above works in this literature review highlighted the importance of careful consideration of each aspect when designing a mooring system. The combination of environmental, material and composition factors ultimately determine the performance and reliability of a potential system. Although there are areas where the research has ethical and

economic limitations, the overall research performed provides solid foundations in order to progress with the proposed task.

## 4. Methodology

### 4.1 Task requirements and assumptions

A successful mooring system design and simulation in the preliminary phase had to satisfy the following demands:

1. Stable and smooth movement pattern

Data collected showing position in the global  $xy$  – plane and  $xz$  – plane i.e., motion pattern. Motion in the  $xy$  – plane represents how the cylinder would move in water seen from a bird's eye view and should ideally follow an overlapping circular pattern. Motion in the  $xz$  – plane represents how much the cylinder would move up and down in the water and should also ideally follow an overlapping circular pattern.

2. Dry length  $\geq 50\%$

Dry length is defined as the length of the cylinder consistently above the water surface to ensure satellite communication.

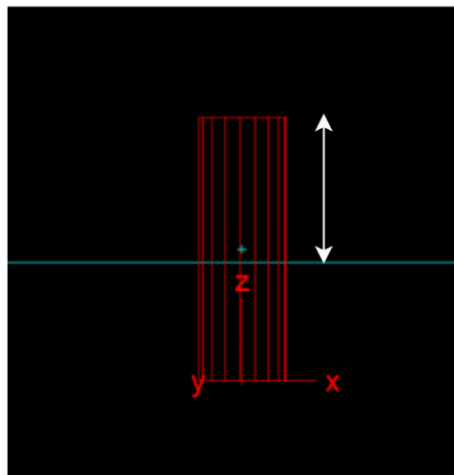


FIGURE 7: DRY LENGTH ILLUSTRATION

3. Declination  $< 2$  deg

Declination is defined as the angle the direction makes with the  $z$  – axis, so is there for 0 deg for positive  $z$  direction, 90 deg for any direction in the  $xy$  – plane, and 180 deg

for negative z direction. The cylinder should not oscillate more than 2 degrees relative to global z – axis after it has reached equilibrium.

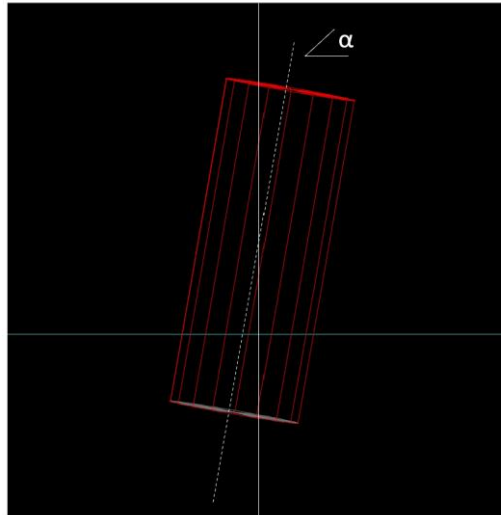


FIGURE 8: CYLINDER DECLANATION

#### 4. No excess line in contact with the seabed

The last demand the simulation had to satisfy was to indicate that the mooring line would not be in contact with the seabed. This was to not disturb and potentially damage the seabed and marine life at any given location.

Any simulation failing to meet these demands was deemed as not successful.

##### 4.1.1 Task assumptions and parameters

*Assumption 1.* The ocean current ( $V_c$ ) is constant through the whole water column and flow is always the same direction which is 180 degrees relative to global x – axis in positive direction.

*Assumption 2.* Wind speed and wind direction is constant at 180 degrees relative to global x-axis in positive direction.

*Assumption 3.* Wave height, frequency and period are constant.

*Assumption 4.* The mooring system experiences perfect waves through the simulations.

*Assumption 5.* The anchor has infinite weight and will not fail or move.

*Assumption 6.* The connection between the mooring line and profiler will not fail.

*Assumption 7.* The profiler has predefined dimensions that we are not responsible for changing.

The standard environmental conditions were defined as the following:

Parameter	Value	Unit	Symbol
Ocean depth	100	m	$D_o$
Water density	1025	Kg/m <sup>3</sup>	$\rho_w$
Kinematic viscosity	1.35e-6	m <sup>2</sup>	$\eta$
Ocean temperature	10	°C	$t$
Wave period	12.5	s	$T$
Ocean current (direction)	0.1 (180)	m/s (deg)	$v_c$
Wind speed (direction)	1.7 (180)	m/s (deg)	$v_w$
Time period	600	s	$T_{sim}$

TABLE 1: STANDARD ENVIRONMENTAL CONDITIONS

## 4.2 Concept discussion

As stated earlier, the design we require must be durable, simple, easy to handle and not negatively interfere with the seabed. Due the relatively small mass and low buoyancy of the vertical profiler, we believe that optimizing the design to reduce axial forces in the mooring line is not of immediate importance as the values of these forces do not endanger failure in any of our potential system choices.

After combining the theoretical aspects and information attained from the literature review, we arrived at two solutions for the task at hand. The first concept discussed was the use of a

taut leg mooring system. The taut leg mooring system offered little interference with the seabed and offered very little flexibility in the line, therefore preventing the profiler from diving under the sea surface, both of which were critical criteria to fulfill in line with the task brief. However, due to the lack of subsurface flotation devices, we deduced that heavier chain lines had to be used in this particular system should it be able to tackle more aggressive and deeper waters. This ultimately led to the omission of this design as the mass of the design would be too much to transport and handle for one to two persons.

The second concept discussed was the use of an inverse catenary mooring system. We derived that based on the extremely positive literature written on this system and the nature of its setup, that this system could be a viable approach to the task. As described in the literature review, the system could employ techniques used in both catenary and semi taut mooring designs, therefore the system presented dynamic opportunity for unique material use in our task. The system takes advantage of added flotation devices, could employ lighter mass materials, and be deployed in a variety of ocean conditions with relevant adjustments to the design of the system.

### 4.3 Forming and design

After the previous conclusions, we arrived at four conceptual designs prior to use in the simulation software. The four designs were based on an inverse catenary mooring system.

We then employed the use of ProteusDS Oceanographic Designer, a software produced by the Canadian engineering company DSA Ocean, to digitally represent the hand drawn concept designs we had [23]. It must be noted that this software was used on the basis that the schematics produced were not of the scale or dimensions used in the simulation software. The components chosen were used to graphically represent the hand drawings and the graphics do not illustrate slack in the line that an inverse catenary mooring conventionally offers but models the systems two-dimensionally. The line lengths displayed are a standard function of the software and are negligible values in the following instances.

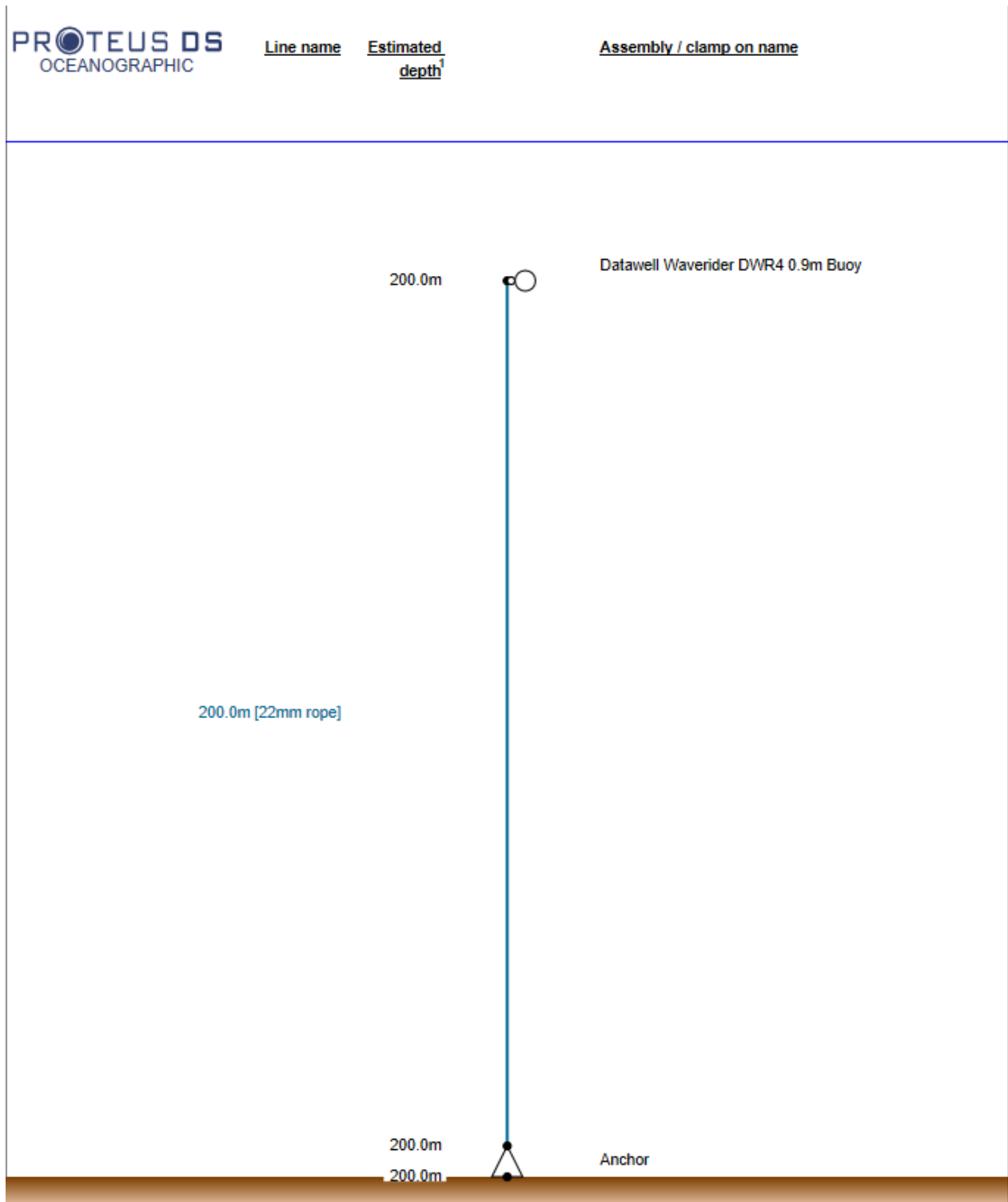


FIGURE 9: DESIGN 1

Design one, as shown above, shows a simple design with no added flotation devices. The surface buoy, or profiler, is attached to a nylon line that spans the depth of the water column

that is in turn attached to the anchor at the seabed. The designs that follow design one are based on the same concept but with added floatation devices.

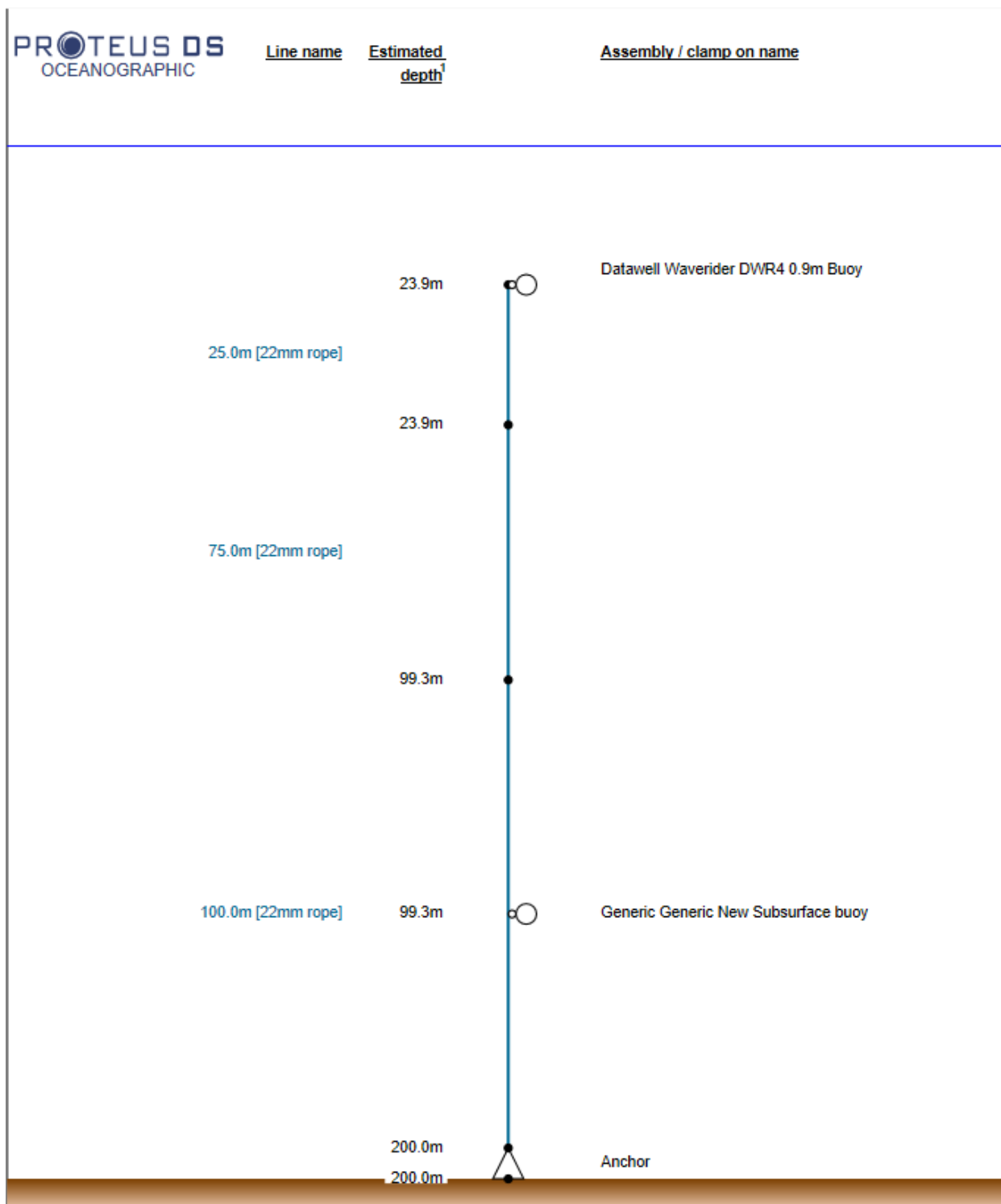


FIGURE 10: DESIGN 2

Design two, is an extension of design one. The line again spans the depth of the water column attached to the anchor at the seabed. At 75m above the anchor, is an added floatation device or subsurface buoy as shown by the caption in the graphic. The added floatation device is used here in order to prevent the line from being in contact with the seabed whilst offering more stability in the system.

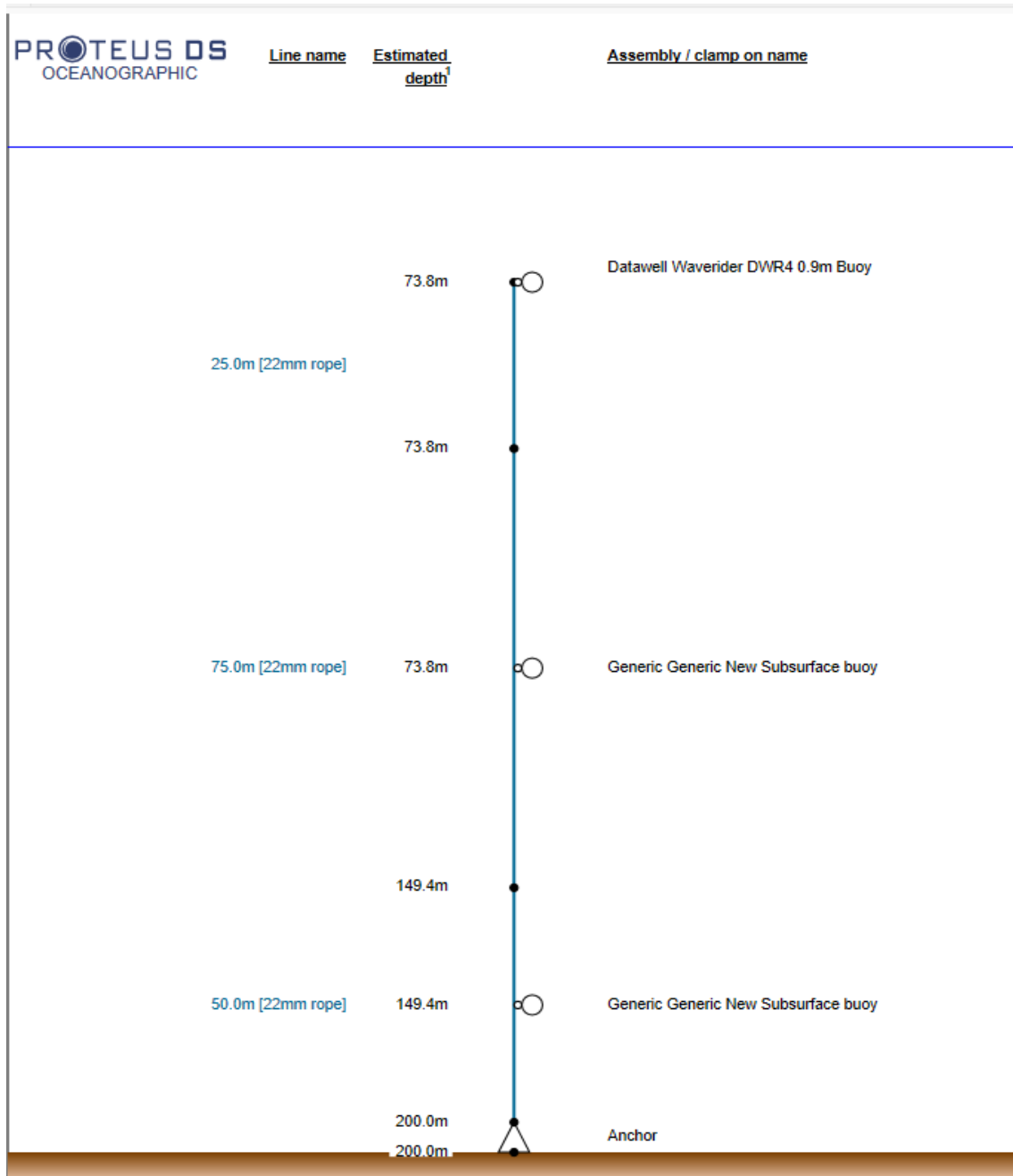


FIGURE 11: DESIGN 3



Design three consisted of two subsurface buoys. The lower of the two subsurface buoys served the same function as in Design two, whilst the subsurface buoy captioned at the midpoint of the system added extra stability in the buoyancy in the system. The added subsurface buoy was included in order to ensure the that the required area of the profiler did not begin diving below the surface.

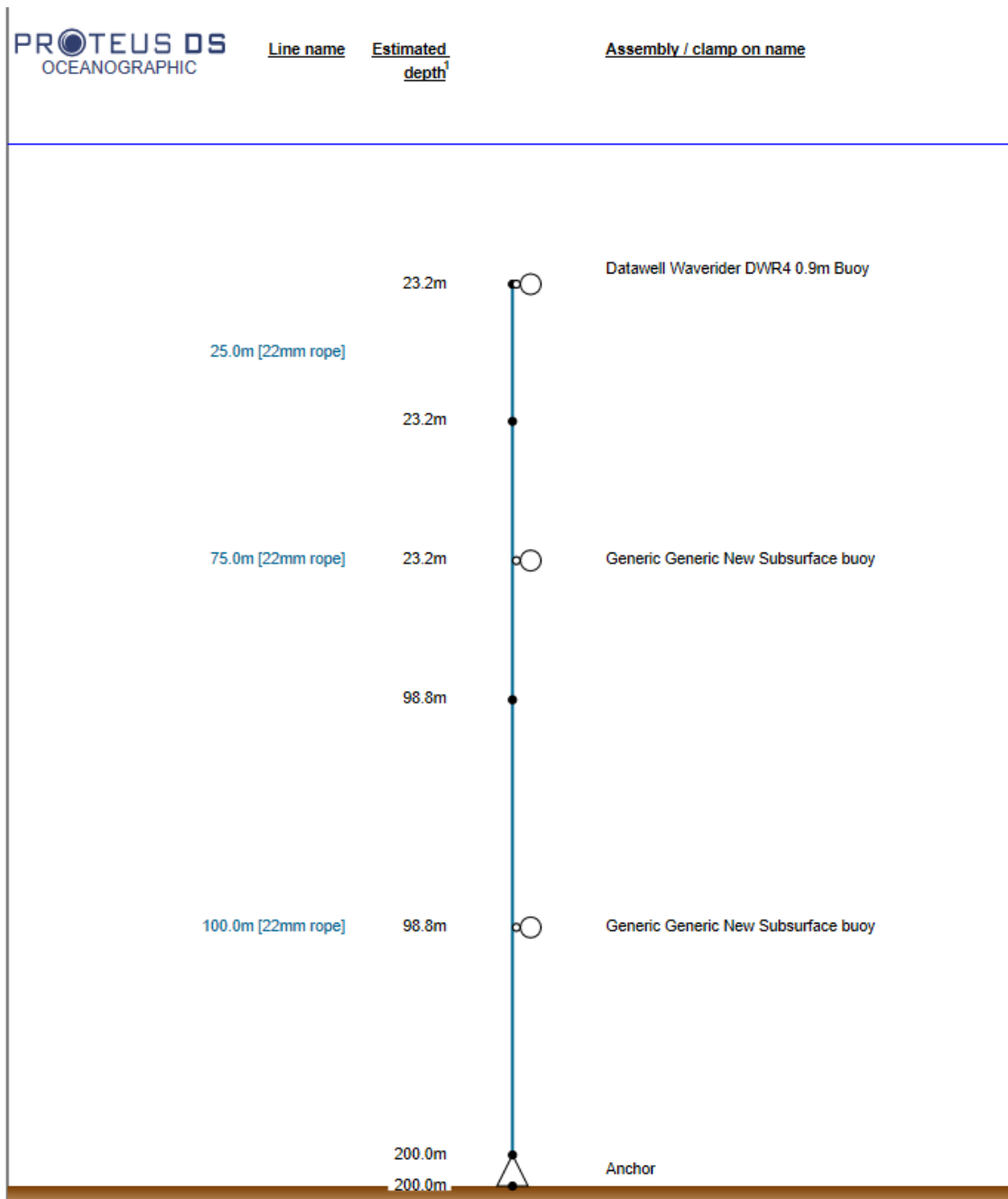


FIGURE 12: DESIGN 4

Design 4 is a modified Design 3. The lower subsurface buoy was again in place to ensure that the lines did not interfere with the seabed. However, in this design, the upper subsurface buoy is situated closer to the profiler or Datawell buoy as captioned, in order to further ensure that the profiler did not begin diving below the sea surface.

#### 4.4 Choice of solution

After some discussion and consideration of the brief's requirements we opted for Design 4 as the chosen design to simulate. As the brief highlighted, the system is required to be handled by one to two people and should therefore have as little mass as possible. The combination of this factor and that the profiler has such little mass compared to other mooring systems, Design 4 was the most viable design.

Design 1 was ultimately too simple and due to the mass of the profiler we concluded that the system would be too unstable and would rely heavily on the deployment environment being extremely calm. There was also no guarantee with this system that the line would not disturb the seabed, a key factor in the project brief that was not fulfilled with this system.

Design 2 accounted for the requirement of the line not being in contact with the seabed due to the inclusion of a subsurface buoy. However, we believe that based on research conducted and due to the small mass of the system, the line itself would not provide sufficient stability for the profiler. For this design to work in the field, we also concluded that the environment in which the system was to be deployed would be limited to calm currents and weather conditions, again conflicting with the task brief.

Design 3 was a viable design but was ultimately not selected due to the positioning of the second subsurface buoy. The inclusion of a second subsurface buoy would significantly increase the system's stability but overall, the hydrodynamic forces on the system would almost certainly result in the submersion of the profiler. Due to this, Design 4 was adapted in order to accommodate for this factor.

Design 4 employed the same fundamental use of components, an anchor, line and two subsurface buoys, but the position of the upper subsurface buoy was adjusted to accommodate for doubts that the net buoyancy was not sufficient to ensure the profiler from diving under the surface. The new position of the buoy should theoretically provide a better platform for buoyancy in the upper portion of the system as it is closer to the surface, therefore balancing the Morison's equation. The lower subsurface buoy serves the same function in this system. The combination of these factors rendered this design the most viable design to model based on the project requirements.

#### 4.5 OrcaFlex guide

To assist the analysis of the stability and simulate the mooring systems the software OrcaFlex from Orcina LTD was used throughout the entirety of the project. The software allows precise and delicate control of every physical factor of each component and for the environment in which the system is to be simulated. The software then outputs result graphically in both two dimensions and three dimensions over a user-controlled time period, in order to see how the system would behave in the real world. The software proved to be a useful and flexible asset to assist the understanding and development of a mooring system design.

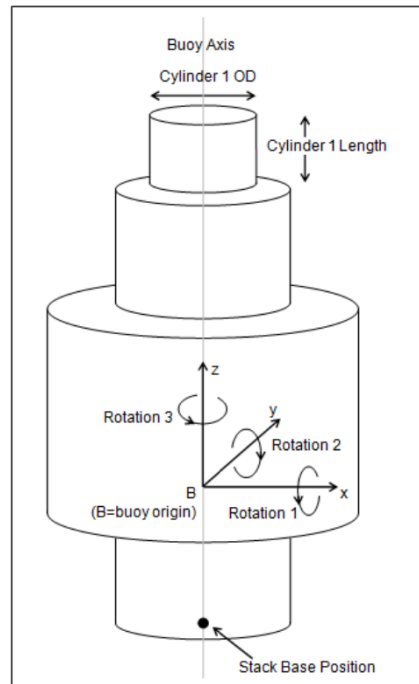
##### 4.5.1 The objects

OrcaFlex is made up of nine modular building blocks or objects. This report focuses only on a few of these objects as the rest is irrelevant. This section introduces each object used in the simulations, their application, types of data input needed and how they form part of the full model. The mooring systems consists of three objects, a 6D buoy, a line and one or more attachments.

##### 4.5.2 6D buoys

6D buoys are rigid bodies with six degrees of freedom, three translations and three rotational denoted as X, Y, Z and 1, 2, 3 respectively. They are intended to be used in the drag and inertia

regime in which Morison's equation applies i.e., its characteristic dimension should be smaller than the wavelength it experiences.



**FIGURE 13: A 6D SPAR BUOY CONSISTING OF MULTIPLE CYLINDERS WITH DIFFERENT DIAMETERS, ALONG WITH LOCAL AXIS AND SIX DEGREES OF FREEDOM.**

Degrees of freedom	Description	Position
1	Surge	Translational motion in x-axis
2	Sway	Translational motion in y-axis
3	Heave	translational motion in z-axis
4	Roll	Rotational motion in x-axis
5	Pitch	Rotational motion in y-axis
6	Yaw	Rotational motion in z-axis

**TABLE 2: AN OVERVIEW OVER DEGREES OF FREEDOM WITH DESCRIPTION AND POSITION.**

OrcaFlex has three types of buoys for different applications, lumped buoys, spar buoys and towed fish. All three share common data to some degree but differ in the ways in which the fluid loads and surface piercing effects are calculated and how the geometries are defined.

A Lumped buoy is the simplest type of 6D buoy with an undefined shape. When this type of buoy pierces the water surface OrcaFlex perceives it as a vertical stick with length equal to its user specified height. The buoyancy changes therefore linearly and vertically, without regard to orientation and neglecting the rotational stiffness that would be experienced by most surface piercing buoys.

Spar buoys are intended for modelling axisymmetric buoys with a vertical axis and where surface piercing effects are important (such as for a profiler). Spar buoys can be modelled as multiple axial cylinders stacked end to end along the local z-axis. This allows the user to define the geometry of the buoy by determining the outer and inner diameter and the height of each cylinder. Spar buoys model surface piercing effects more sophisticatedly than lumped buoys. Effects such as heave stiffness and righting moments in pitch and roll are calculated based on the intersection of the water surface with each of the cylinders making up the buoy allowing for instantaneous position and orientation of each individual cylinder in the wave. Hydrodynamic loads are loading that result from water flowing against and around a rigid body and are calculated using Morison's equation. Added mass and drag are applied to the parts of the buoy which are instantaneously in the water and for partly submerged spar buoys, added mass and drag are scaled according to the proportion of the individual cylinder volume that is submerged.

The last type of 6D buoy is called towed fish and are intended for modelling bodies whose principal axes are horizontal. They are identical to spar buoys except the cylinders are laid out along the x – axis of the buoy and not the z-axis.

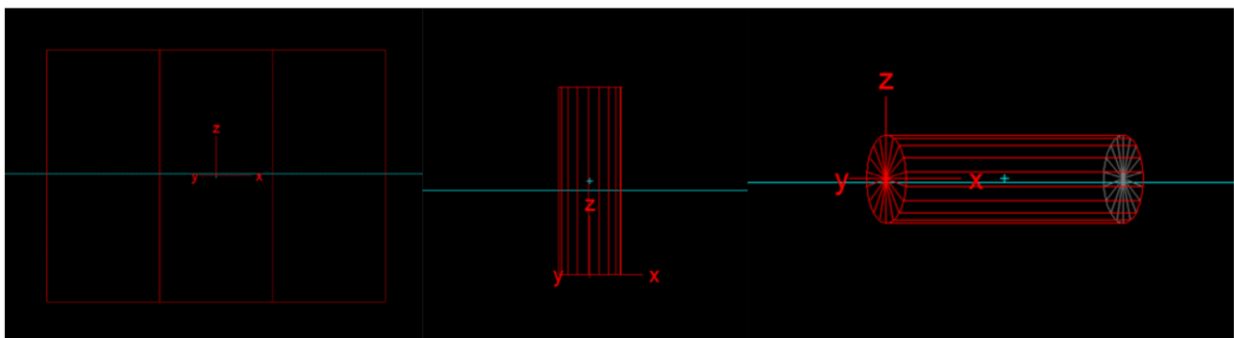


FIGURE 14: FROM LEFT TO RIGHT, LUMPED BUOY, SPAR BUOY AND TOWED FISH

#### 4.5.3 Lines

A line is a flexible linear element and can be used to represent pipes, cables, chains, hoses, and mooring lines. Its mass and hydrodynamic properties are lumped at nodes which are connected by straight massless line segments. The properties of the line can also vary along its length by splitting the line into multiple sections and assigning different properties such as mass per meter, inner and outer diameter, and material, with each effecting the physical behaviour of the line thereafter. The line length, segment length, properties and quantity of nodes are user specified variables, where a greater number of nodes and properties contribute to a more accurate model, but at the expense of simulation run time and file size.

#### 4.5.4 Clumps

A clump is a concentrated attachment connected to a node on a line. It can both be buoyant or heavy and represents a body that experiences forces such as weight, buoyancy or drag. A clump is not free to move but constrained to move with the node to which it is attached to, so the forces acting on the clump are transferred to that node. It therefore adds to the mass, buoyancy, and hydrodynamic force of the line at the connecting node. The clump can again be fully user defined in the same manner as a buoy or line. A clump will from this point be referred to as a subsurface buoy or SSB.

#### 4.5.5 Object states and connections

Model objects can either be fixed, anchored, free or connected to another object, the latter is referred to as parent – child connection. The parent refers to the model object that a child is connected to. The child is described to be linked to the parent rather than the other way around by convention. Connections are made relatively and with respect to local axes of the objects and once a connection has been defined by the user, the point  $p$  at which the child is connected to the parent will be treated as if they were rigidly attached with a standard connection that the software determines itself.

Objects that are either fixed or anchored will always remain fixed to a user specified point relative to the global axes. Free objects move independently of other objects and move in

response to wave loads, connected lines and subsurface buoys, where the motion of the child is controlled by its parent. To clarify, a line can be connected to a buoy and a buoy can be connected to a line, the difference being that the parent will act as the main body or point A that affects the motion and forces acting on the child object at point B.

#### 4.5.6 Control bar

Upon opening OrcaFlex, the user is met with the following screen.

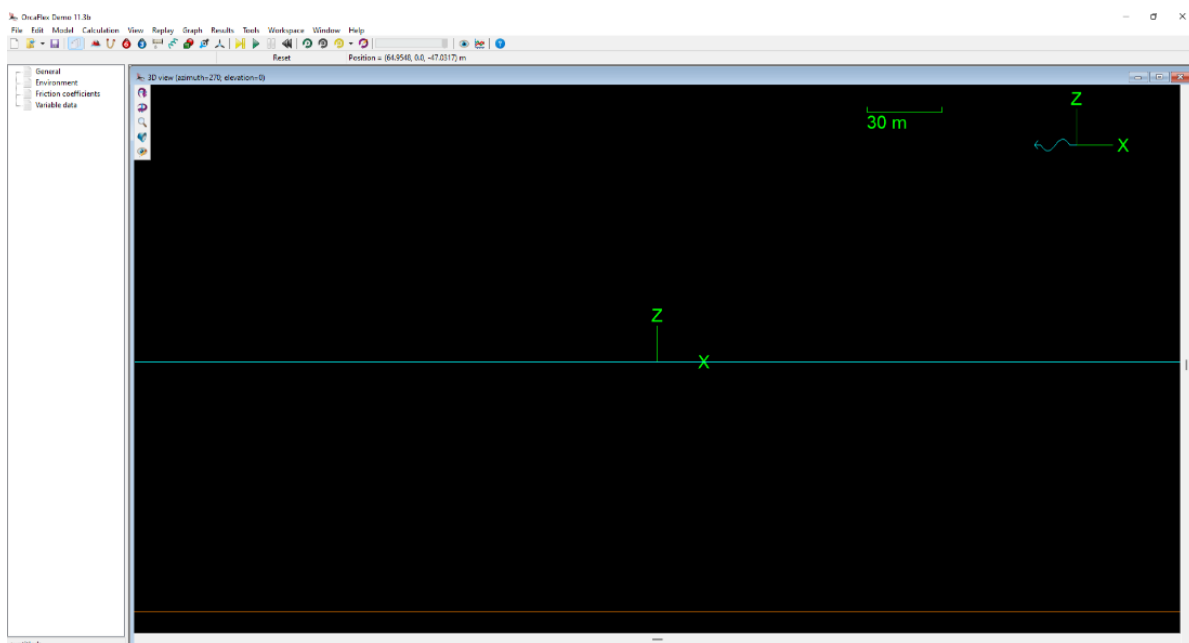


FIGURE 15: ORCAFLEX OPENING WINDOW WITH TWO-DIMENSIONAL VIEW

The screen shows the global axis in the centre, the toolbar at the top and the control bar at the left of the screen. The blue line represents the sea surface and the orange line the seabed. The first useful shortcut is a shortcut to change the graphic view on the users' screen, by using CTRL+G, the user can toggle between the two-dimensional and three-dimensional views OrcaFlex offers. As seen below, the 3D view is also a graphical model of an ocean.

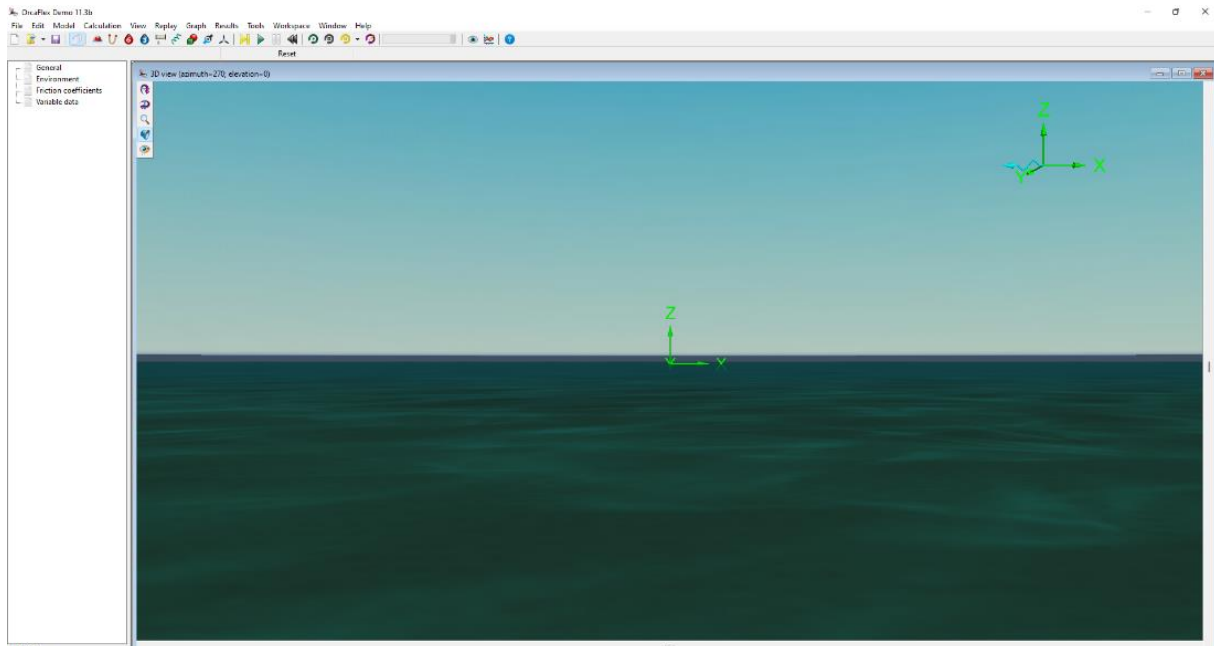


FIGURE 16: 3D VIEW OCEAN VIEW IN ORCAFLEX

Starting with the control bar at the left of the screen, there are four options upon startup in OrcaFlex. These options are General, Environment, Friction coefficients and Variable data. These options are the fixed variables the user can set and control before commencing a simulation. The “General” option allows the user to set units used in the post simulation phase, the starting velocity of the water and the number of iterations the software should perform whilst solving the statics and dynamics under the simulation period. As displayed below, the user can input their own parameters to control the constraints of the simulation.



Edit general data

Model type: standard

Units:

System	Length	Mass	Force	Time	Temperature	g (m/s <sup>2</sup> )
SI	m	te	kN	s	°C	9.80665

Comments   Reset   Analysis   **Statics**   Dynamics   Restart state   Results   Post calculation actions   User defined results   Drawing   Tags

Buoy degrees of freedom included in static analysis:

Starting velocity:

Speed (m/s)	Direction (deg)
0.0	0.0

Line statics step 1 policy:

None  
 Parent lines excluded  
 All lines included

Line statics step 2 policy:

None  
 Parent lines excluded  
 Solve coupled systems

Whole system statics enabled

Whole system statics convergence parameters:

Max iterations	Tolerance	Min damping	Max damping
400	1e-6	1.0	10.0

FIGURE 17: GENERAL TAB WITH USER-DEFINABLE SETTINGS

In the environment tab the user can define several parameters used for the simulation including current velocity, wave height and wind speed. This tab provides a clear overview of the environments' variables and allows the user to simulate a specific real-life scenario, such as in the North Sea or in the Black Sea, should they see fit. The figure below shows the further parameters than can be defined in the environment control window.

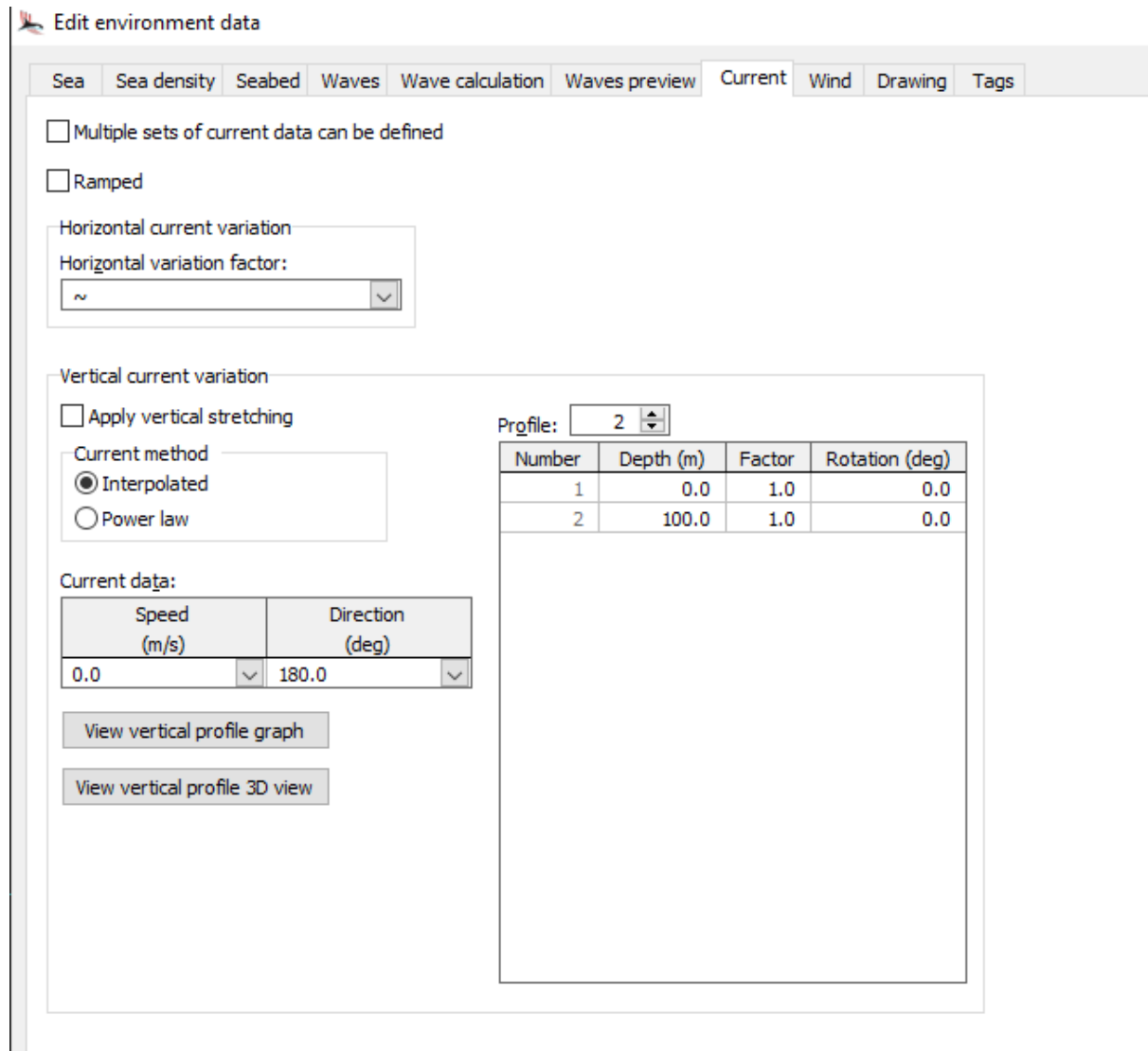


FIGURE 18: ENVIRONMENT CONTROL WINDOW

The user can also set the depth of the seabed and the temperature of the sea using the seabed and sea tabs respectively.

The Friction Coefficient window allows the user to control the friction models of each shape that is present in the simulation. OrcaFlex uses the Coulomb friction model [5] if the user chooses not to customise this setting. In the case of this project, the Coulomb was representative enough in order to produce a steady and viable simulation, this will apply to most simulations.

The final tab in the control bar is the Variable Data bar. This allows the user to control which plots are outputted in the post phase of the simulation. Here the user can choose to compare

several elements of the simulation and the tool outputs the correlation between the two (or more) results chosen in an Excel graph.

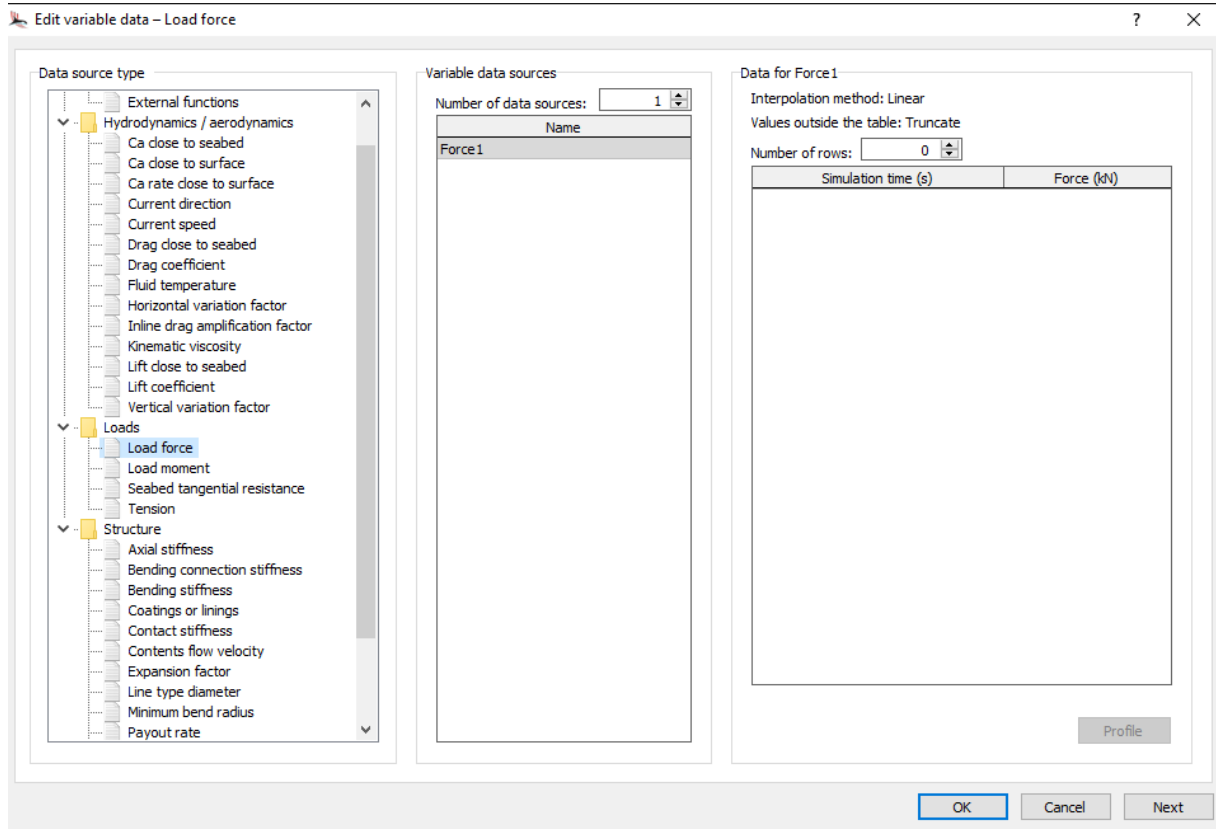


FIGURE 19: VARIABLE DATA CONTROL

For example, as seen in the figure above, the user can choose to compare Load force and Current speed after a simulation has been run, in order to interpret and understand the correlation between the two factors. This has proven to be a very useful tool throughout this project as it allows for graphical understanding of how and why two variables can influence one another; a key part in understanding both the setting up of a model and changing of a model based on the results shown.

#### 4.5.7 The help tab

If the user should require extensive help on all or any elements within the software, OrcaFlex provides a precise, in-depth Help tab, located on the far right of the toolbar at the top of the

screen. This guide provides a tutorial on how to use OrcaFlex, information guides on how to improve the quality of a simulation and extensive background information on the theoretical aspects of a simulation, including equations.

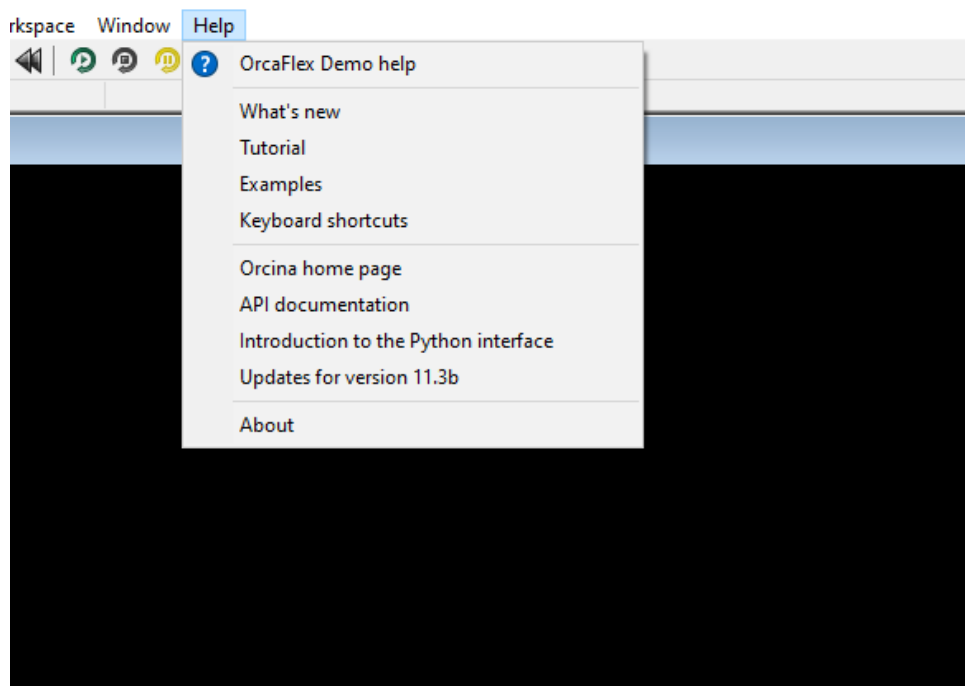


FIGURE 20: ORCAFLEX HELP WINDOW

#### 4.5.8 Basic controls

In order to move around the screen and model within OrcaFlex there are a few basic key and mouse click combinations. Firstly, in order to move around the screen horizontally and vertically, or along a theoretical X and Y axis, the user must hold SHIFT and then, using the mouse, move the screen to the desired location.

A similar combination is used in order to rotate the model through the X, Y, Z axes, here the user must hold the CTRL and, again using the mouse, move the screen to the desired location to improve the viewing angle of the model.

If the user wishes to zoom into any aspect of the model, this can be done by holding the CTRL key and using the scroll wheel in order to zoom into the model. Here it is important to note

that the screen will zoom based on the position of the cursor on the screen. Therefore, to perform a precise zoom, the user must move the cursor to the desired zoom position before zooming in on the model.

As previously mentioned, the user can toggle between 2D and 3D views using the CTRL+G shortcut within OrcaFlex.

Finally, if at any point the user would like to return to the standard origin view, this can be done by using the shortcut CTRL+T. This tool is particularly useful in situations where the user may have zoomed or rotated slightly wrong and wishes to reset the model view in order to rotate around the model again.

#### 4.5.9 Setting up a model

In this part of the OrcaFlex walkthrough, we will introduce setting up a basic model. We will start by looking at the component tool bar, located in the centre at the top of the OrcaFlex window.

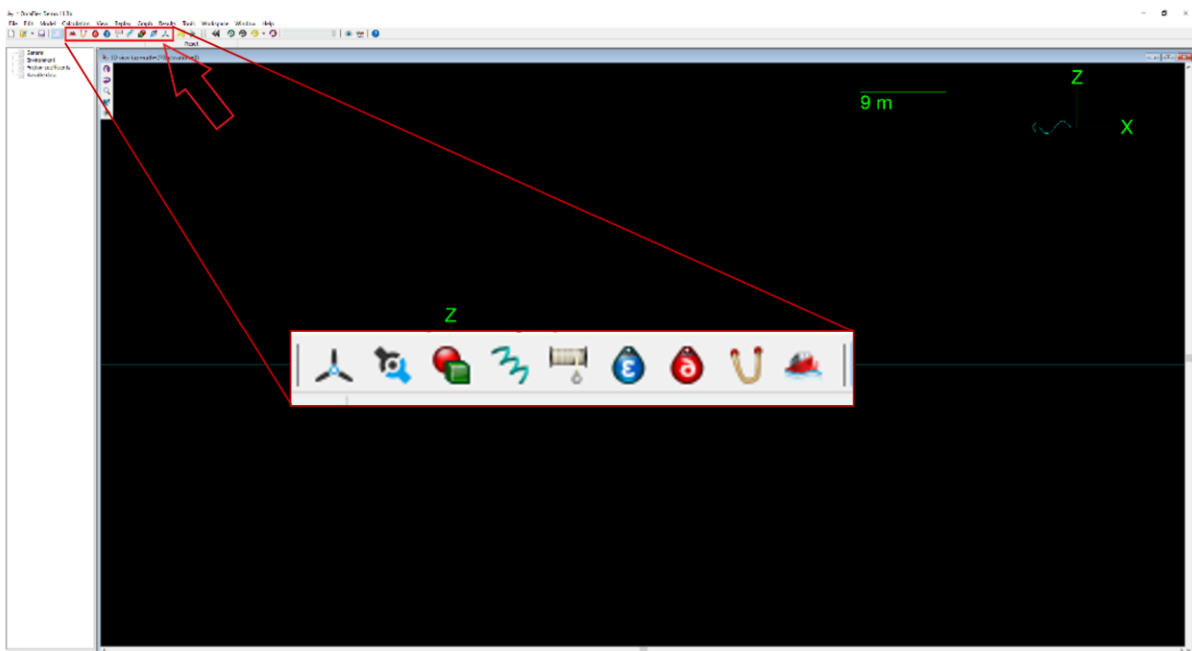


FIGURE 21: COMPONENT TOOL BAR LOCATION

From here, there are nine components we can chose from. However, for our particular application we will only require the Line, 6D buoy and 3D buoy components located on the tool bar.

For ease-of-use purposes, we will only be changing one of the environmental properties and the rest of the settings will remain at default. Navigate to the “Environment” tab on the control bar and select the “Waves” tab. Navigate to the “Wave data” window and edit the height to 1.

Firstly, we will start by selecting the line tool from the toolbar. After selecting this tool, use the mouse to click on the screen to assign the point in which point A of the line will reside; we recommend choosing the vertex of the Z-X axis displayed on the screen. The result should be similar to the figure below.

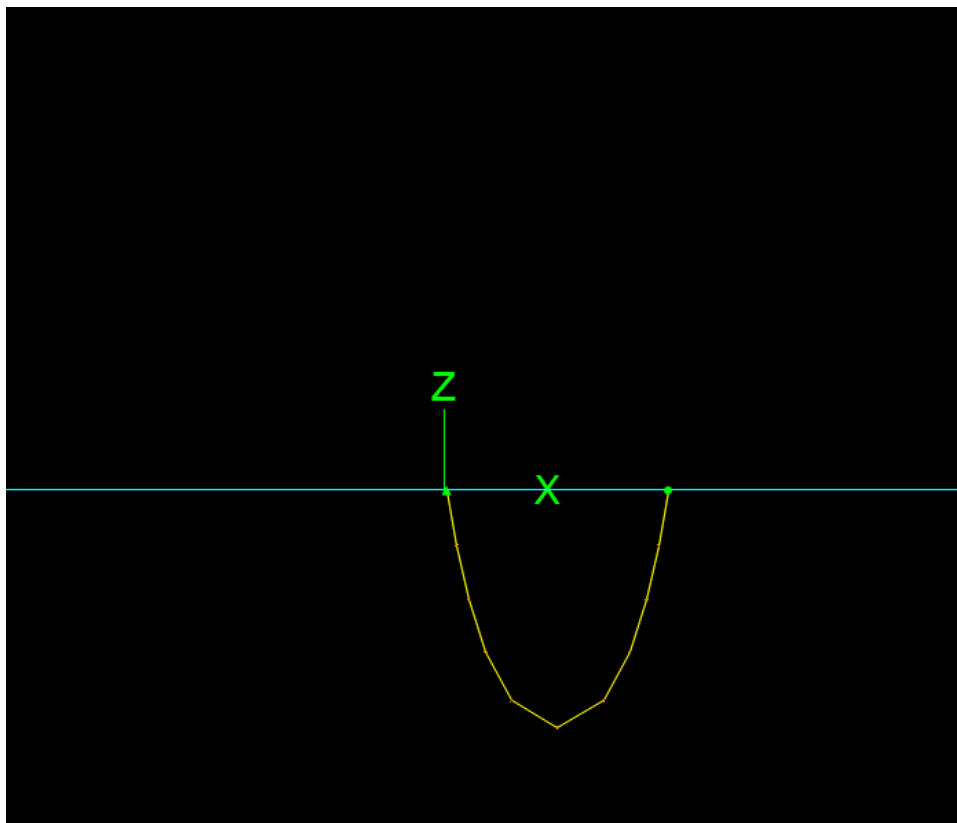


FIGURE 22: FIRST LINE POSITION

Here after, the user can drag the line around the screen to assign it to a new point or drag point B (right hand green point) to a different position. If we navigate to the control bar, we can now see that a new window with the text “Line1” has appeared.

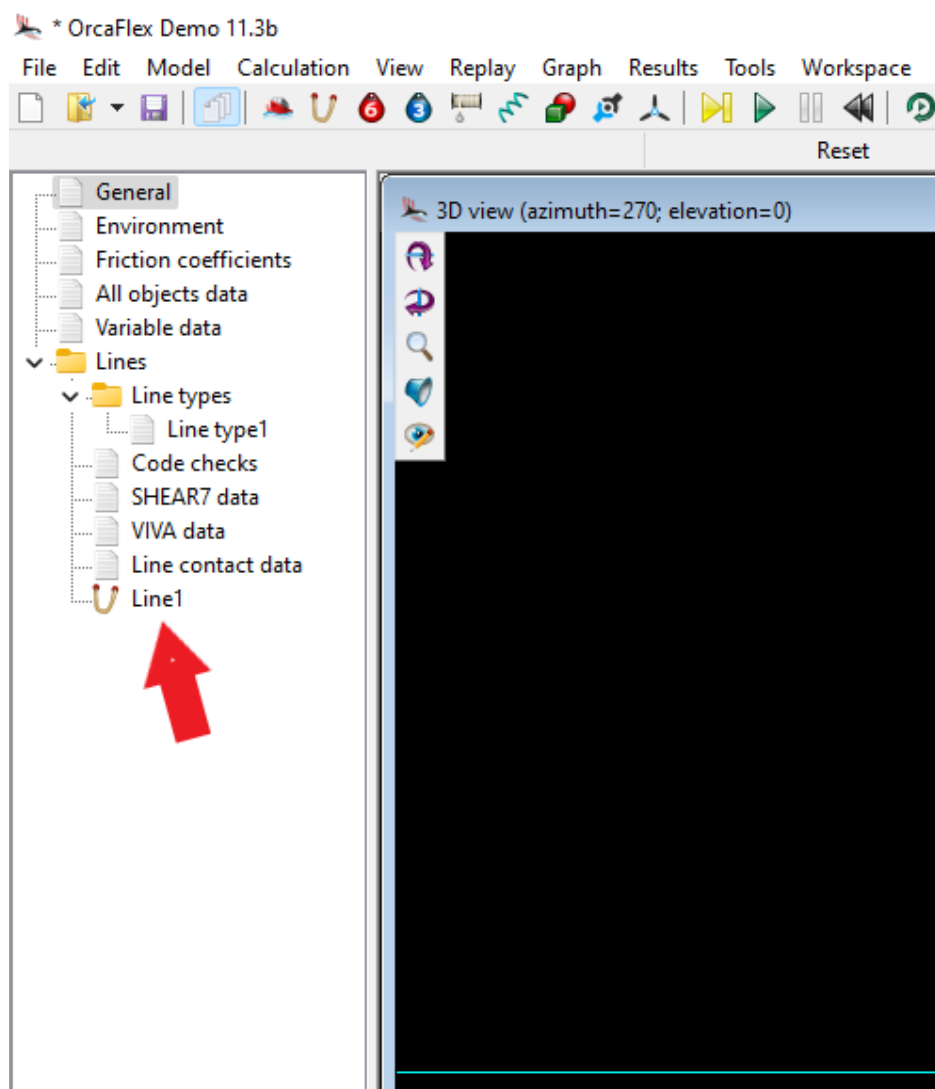


FIGURE 23: LOCATION OF LINE1

From here the user can double click on Line1 and edit length, segment length and number of segments or nodes, as seen below. We will edit the line length to be 150m. The user can also select between the three states previously mentioned, fixed, free, or anchored at point A and B respectively. In this guide we will select point B to be anchored, the line should now be fixed

to the orange line at the bottom of the screen. If this does not occur, the user can drag point B to the orange line.

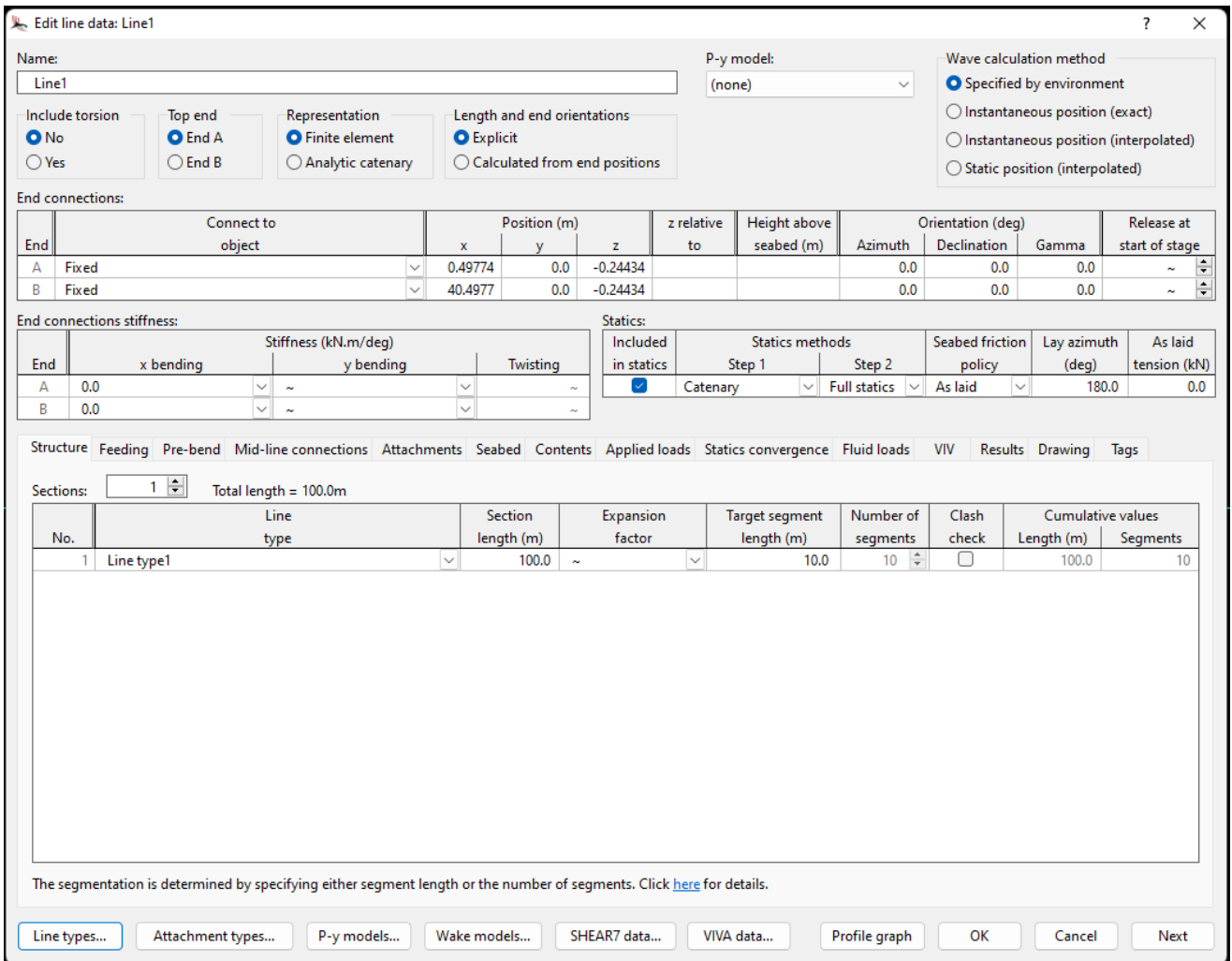


FIGURE 24: LINE EDITING

By selecting “Line types” in the bottom left corner, the user can then edit the outer and inner diameters of the line, mass per meter of line and the bulk modulus where necessary. The bulk modulus refers to the pressure increase in line where the volume decreases, but this value is usually a negligible factor as it usually refers to pipes dealing with pressures between 30,000psi and 300,000psi [24].

By now, the model should appear as follows:



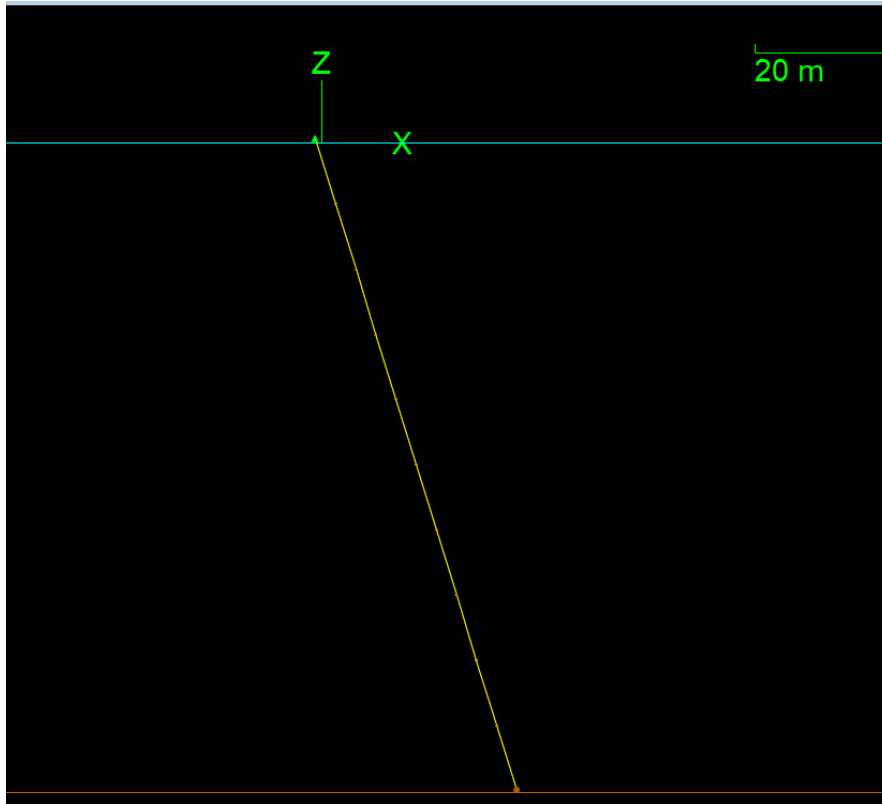


FIGURE 25: FIRST LINE ANCHORED

We will now proceed to the setup of the profiler. We will now choose the “6D buoy” option from the tool bar. We can place this buoy at any location on the screen for now. The control bar will now show “6D buoy1”, similarly to the “Line1” tab. By double clicking on “6D buoy1” we can set the properties and attachment points for this component.

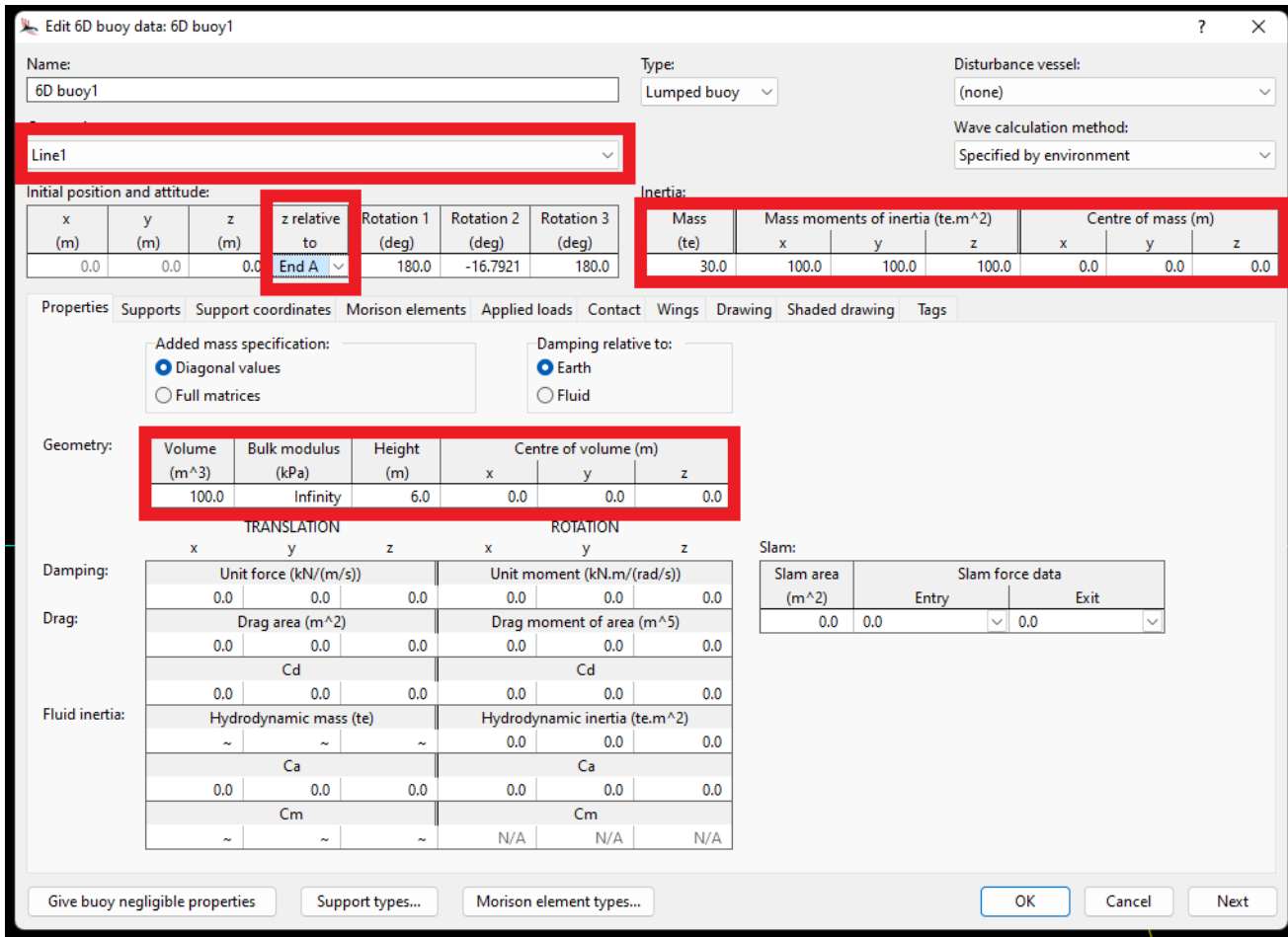


FIGURE 26: PROFILER PROPERTIES

The highlighted red boxes refer to which properties are the most important to edit. Here we can edit mass, the point at which the profiler is attached to, the state of the buoy and the volume and height of the profiler. Here we will change the state to be attached to Line1 (top red box), the point at which the profiler is attached to End A (left centre red box), the mass to 20 (right centre red box), the volume 20 and the height to 1 (bottom red box). We will also change the type of buoy to “Spar buoy” as it is a profiler we wish to model. The result should be as shown below.

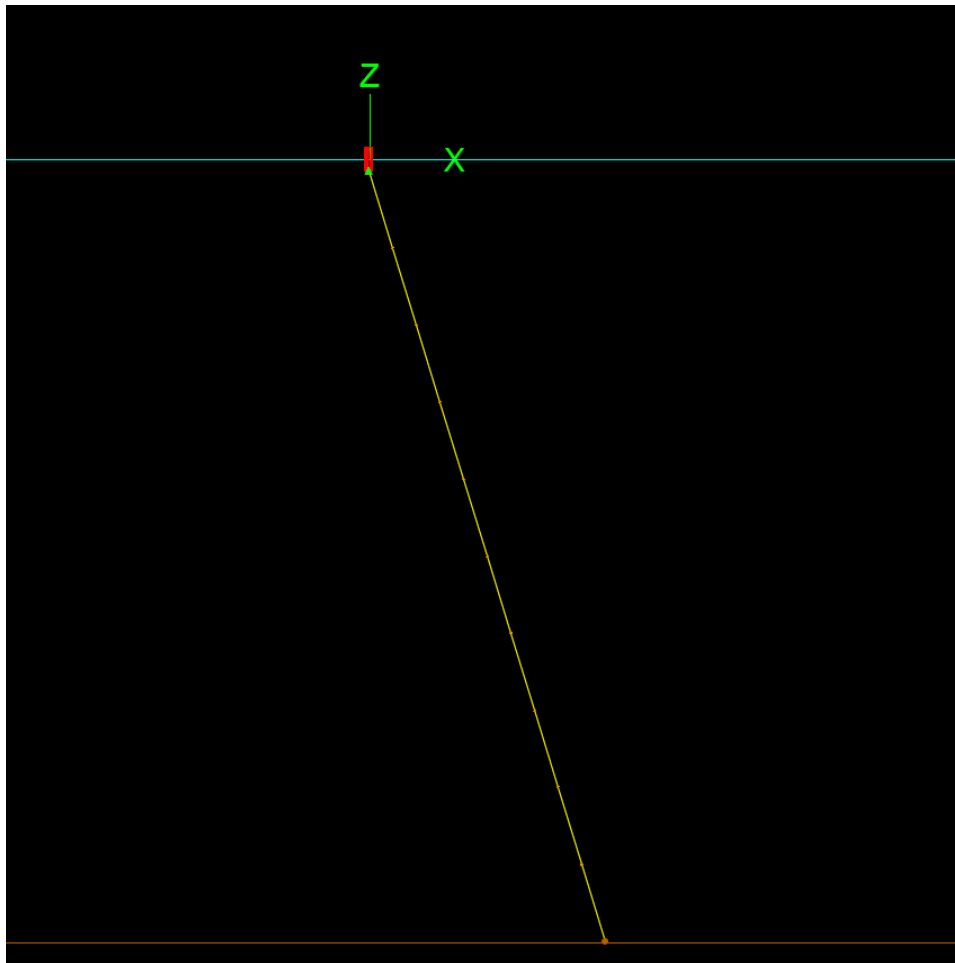


FIGURE 27: SYSTEM WITH BUOY

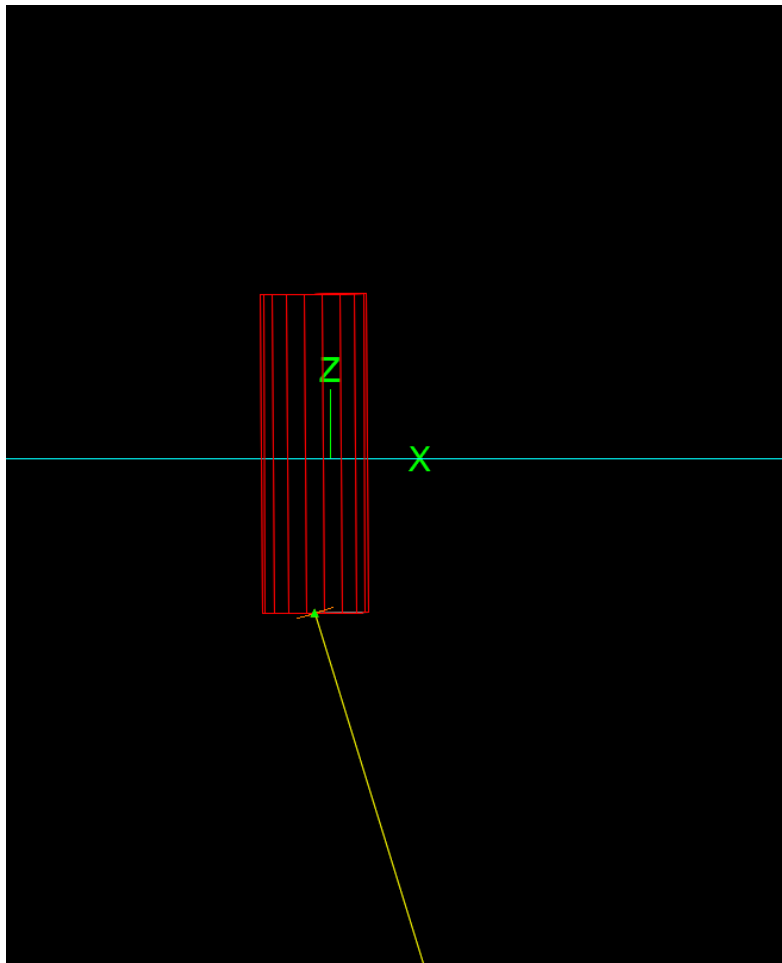


FIGURE 28: BUOY ZOOMED

As we can see, the system now shows a profiler at the sea surface attached to a line anchored to the seabed. As we have changed the volume and dimensions of the profiler, we can now see that it shows as a cylindrical geometry.

For added stability we will now attach a sub-surface buoy (SSB). This buoy will act similarly to the profiler but ultimately has the ability to float whilst being submerged, offering more stability to the system. It is not always necessary to add a sub-surface buoy in shallow waters, but in open waters where currents, wind and waves are a dynamic factor that effect the system, the user will generally require a sub-surface buoy. In this case, we will be adding a sub-surface buoy 15 metres from point A of the line. To do this, we will again double click on "Line1", from here we will navigate to "Attachment types", second from the left at the bottom of the window.

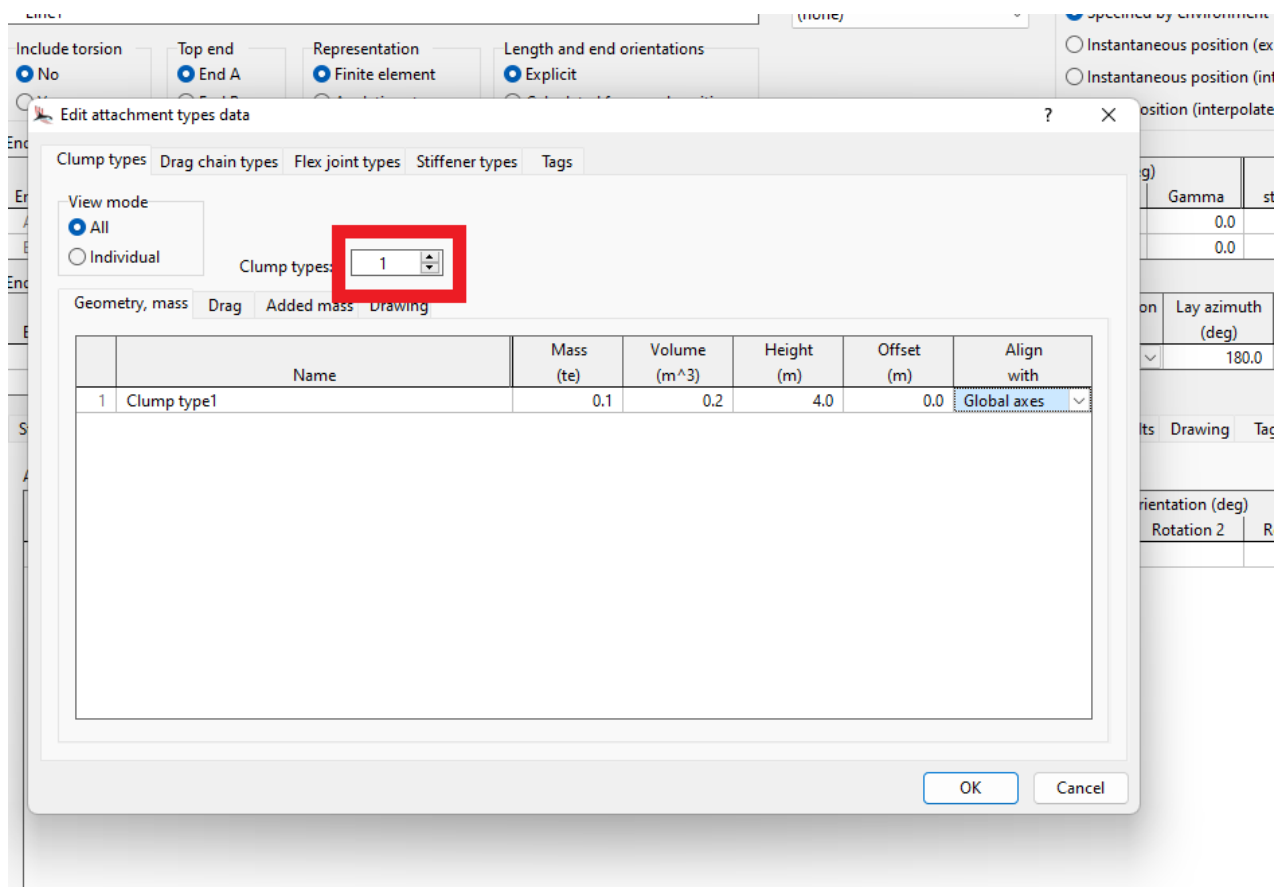


FIGURE 29: CLUMP WINDOW

From here, we will set the “Clump types” tally to 1 (or more depending on the simulation the user wishes to run) by clicking up on the arrow in highlighted red box. Here we can see that a new clump “Clump type1” in the window below. We will now change the mass, volume, and height of the clump to 20, 20 and 1, respectively, before clicking OK. The new clump or SSB will now be saved as “Clump type1”. We will now add the clump to the line by navigating to the attachment tab in the window.

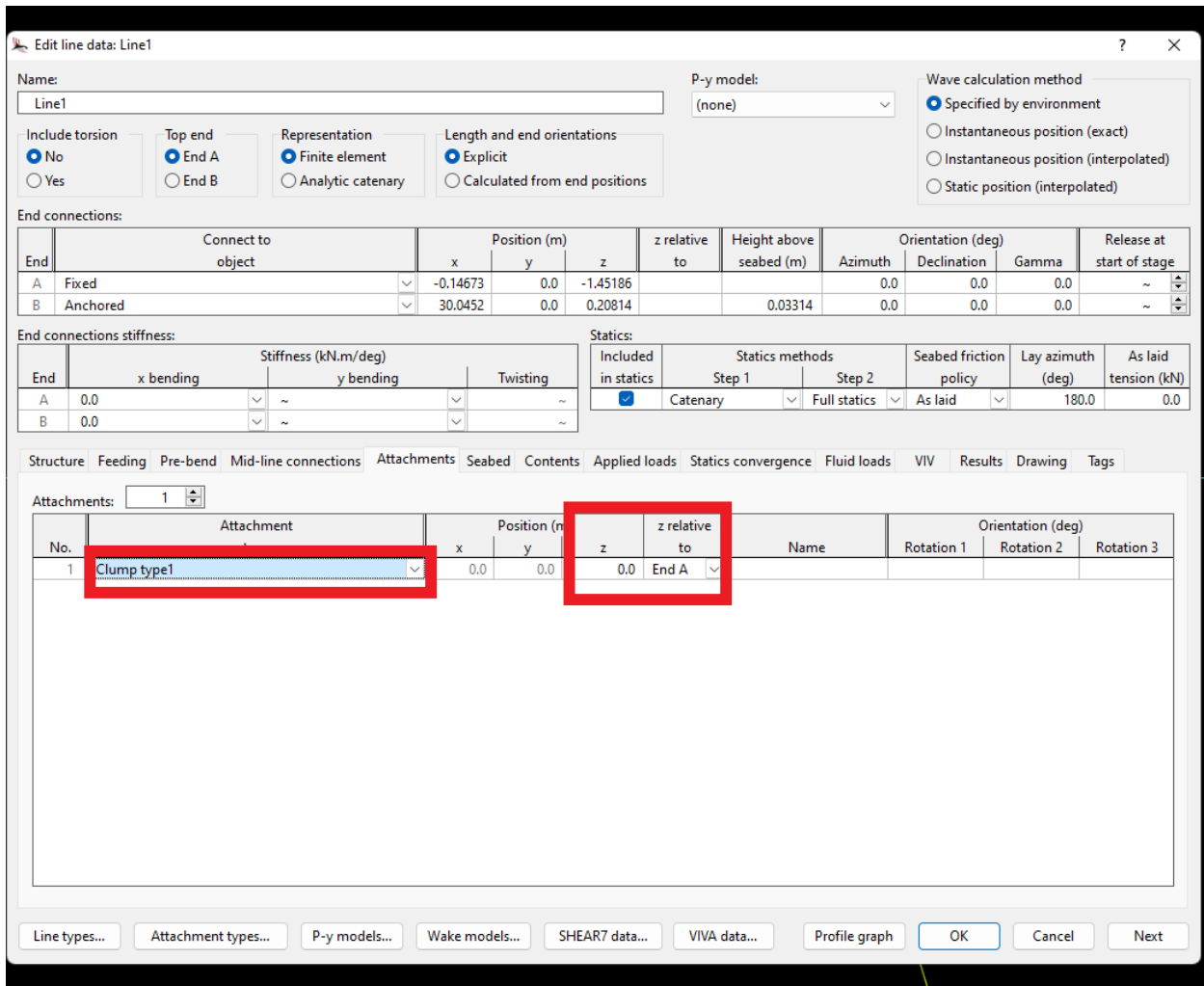


FIGURE 30: ATTACHMENT TAB

After finding the attachment tab we will click on the drop-down menu, highlighted in the red box, and select “Clump type1” and set the clump position relative to End A with a Z position set to 15. The model should now appear as shown below.

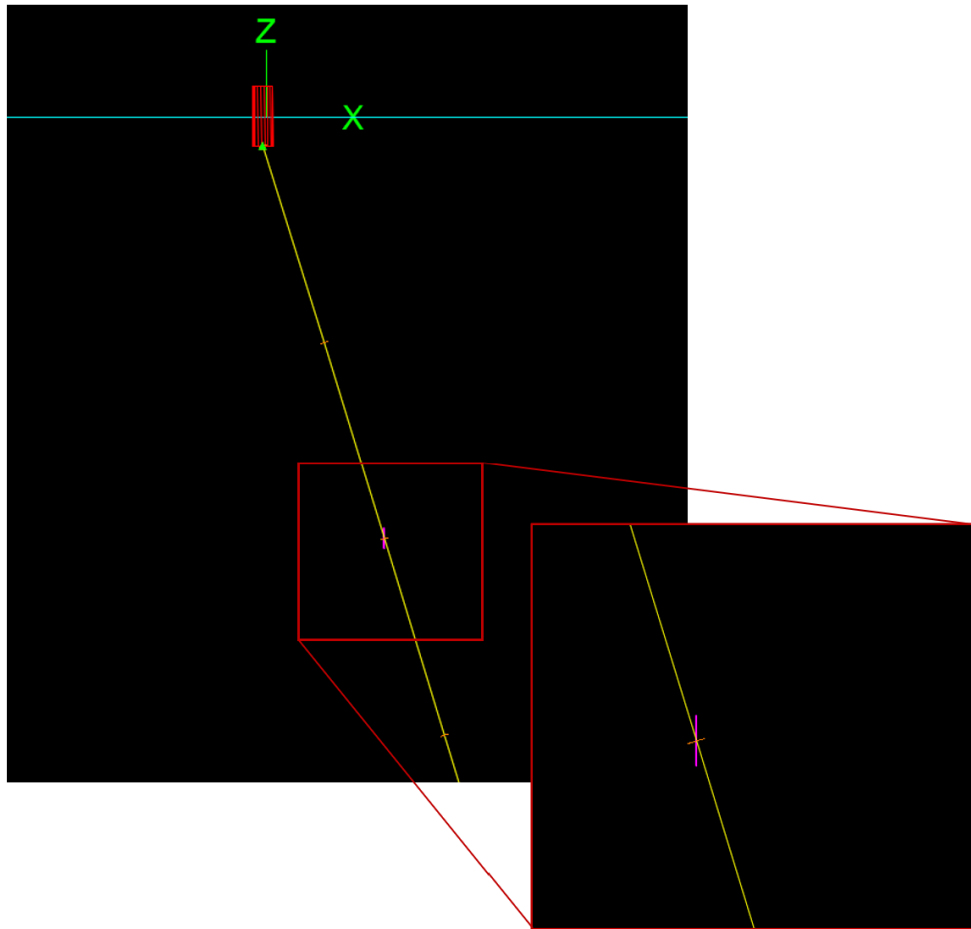


FIGURE 31: MODEL WITH SSB ADDED

The SSB is graphically represented by the purple geometry shown. We are now ready to run the simulation.

#### 4.5.10 Running a simulation

To run the simulation, we find the “Run dynamic simulation” button on the toolbar at the top of the window.

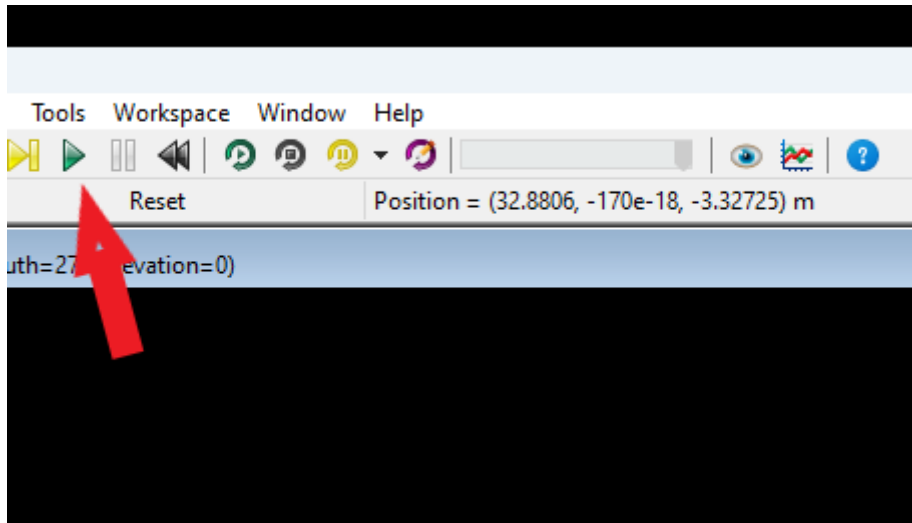


FIGURE 32: RUN SIMULATION BUTTON

By pressing this button, OrcaFlex will begin a simulation of the system. When the simulation is finished, the screen will return to a static state. To replay the simulation, the user can use the “Replay” button located three buttons to the right of the “Run” button the user has just used. The replay will then playback the simulation using the time period given in the default settings, again this setting is available for the user to change under the “General” tab in the control bar. The user can also toggle between a graphical and non-graphical view by using CTRL+G. The screen should now show as follows.



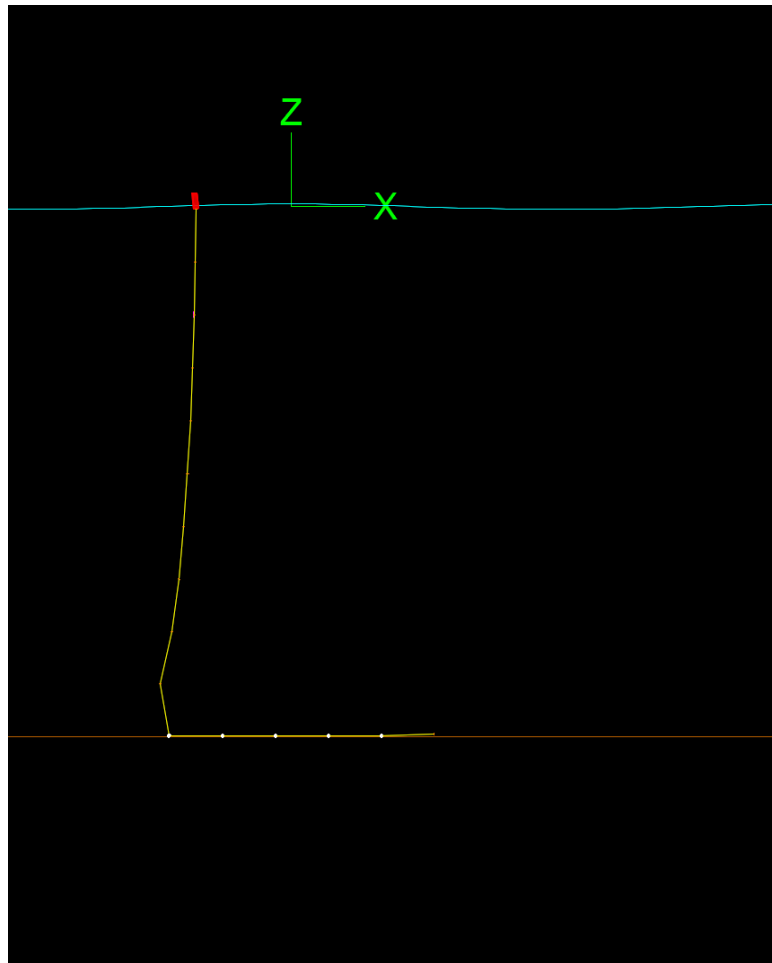


FIGURE 33: SYSTEM AFTER RUNNING SIMULATION

As we can see the profiler remained above the sea surface, but the lower part of the line drags along the seabed. This is normal practice for many mooring systems, but should the user wish to have minimal sea drag, the user can change the line length or add another line with a different length to satisfy the requirements of the system and run the simulation again.

#### 4.5.11 Post simulation

The user is now free to gather whatever information necessary by navigating to the “Results” tab at the top of the toolbar. After selecting “Select results” the user is met with the following window.

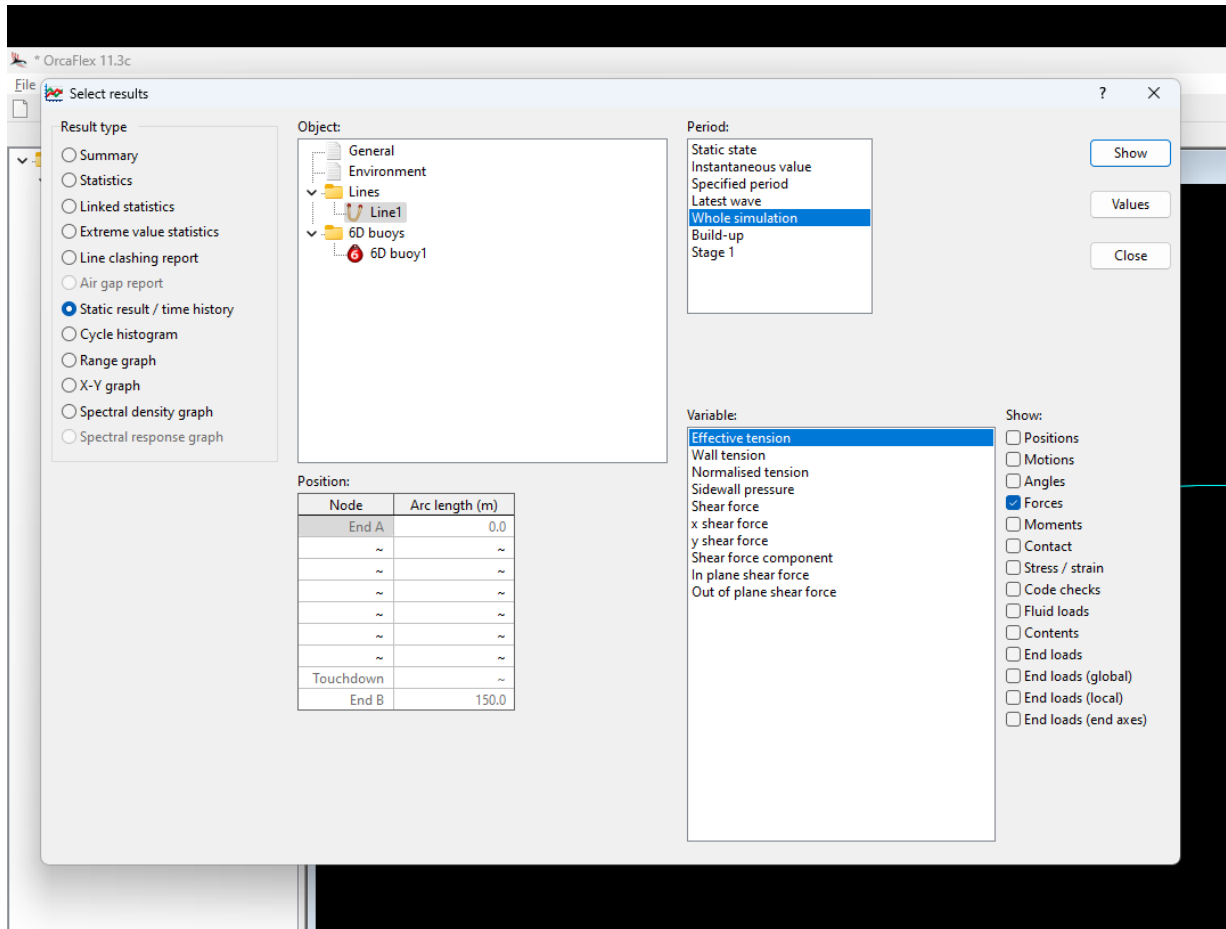


FIGURE 34: RESULTS WINDOW

The user can now select the object they wish to observe data for, the type of data and the period in which the data is outputted for. For instance, we have chosen the effective tension in Line1 at point A. After selecting the desired data set for the desired object, the user can press “Show” to display a graph of the chosen parameters.

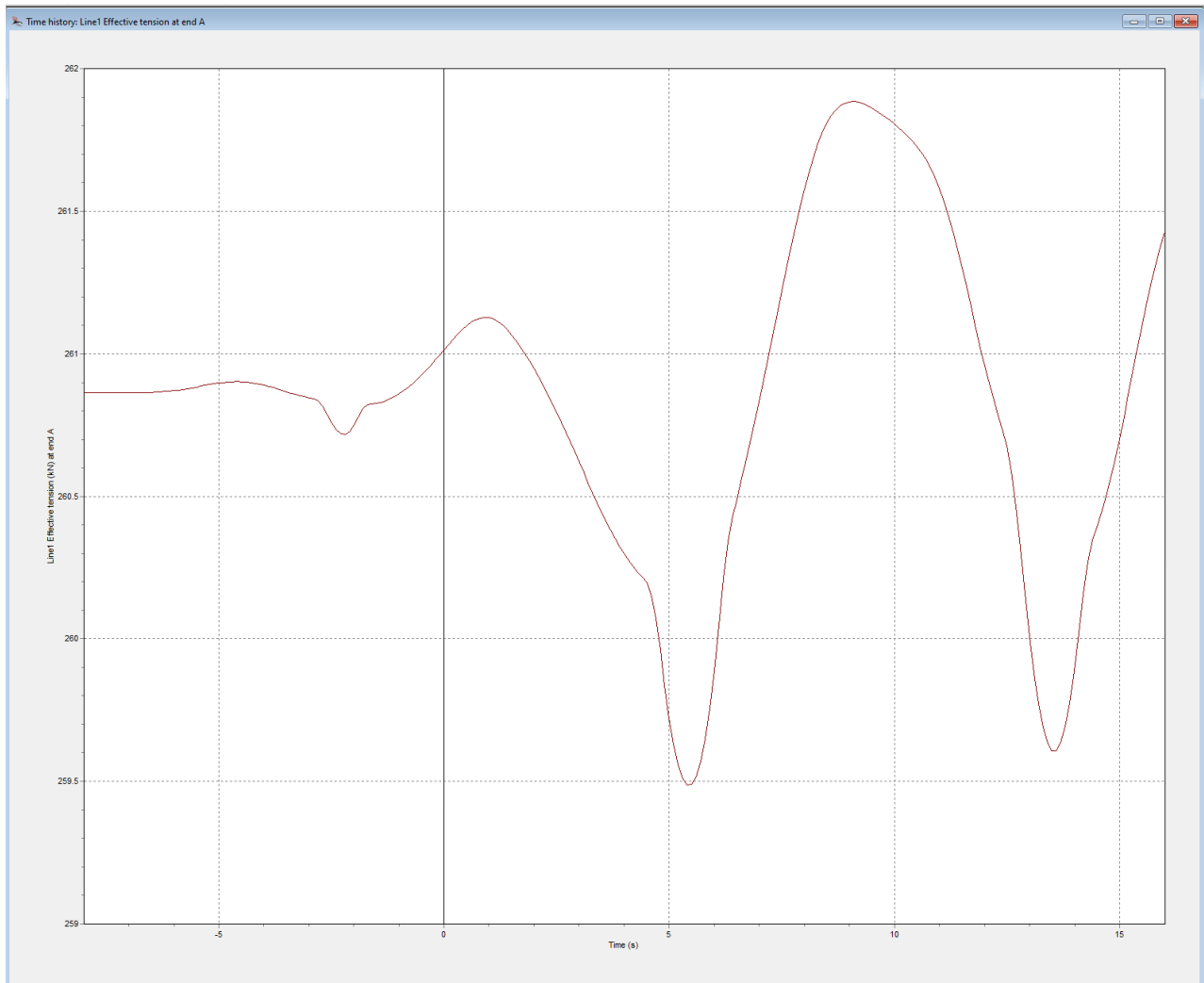


FIGURE 35: GRAPH SHOWING TENSION PLOTTED AGAINST TIME

This example graph shows tension at point A plotted against time for the whole simulation's time period. Here we can see an increase and decrease in tension at points where the waves oscillate, creating a contract and relax effect in the line, in which the pattern is shown on the graph, which concurs with the theoretical aspects of the system.

#### 4.6 Preliminary simulations

The goals in the preliminary stage of design were to ensure that the mooring system would provide adequate stability to ensure that the profiler, illustrated as a simple cylinder, would

remain afloat given a wide range of metocean conditions. Metocean conditions refers to wind, wave, current and climate at a specific location. i.e., ocean and weather conditions. Ideally, the profiler would have a stable motion pattern with minimal change in angle or declination, thus not disturbing the satellite communication device built into the profiler. This meant that ideally the very top of the profiler would not be in contact with water and the methods below aim to achieve this.

The preliminary stage consisted of multiple iterations of the mooring system where different parameters and system setups were tested against each other and compared, as well as obtaining knowledge about OrcaFlex. The preliminary simulations were based on an inverse catenary mooring, as deduced from the design and discussion process, as this was deemed to be the most fitting mooring system for the given conditions the system would experience. The mass of the profiler was 20 kg in every iteration and the mooring line in every system setup was attached to the profiler at end A at point  $p(0, 0, 0)$  on the 6D buoy, and anchored to the seabed at end B.

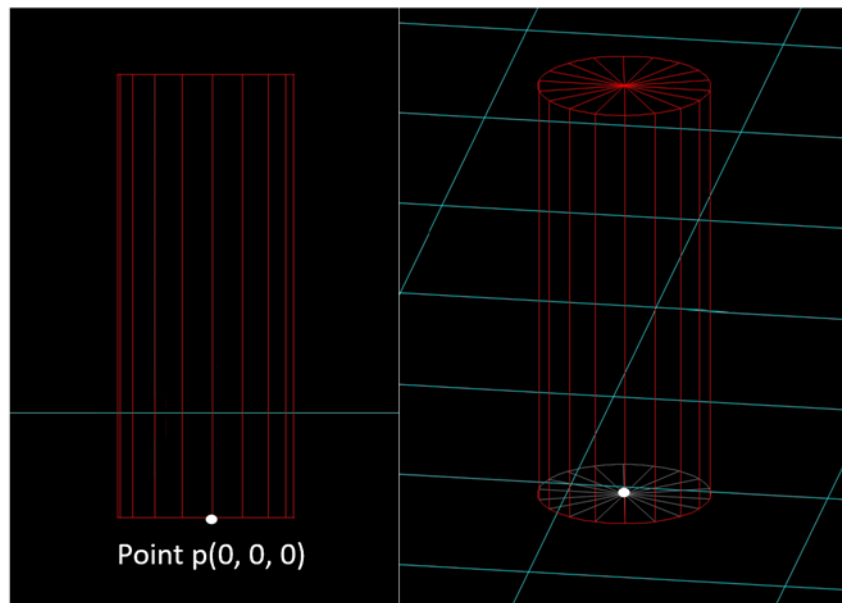


FIGURE 36: POINT P ON THE CYLINDER

The process of running the simulations is demonstrated in the flowchart below, see Figure 37.

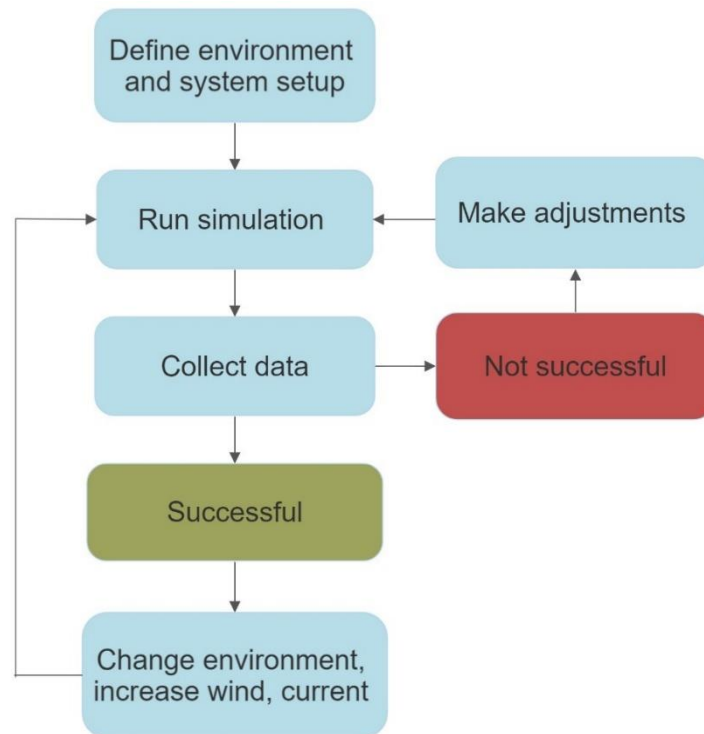


FIGURE 37: PROCESS OF RUNNING THE SIMULATIONS

We start by deriving some assumptions about the general environmental setup in OrcaFlex regarding the metocean conditions and system.

*Assumption 1.* The ocean current ( $V_c$ ) is constant through the whole water column and flow is always the same direction which is 180 degrees relative to global x – axis in positive direction.

*Assumption 2.* Wind speed and wind direction is constant at 180 degrees relative to global x-axis in positive direction.

*Assumption 3.* Wave height, frequency and period are constant.

*Assumption 4.* The mooring system experiences perfect waves through the simulations.

*Assumption 5.* The anker has infinite weight and will not fail, i.e., move.

*Assumption 6.* The connection between the mooring line and profiler will not fail.

The standard environmental conditions were defined as the following:

Parameter	Value	Unit	Symbol
Ocean depth	100	m	$D_o$
Water density	1025	Kg/m <sup>3</sup>	$\rho_w$
Kinematic viscosity	1.35e-6	m <sup>2</sup>	$\eta$
Ocean temperature	10	°C	$t$
Wave height	0.1	m	$h_w$
Wave period	12.5	ul	$T$
Ocean current (direction)	0.1 (180)	m/s (deg)	$v_c$
Wind speed (direction)	1.7 (180)	m/s (deg)	$v_w$
Time period	600	s	$T_{sim}$

TABLE 1: STANDARD ENVIRONMENTAL CONDITIONS

#### 4.6.1 First iteration

For the first iteration the main target was to obtain enough knowledge about OrcaFlex in order to achieve viable results. This section also includes a comparison of the effects a hollow section in an otherwise solid cylinder versus a completely solid cylinder would influence the mooring system.

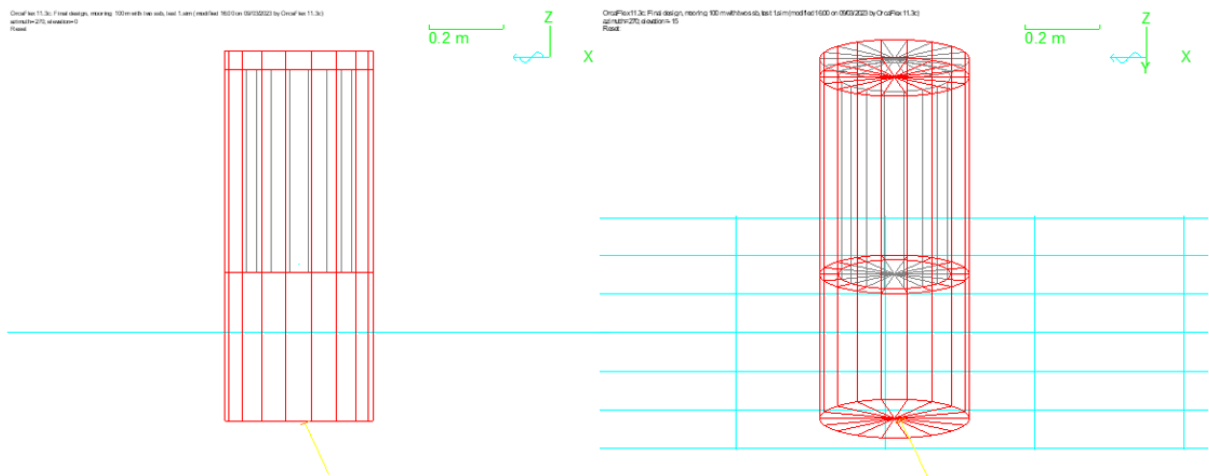
We start by defining the environment, see Table 1, and setting up a simple mooring system in OrcaFlex using a 6D spar buoy as a profiler and a default line. The hollow and solid buoys in the shape of cylinders, have the following dimensions and properties.

Cylinders	Outer diameter [m]	Inner diameter [m]	Length [m]	Cumulative length [m]
1	0.4	0.0	0.05	0.05
2	0.4	0.3	0.55	0.6
3	0.4	0.0	0.4	1.0

**TABLE 3: DIMENSIONS OF THE HOLLOW CYLINDER**

Cylinders	Outer diameter [m]	Inner diameter [m]	Length [m]	Cumulative length [m]
1	0.4	0.0	1.0	1.0

**TABLE 4: DIMENSIONS OF THE SOLID CYLINDER**



**FIGURE 38: ILLUSTRATION OF THE 6D SPAR BUOY WITH A HOLLOW SECTION**

The blue grid represents the ocean, and the yellow line represents the mooring line.

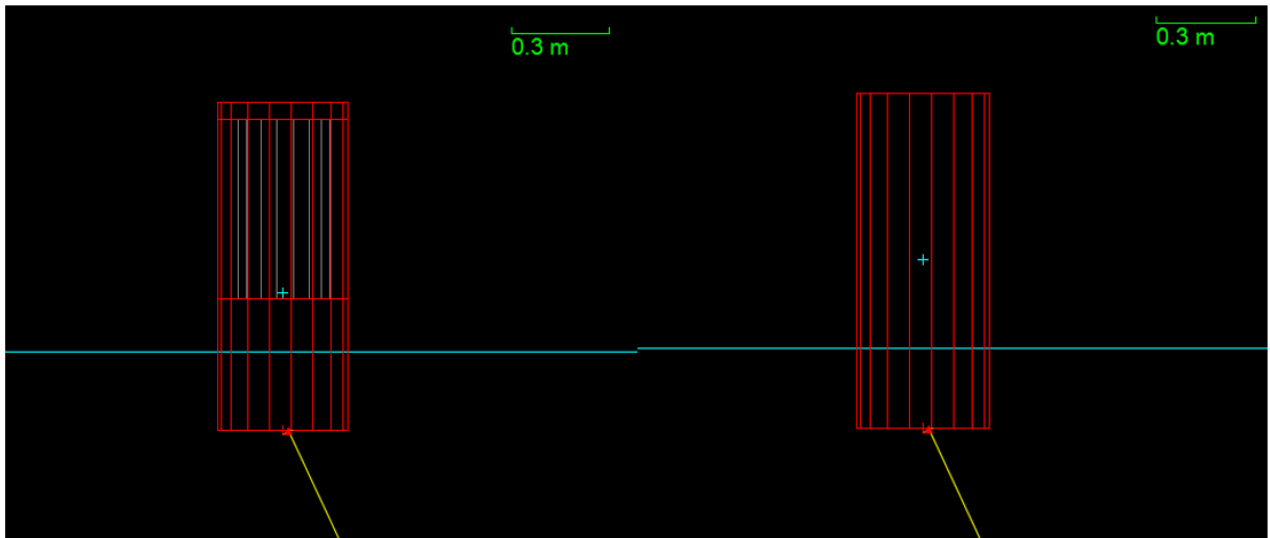


FIGURE 39: CENTRE OF GRAVITY IN THE HOLLOW AND SOLID CYLINDER RESPECTIVELY

To achieve a lower centre of gravity a hollow section in an otherwise solid cylinder was included in an attempt to achieve a greater average dry length. Notice how the hollow section affects centre of gravity and shifts it lower in the cylinder in Figure 39.

The default line in OrcaFlex has the following dimension and properties:

Material	Mass per unit length [kg/m]	Outer diameter [m]	Inner diameter [m]	Length [m]
Default	0.718	0.35	0.25	109

TABLE 5: DEFAULT LINE DIMENSIONS



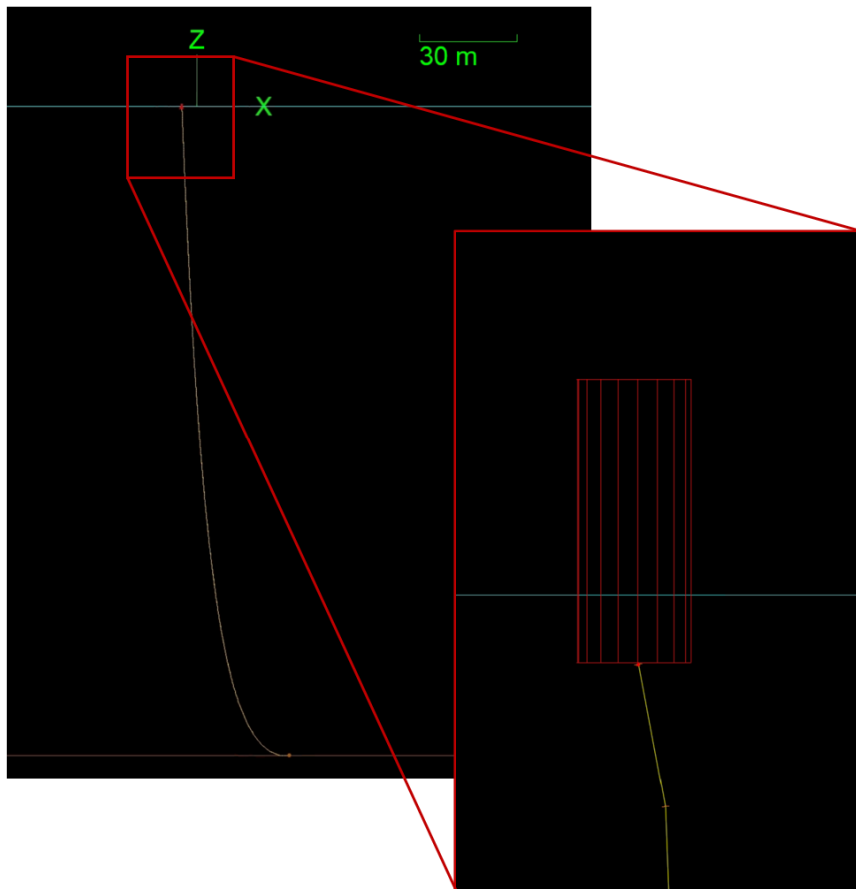
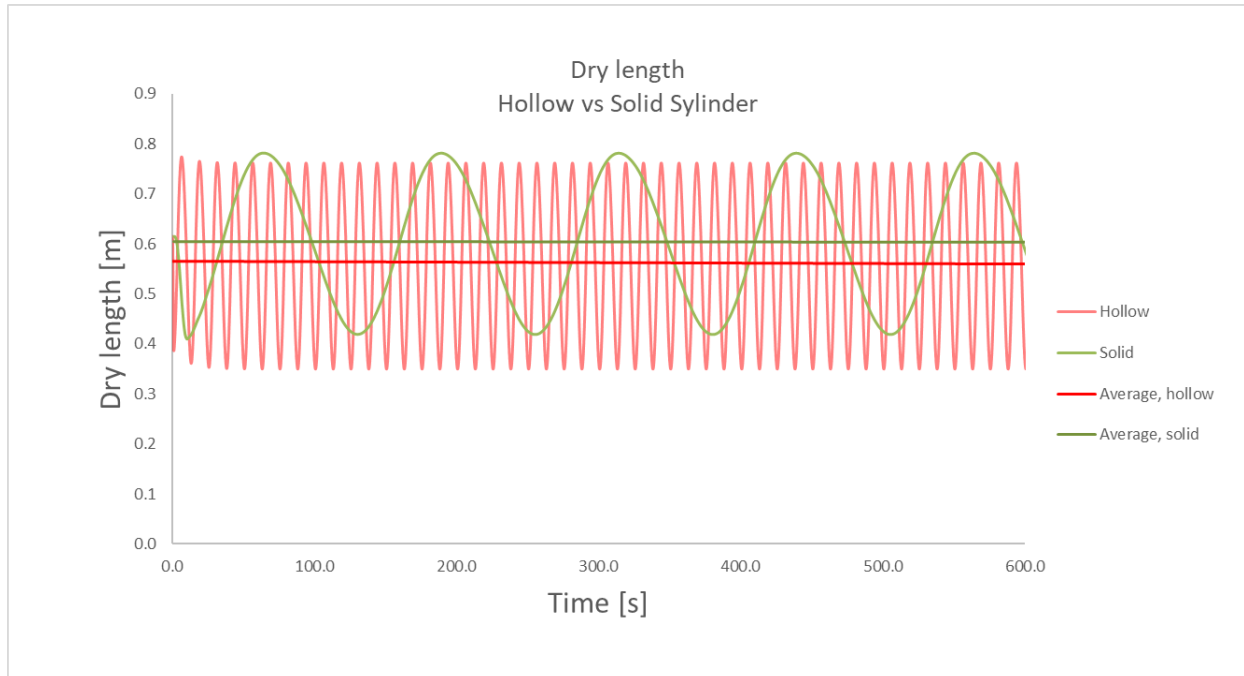


FIGURE 40: SYSTEM SETUP FOR THE FIRST ITERATION



**FIGURE 41: A COMPARISON IN THE DIFFERENCE IN DRY LENGTH BETWEEN A HOLLOW AND SOLID CYLINDER.**

From the graph in Figure 41, we experienced a somewhat surprising result. We initially expected to see a greater average dry length for the hollow cylinder since the centre of gravity is lower, but the opposite can be observed. The trend line for the solid cylinder is greater than the hollow one, although the difference is small with 0.04 m. The difference in movement along the global z – axis, or motion up and down is also very apparent, the solid cylinder appears to be more stable in the water as the graph does not oscillate as much.

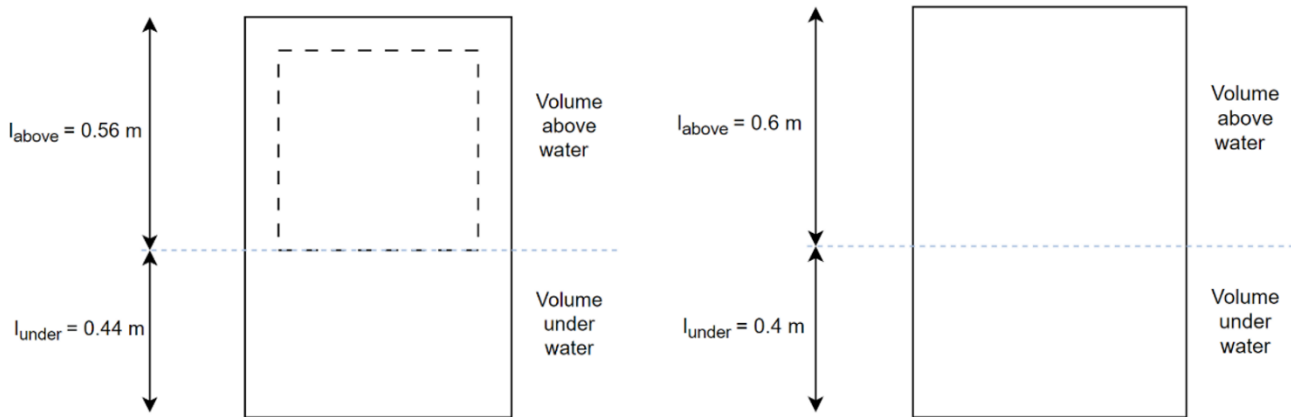


FIGURE 42: ILLUSTRATION OF THE DIFFERENCE IN DRY LENGTH.

Where  $L_{\text{above}}$  is the length of the cylinder above water and  $L_{\text{under}}$  is the length under water.

A hollow section in the cylinder did not contribute to a greater average dry length but did rather the opposite, furthermore it also contributed to less stability. Further preliminary simulations consisted of a 6D spar buoy with the geometry of the completely solid cylinder as profiler.

#### 4.6.2 Second iteration

The second iteration built on the first iteration but consisted of a more complex system setup. The main objective for the second iteration was to test out the mooring system in different ocean conditions and obtain knowledge about its strengths and weaknesses. Multiple simulations with variations in metocean conditions, see Table 6, were performed and results of interest were the motion pattern, dry length, declination and Morison's force, along with visual impressions.

Three simulations/tests for the same system setup were performed using the following metocean conditions in Table 6.

	Waves [m]	Current [m/s]	Wind [m/s]	Period [s]	Time [s]
<b>Test 1</b>	0.1	0.1	1.7	12.5	600
<b>Test 2</b>	0.5	0.5	2.0	12.5	600
<b>Test 3</b>	1.0	1.0	2.3	12.5	600

TABLE 6: METEOCEAN CONDITIONS

We start of by setting up a more complex mooring system in OrcaFlex using a 6D spar buoy as profiler, a user defined line and two subsurface buoys. The dimensions and properties of the 6D spar buoy are identical to the solid cylinder from first iteration. The subsurface buoys are attached to the line, subsurface buoy 1 is attached halfway up the line relative to end B, or seabed, and subsurface buoy 2 is attached 10m below the surface or End A.

The line, which is a default nylon line in OrcaFlex, has the following dimensions and properties:

Material	Mass per unit length [kg/m]	Diameter [m]	Length [m]
Nylon (8 strand)	0.582	0.0255	108

TABLE 7: NYLON DIMENSIONS

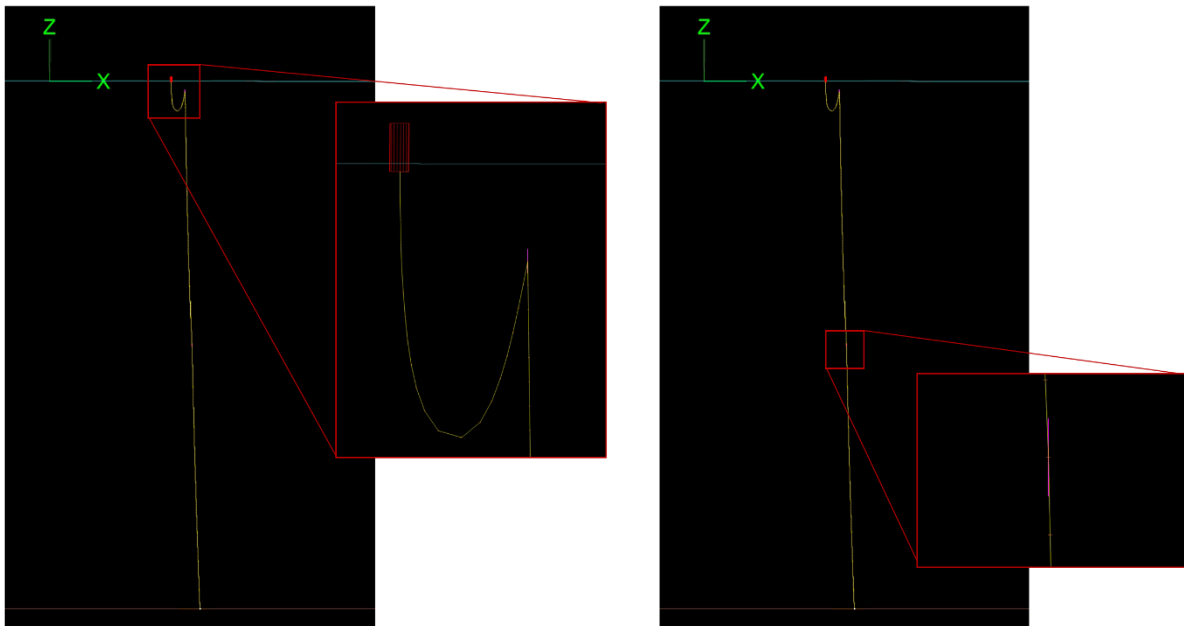


FIGURE 43: SYSTEM SETUP IN 2D VIEW, TO THE RIGHT IS SSB 1 AND TO THE LEFT IS SSB 2

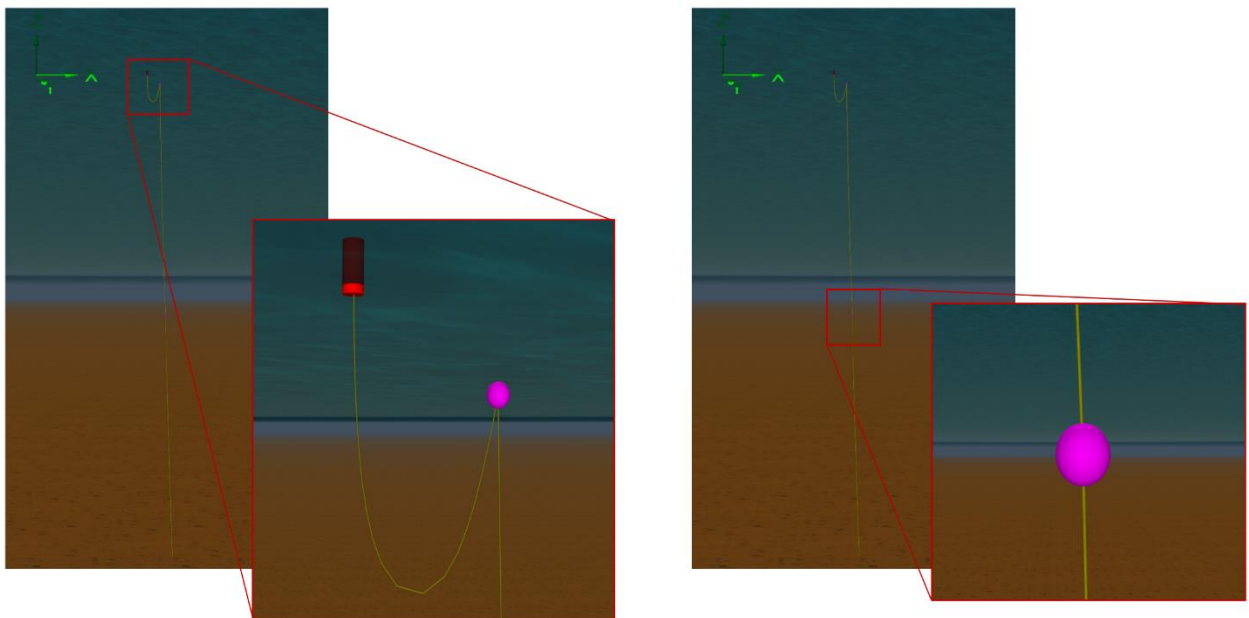


FIGURE 44: SYSTEM SETUP IN 3D VIEW, TO THE RIGHT IS SSB 1 AND TO THE LEFT IS SSB 2

Results of interest included buoyancy, motion pattern, dry length, declination, Morisons force and tensile strength, along with visual impressions.

The buoyancy and weight of the profiler and mooring line were constant for all tests as shown in Table 8.

	Profiler	Line including attachments	Total [kN]
Weight [kN]	0.196	0.760	0.956
Buoyancy [kN]	1.263	0.567	1.830

TABLE 8: BUOYANCY AND WEIGHT VALUES

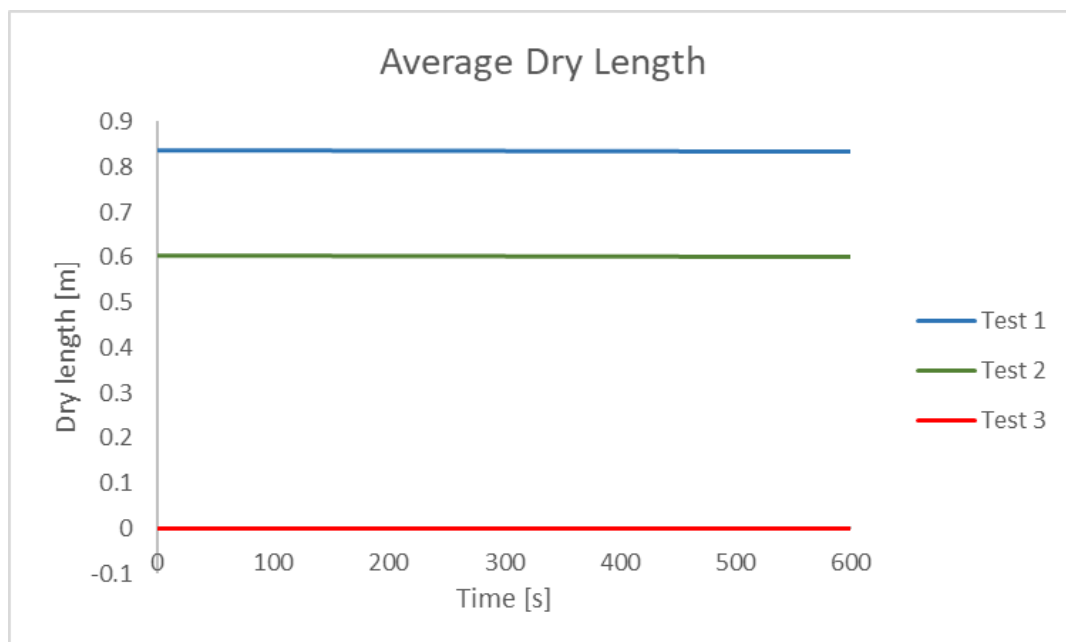


FIGURE 45: AVERAGE DRY LENGTH

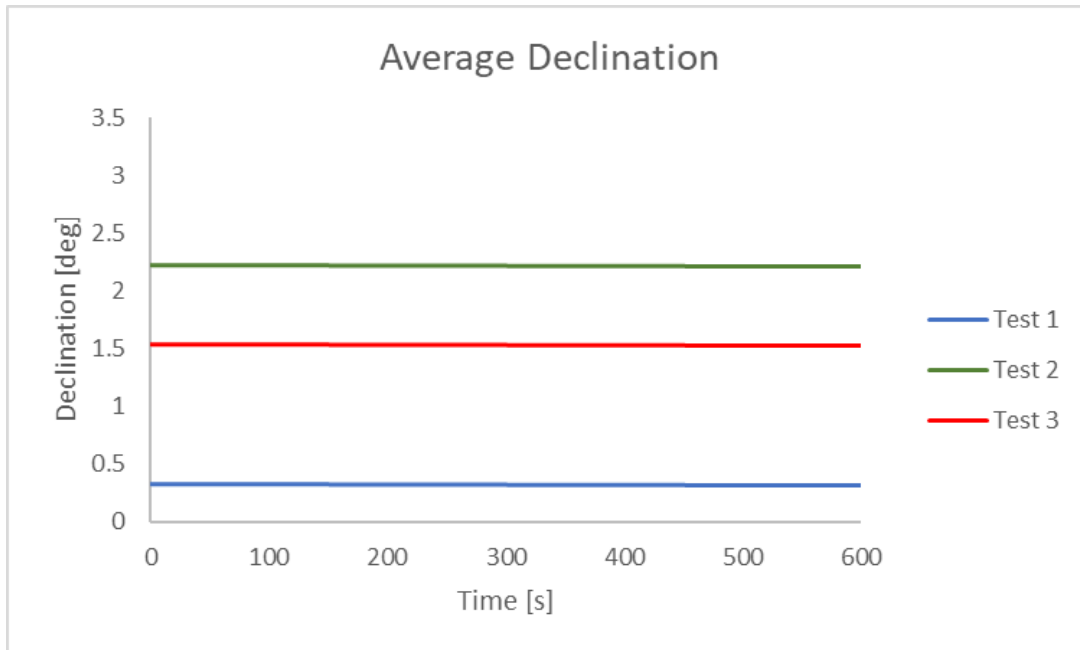


FIGURE 46: AVERAGE DECLINATION

Figures 45 and 46 show the average dry length and declination respectively, for all three tests.

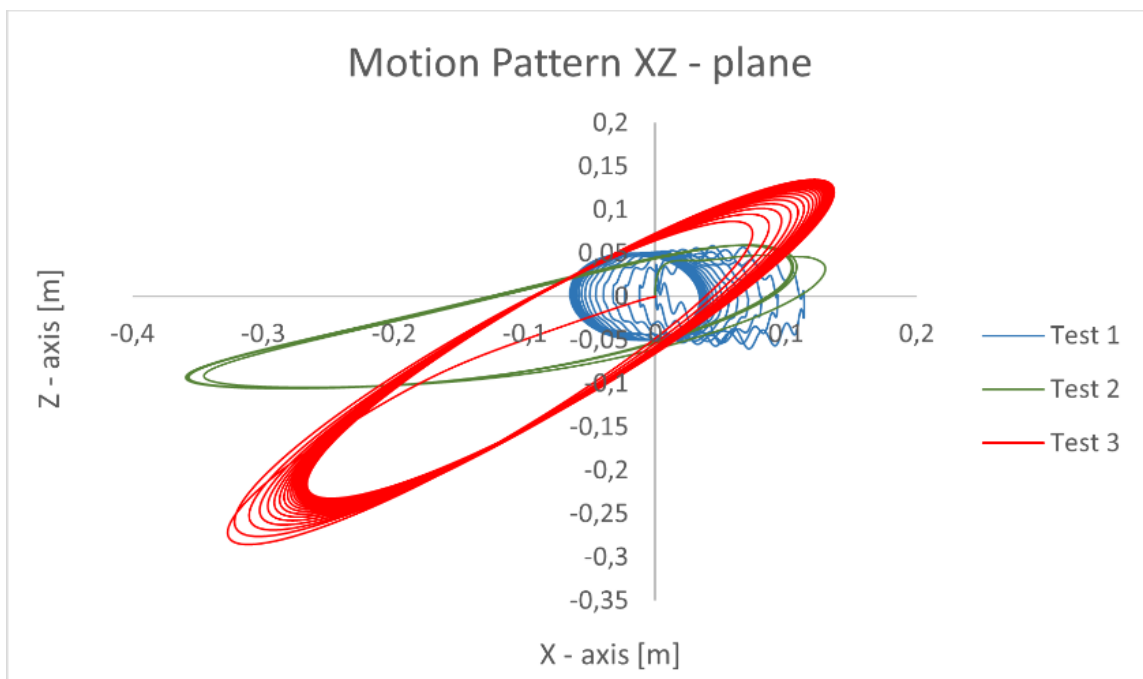


FIGURE 47: MOTION PATTERN XZ-PLANE

Figure 47 show the profilers motion pattern for each test in the XZ – plane.

Test 1 had the greatest dry length but was the most unstable. When looking at the graph for motion pattern XZ – plane, Figure 47, the profiler in Test 1 oscillates significantly more in comparison with Test 2 and Test 3 but did not move over such a large area. The declination and dry length values in Test 1 and Test 2 were also observed to fulfill the requirements set in the task brief. However, Test 3 was not successful as the dry length was zero, meaning the profiler was dragged completely under water.

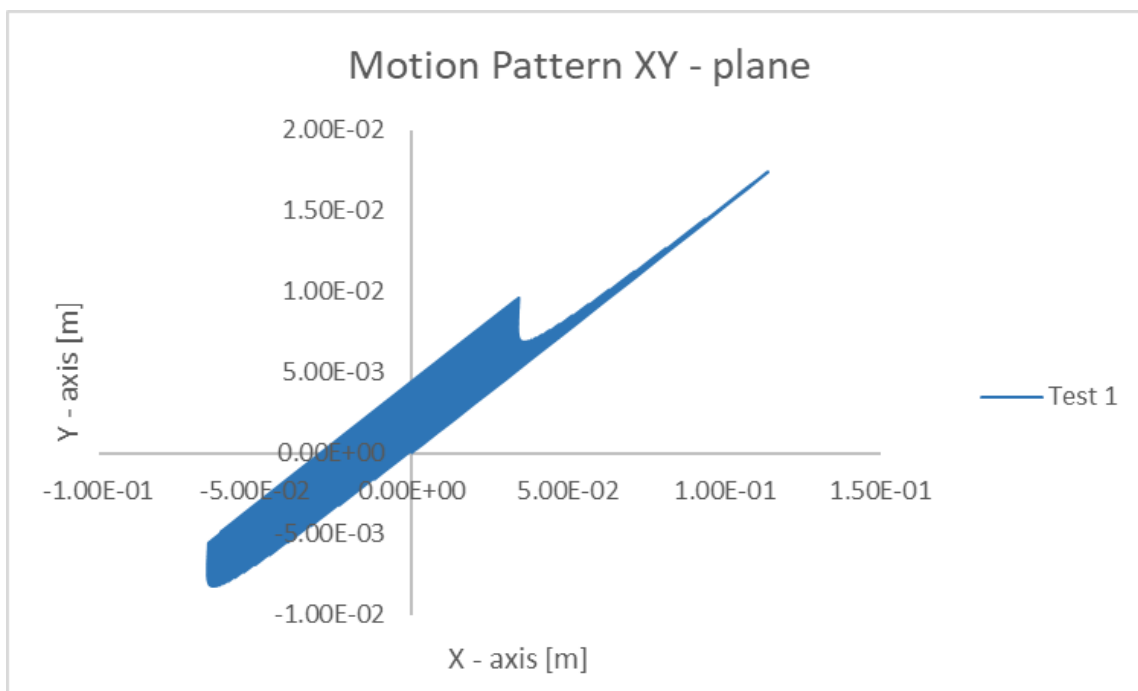
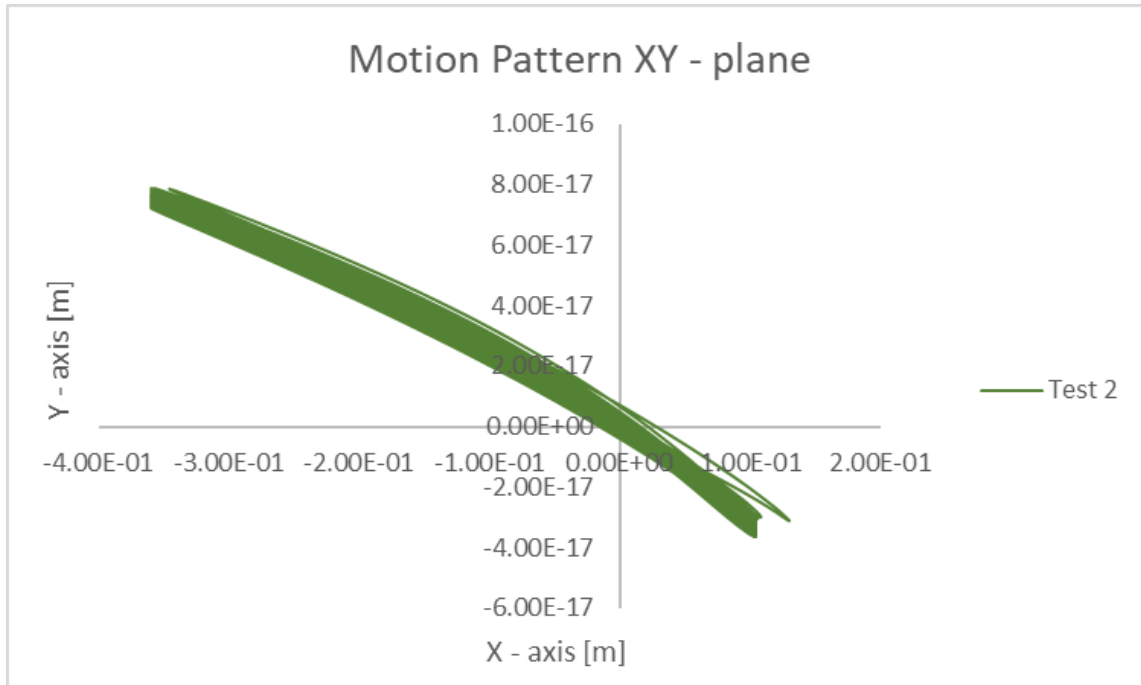
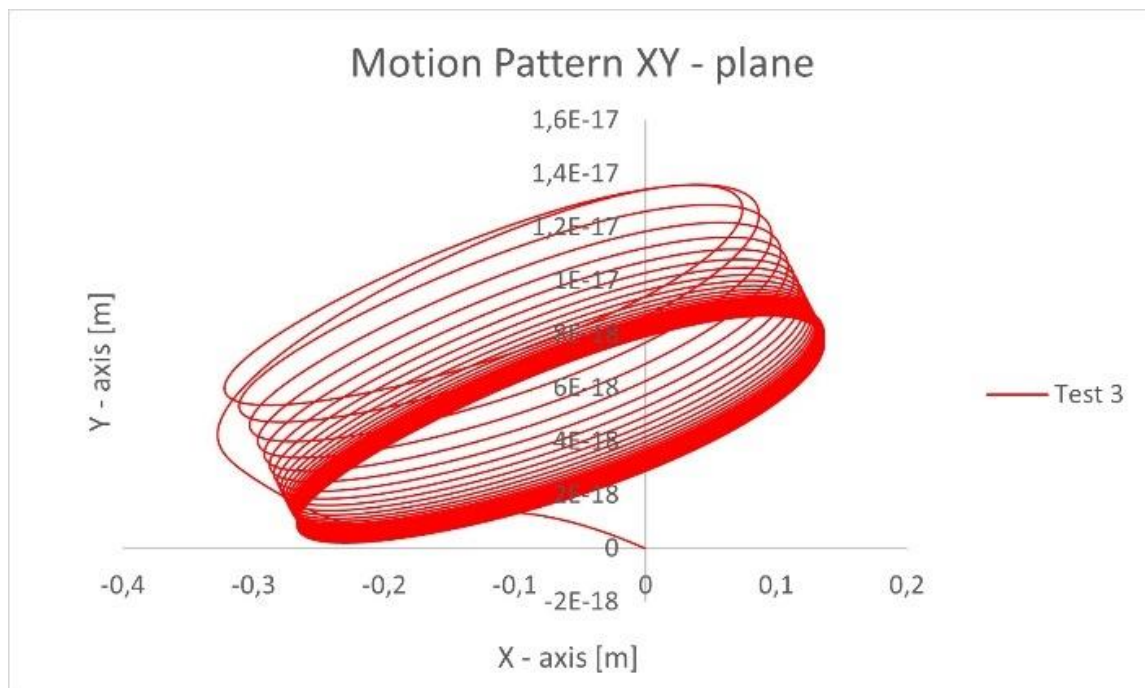


FIGURE 48: MOTION PATTERN XY – PLANE FOR TEST 1





**FIGURE 49: MOTION PATTERN XY – PLANE FOR TEST 2**



**FIGURE 50: MOTION PATTERN XY – PLANE FOR TEST 3**

Figures 48, 49 and 50 show the profiler's motion pattern in the XY – plane, or how the profiler moves as seen from above.

Test 1 and Test 2 have a similar motion pattern where the profiler moves linearly back and forth, whereas the profiler in Test 3 moves in a harmonic circular pattern, although under water. The motion pattern in both the XZ – and XY – plane for all three tests show a level of predictability and help forecast the movement of the profiler after 600 seconds. On the other hand, the metocean conditions defined in OrcaFlex are constant throughout the entire simulations making them not as realistic as possible but rather give an indication of how the mooring system would possibly behave.

The mooring line in Test 1 was prone to folding back on itself due to the low current, at the line segment where the SSB is attached the line bended more than 160 degrees. This may result in tangling and cause damage to the line. In addition to this, the top subsurface buoy (SSB 2) was approximately 2 m under the water line which may limit the effect it has on the system stability as a whole, as it is very close to the profiler. The line in Test 2 did not have much slack in the upper section, meaning the profiler was vulnerable to being completely submerged, as observed in Test 3, where the profiler was dragged 14m under the surface.

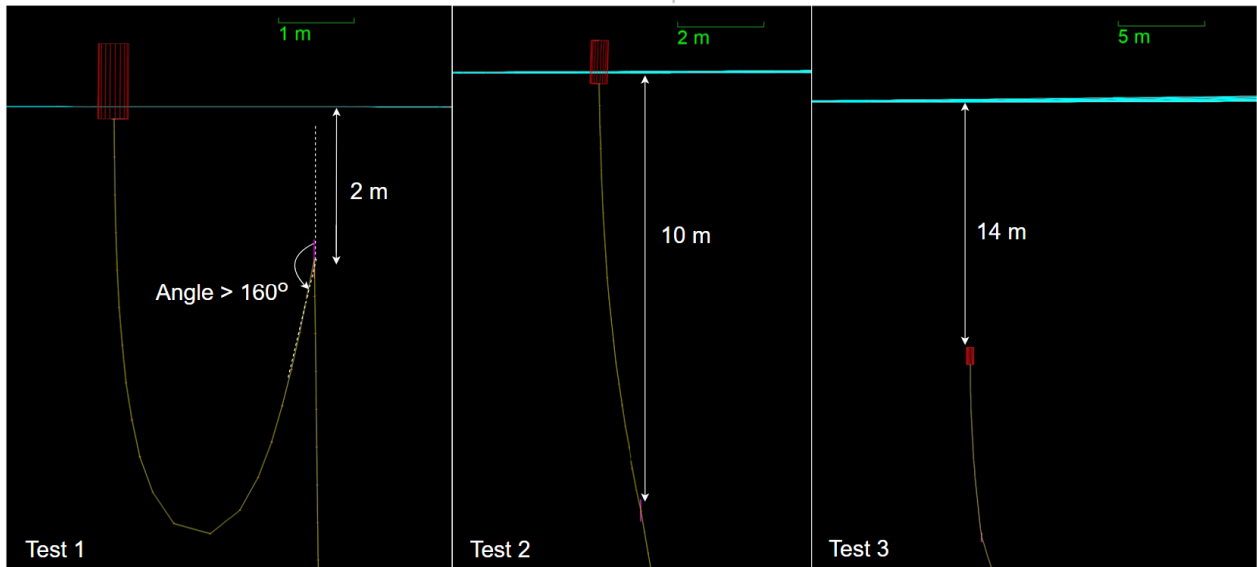


FIGURE 51: TEST COMPARISONS

Morison's equation is an equation that relates the force exerted on a body by a fluid flow to the velocity and acceleration of the fluid flow and takes into account the fluid flow force, along with the drag force and the added mass force [5].

Morison's equation is defined as

(EQUATION 5)

$$f = (\Delta a_f + C_a \Delta a_r) + \frac{1}{2} \rho C_d A |v_r| v_r$$

A mooring system will keep afloat providing that the following simplified equation using Morison's force is satisfied. The buoyancy force should be larger than the sum of Morison's force per unit length and the force of gravity acting on the system. This will be referred to as the following equality.

(EQUATION 14)

$$F_b > f_m L + G$$

Where  $F_b$  is the total buoyancy of the system,  $f_m$  is Morison's force,  $L$  is the line length and  $G$  is the total force of gravity.

	Maximum Morisons Force $M_f$ [kN/m]	Maximum tensile stress [kN]
Test 1	0.000171	0.643
Test 2	0.00732	0.783
Test 3	0.0183	1.089

TABLE 9: TABULATED MAXIMUM MORISONS FORCE AND TENSILE STRESS

In the table above, we have recorded the Maximum Morison's Force and Maximum tensile stresses for tests 1, 2 and 3 respectively. The ultimate strength of nylon is listed as 45-90MPa or 4.5-9·10<sup>6</sup>MPa and as we can see from the table above, each test was comfortably within the breaking stress value for the chosen line material [25]. As we can see from the table above, each test was comfortably within the breaking stress value for the chosen line material.

The calculations from each test regarding this equality are shown below.

For test 1 we obtain

$$F_b > f_m L + G$$

$$1.830 \text{ kN} > 0.000171 \frac{\text{kN}}{\text{m}} * 108 \text{ m} + 0.956 \text{ kN}$$

$$1.830 \text{ kN} > 0.974 \text{ kN}, \text{ ok}$$

For test 2 we obtain

$$F_b > f_m L + G$$

$$1.830 \text{ kN} > 0.00732 \frac{\text{kN}}{\text{m}} * 108 \text{ m} + 0.956 \text{ kN}$$

$$1.830 \text{ kN} > 1.746 \text{ kN}, \text{ ok}$$

For test 3, which was not successful, we obtain

$$F_b > f_m L + G$$

$$1.830 \text{ kN} > 0.0183 \frac{\text{kN}}{\text{m}} * 108 \text{ m} + 0.956 \text{ kN}$$

$$1.830 \text{ kN} < 2.932 \text{ kN}, \text{ fail}$$

The mooring system in the given metocean conditions for Test 1 and Test 2 did not experience a resultant force greater than the systems' total buoyancy and therefore stayed afloat. The environmental conditions in Test 3 resulted in a greater Morison's force and a greater resultant force and the system therefore failed.

Test 1 and Test 2 were both "Successful" whereas Test 3 was marked as "Not successful".

This was due to the dry length being less than the required value after the system experienced a greater resultant force than the total buoyancy.

The mooring system for the second iteration proved to be successful for the metocean conditions in Test 1 and Test 2 but failed for Test 3, where the system experienced a greater current than it could withstand which resulted in the profiler being submerged 14m below the surface. The ocean current appears to be the parameter which affects the system the most as it induces a greater Morison's force.

#### 4.6.3 Third iteration

The third iteration of the mooring system consisted of a 6D spar buoy with no hollow section, only one subsurface buoy and a user defined line. Unlike previous iterations where the main objective was to achieve a significant dry length, this iteration focused heavily on controlled buoyancy and user friendliness, meaning the entire system should ideally be deployed by one person. This factor affects the maximum volume of the subsurface buoy and total weight of mooring line.

The goal for this iteration was to achieve a net buoyancy of approximately 15 N as this was a new requirement from Oceanlab along with the preference of only one relatively small SSB. The requirement of 50% dry length was also changed to larger than 0%. This was achieved by defining the volume and dimensions of the cylinder in order to accomplish said buoyancy as

the mass was already given at 20 kg. If the weight of the mooring line is neglected, the following equations can be derived.

(EQUATION 6)

$$F_b = \rho g V$$

I:

$$F_b - mg = 15 \text{ N}$$

$$F_b - 20 \text{ kg} * 9.81 \frac{\text{m}}{\text{s}^2} = 15 \text{ N}$$

$$F_b - 196.2 \text{ N} = 15 \text{ N}$$

$$F_b = 211.2 \text{ N}$$

II:

$$F_b = \rho g V$$

$$F_b = 1025 \frac{\text{kg}}{\text{m}^3} 9.81 \frac{\text{m}}{\text{s}^2} * V$$

By substituting the value of  $F_b$  in Equation II we determine the volume of the cylinder which is submerged underwater.

II:

$$F_b = \rho g V \Rightarrow V = \frac{F_b}{\rho g}$$

$$V = \frac{211.2 \text{ N}}{1025 \frac{\text{kg}}{\text{m}^3} 9.81 \frac{\text{m}}{\text{s}^2}}$$

$$V = 0.021 \text{ m}^3$$

$$V = 21 \text{ L}$$

$V$  represents the volume of the cylinder which is submerged under water and not the total volume, i.e., the volume of the displaced water. 15 N represents the mass of the remaining theoretical displaced water and through the 1:1 relationship between volume and mass of water, we determine the remaining volume of the cylinder which equals 1.53 kg or 1.53 L of water. If the net buoyancy of the 20 kg cylinder should be 15 N, the total volume of the cylinder is 0.0225 m<sup>3</sup> or 22.5 L, when neglecting the weight of the mooring line, see equation below.

(EQUATION 15)

$$V_{tot} = V_{above} + V_{under}$$

$$V_{tot} = 21.00 L + 1.53 L$$

$$V_{tot} = 22.53 L$$

The new cylinder has the following dimensions and mass moment of inertia.

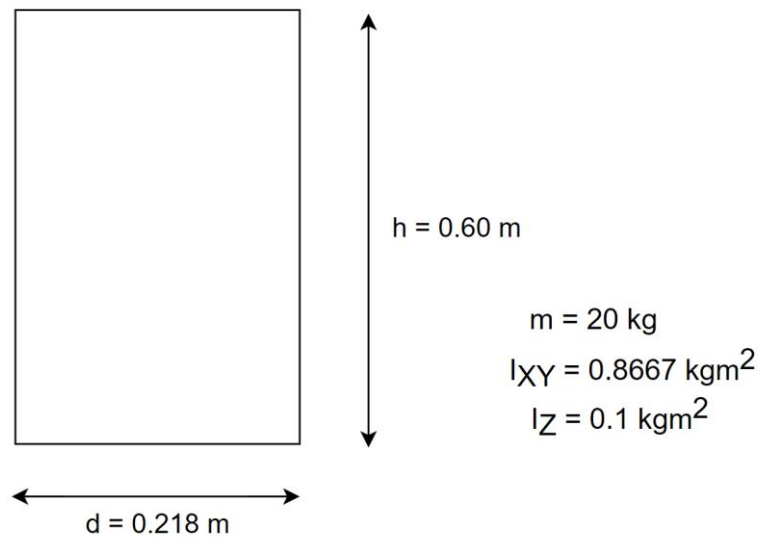


FIGURE 52: DIMENSIONS OF THE FINAL PROFILER

The metocean conditions for each simulation were as follows.

	Waves [m]	Current [m/s]	Wind [m/s]	Period [s]	Time [s]
<b>Test 1</b>	0.1	0.1	1.7	12.5	600
<b>Test 2</b>	0.5	0.5	2.0	12.5	600
<b>Test 3</b>	1.0	1.0	2.3	12.5	600

TABLE 10: METOCEAN CONDITIONS FOR THIRD ITERATION

We start of by setting up a similar system to that of the one used in the second iteration using a 6D spar buoy as a profiler with the new volume and inertia values, a user defined line but with only one subsurface buoy. As the deployment of the entire system should ideally be

achievable by one person, the subsurface buoy cannot have a greater volume than what one person can carry. Two different volumes of subsurface buoy, 15L and 30L, both having a mass of 5kg were tested in OrcaFlex to observe how increasing the volume would affect the mooring systems resistance to failing. The diameter of the mooring line was kept the same as for the second iteration as to isolate the effects of the subsurface buoy and keep control over the parameters.

Another constraint set by Oceanlab was that the subsurface buoy should be approximately 10m below the sea surface when current, wind and wave height was zero or negligible. The subsurface buoy was therefore attached 10 m down the line relative to end A. The line, which is a default nylon line in OrcaFlex, has the same dimensions and properties as that from table 7.

The results of visual interest were dry length and declination. Quantitative data such as buoyancy and weight, Morison's force and line tensile stress were also used to reinforce the visual results.

#### Buoyancy and weight

	<b>Profiler</b>	<b>Line including attachments</b>	<b>Total [kN]</b>
<b>Weight [kN]</b>	0.196	0.664	0.861
<b>Buoyancy [kN]</b>	0.225	0.834	1.059

**TABLE 11: BUOYANCY AND WEIGHT**

#### Dry length and declination

Test 1 Average dry length = 0.0501 m

Test 2 average dry length = 0

Test 1 average declination = 0.161 deg

Test 2 failed as it ended up completely under water.



The mooring system for Test 1 satisfied the predefined demands for a successful simulation, with both dry length and declination below the maximum value.

Morisons force and tensile strength

	Maximum Morisons Force $f_m$ [kN/m]	Maximum tensile stress [kN]
Test 1	0.000174	0.0108
Test 2	0.00431	0.0295

TABLE 12: TABULATED MAXIMUM MORISON'S FORCE AND TENSILE STRESS

In the table above, we have recorded the Maximum Morison's Force and Maximum tensile stresses for Tests 1 and 2 respectively and did not include the data from Test 3 as the simulation for Test 2 was not successful. The ultimate tensile strength of nylon is listed as 45-90 MPa or  $4.5 \cdot 10^6$  MPa and as we can see from the table above, each test was comfortably within the tensile stress value for the chosen line material [25]. As we can see from the table above, each test was comfortably within the tensile stress value for the chosen line material.

For Test 1 we obtain:

$$F_b > f_m L + G$$

$$1.059 \text{ kN} > 0.000174 \frac{\text{kN}}{\text{m}} * 108 \text{ m} + 0.861 \text{ kN}$$

$$1.059 \text{ kN} > 0.879 \text{ kN}, \text{ ok}$$

For Test 2, which was not successful, we obtain:

$$F_b > f_m L + G$$

$$1.059 \text{ kN} > 0.00431 \frac{\text{kN}}{\text{m}} * 108 \text{ m} + 0.861 \text{ kN}$$

$$1.059 \text{ kN} < 1.326 \text{ kN}, \text{ fail}$$

The environmental conditions in Test 2 resulted in a Morison's force greater than the total buoyancy and the system failed.

## 5. Results

### 5.1 Final design

The design used in the final simulations is a modified inverse catenary mooring system as pictured below. The final mooring system was a product of the results obtained in the preliminary stage, and the constraints received from Oceanlab.

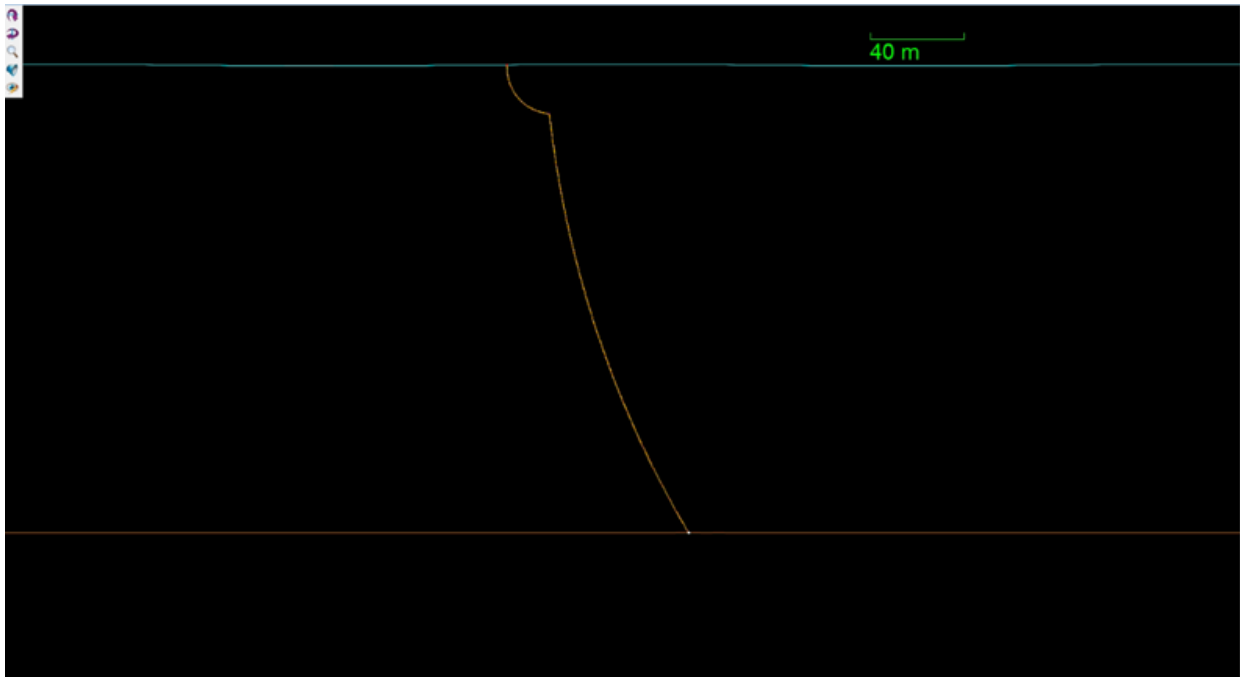


FIGURE 53: FINAL DESIGN

The system consists of three main elements. The upper line stretching from the connection point to the vertical profiler to the connection point on the subsurface buoy, the middle line consists of the subsurface buoy, and the lower line connecting the subsurface buoy to the seafloor.

This section presents the results from three series of simulations investigating the effects of SSB volume (buoyancy), slack length and line diameter. As discussed already in the report, the mooring system must be able to withstand as much current as possible and maintain a dry length throughout the duration of its deployment period. The following graphs present data that greatly influenced the final design. We define current resistance as the current [m/s] when dry length is 0.

Two assumptions we make is that the anchor has infinite weight and that the current is uniform throughout the whole water column.

The constant parameters for the following three sets of simulations are as follows.

Depth of water column:	200 m
Wave height	0.1 m
Wave period	12.5 s
Sea density	1025 kg/m <sup>3</sup>
Wind speed	1 m/s
Mooring line diameter	15mm
Mooring line mass (wet)	0.19 kg/m
Mooring line material	braided nylon (8 strand)
Subsurface buoy mass	5 kg

**TABLE 13: CONSTANT PARAMETERS FOR THE THREE SETS OF SIMULATIONS**

The parameters investigated for each series of simulations are listed above in the tables above each new data set.

**Volume vs current resistance**

Line type	Slack (m)	SSB volume (L)
15mm Braided nylon	20	variable

TABLE 14: RELEVANT PARAMETERS FOR FIGURE 54

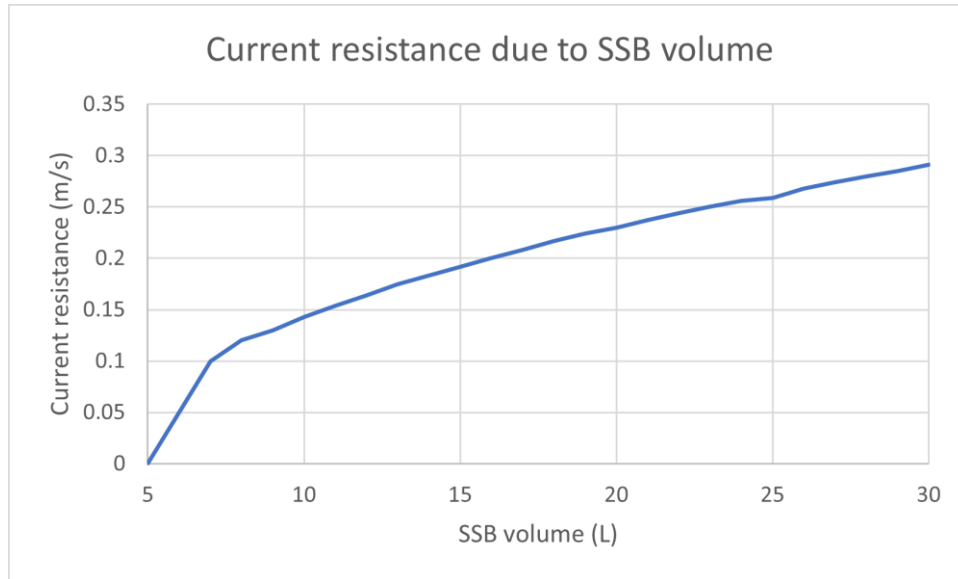


FIGURE 54: CURRENT RESISTANCE DUE TO SSB VOLUME

The first graph shows a plot of SSB volume against current resistance. Here we can see that there is a correlation between increasing the volume of the SSB used in the system and its ability to withstand current. We concluded that the largest realistic manageable volume was 30L and therefore show this to be the largest SSB volume in this data set. The graph illustrates that after 7.5L of volume, the SSB volume drastically effects the system’s ability to withstand current and therefore stay afloat in more challenging conditions. We found that increasing the size of the buoy has a significant effect on the systems resistance to current. From the graph above we can see that doubling the size of the buoy increases the systems resistance to current by approximately 62%. It is therefore advantageous to employ the use of as large a SSB as possible.

**Slack vs current resistance**

Line type	Slack (m)	SSB volume (L)
15mm Braided nylon	variable	15L

TABLE 15: RELEVANT PARAMETERS FOR FIGURE 55

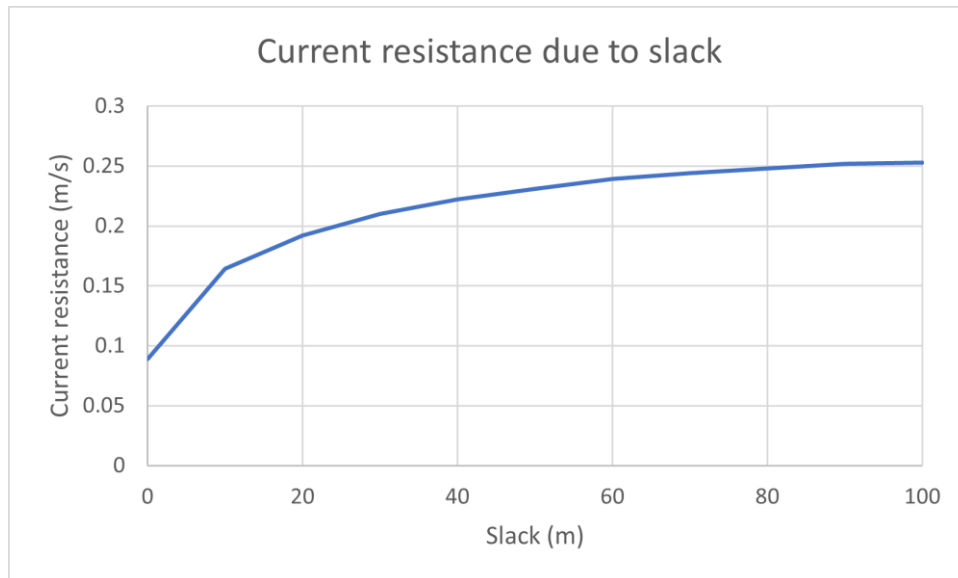


FIGURE 55: CURRENT RESISTANCE DUE TO SLACK

The second graph illustrates the total slack or excess length in the upper portion of the mooring system and how this also effects current resistance. We read from the graph that increasing the slack in the upper portion of the system, above the SSB, provides greater stability in greater currents. This concurs with previous literature studies, stating that an inverse catenary mooring was an effective solution to the majority of mooring problems. However, the schematic also illustrates that there is very little change in resistance after 40m of slack and therefore any increase after this value would be seen as added length and mass with no real effect.

### Line diameter vs current resistance

Line type	Slack (m)	SSB volume (L)
Variable	20	15

TABLE 16: RELEVANT PARAMETERS FOR FIGURE 56

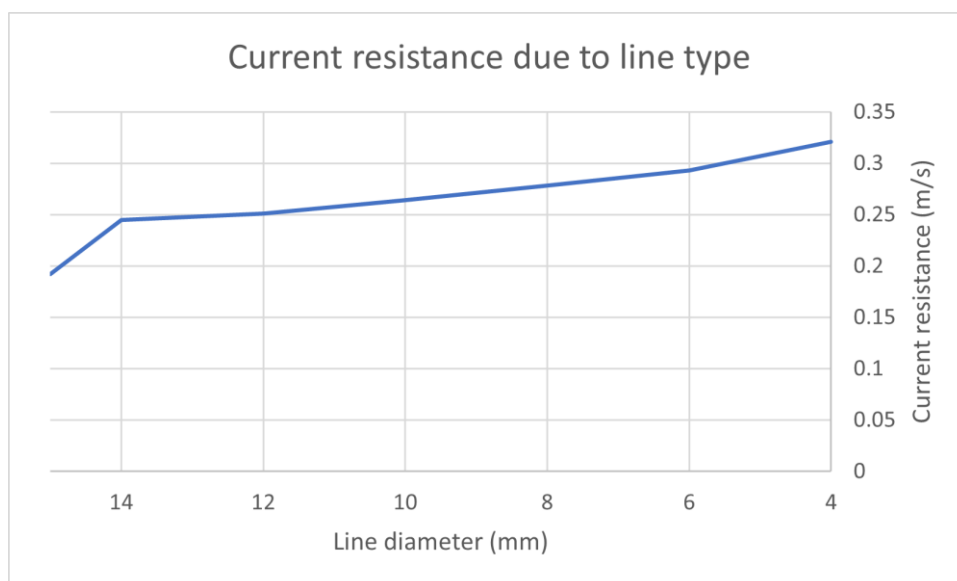


FIGURE 56: CURRENT RESISTANCE DUE TO LINE TYPE

The final graph presents line thickness plotted against current resistance. In this graph we observe that a smaller diameter line provided a greater resistance to current. This is due to the effects of Morison’s equation, as the drag force increases proportionally to the cross-sectional area of the line. However, similar to the effect in Figure 56, we can see that after 8mm in diameter, the diameter difference does not present a significant current resistance result.

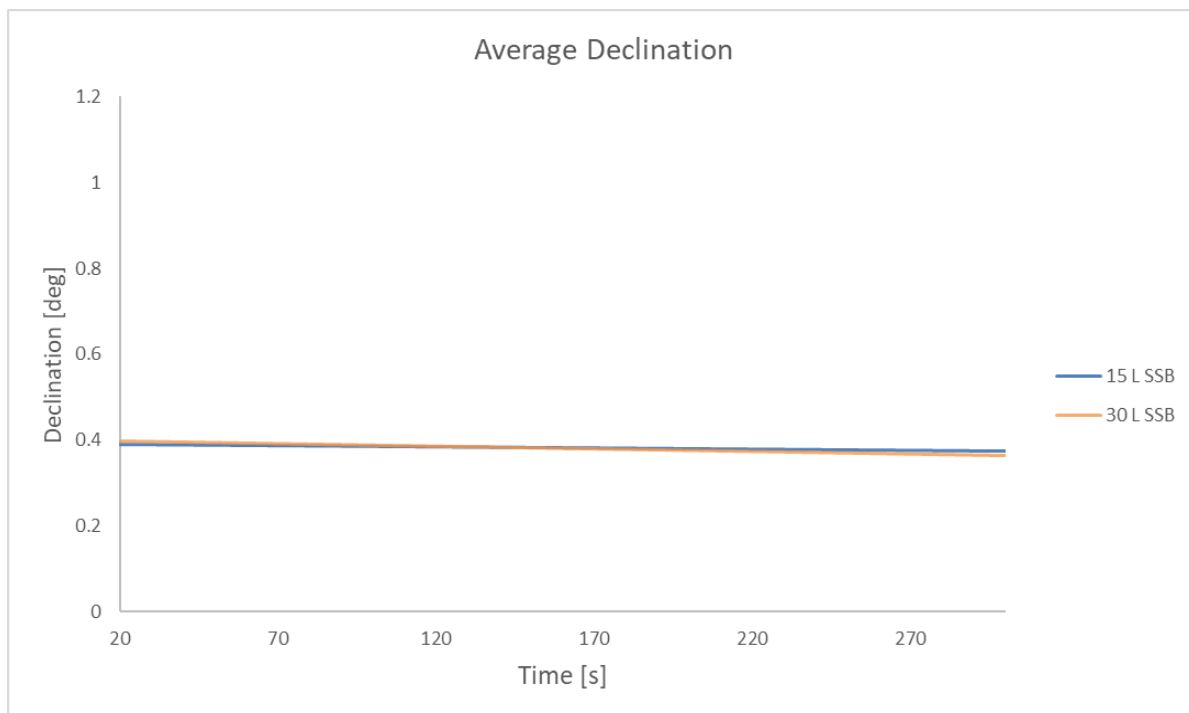
The table below shows the wet weights and breaking forces for all the diameters and line types used [26]. We can see that the Ultimate Tensile Strengths for these lines are considerably larger than the tensile strains experienced in the following simulations due to the small masses involved.

Line type	Wet weight [kg/m]	Minimum breaking force [kN]
15mm braided nylon	0.19	39.9
14mm Sk-78 Dyneema line	0.12	214.3
12mm Sk-78 Dyneema line	0.093	161.1
10mm Sk-78 Dyneema line	0.061	105.4
8mm Sk-78 Dyneema line	0.038	65.5
6mmSk-78 Dyneema line	0.023	40.8
4mm Sk-78 Dyneema line	0.011	20

TABLE 17: WET WEIGHTS AND BREAKING FORCES

In the following series of simulations, we compare a system with a 15L subsurface buoy to a system with a 30L subsurface buoy and investigate the declination and motion pattern. The volumes used were determined to be the most viable volumes to simulate as they were deemed to be the best combination of both current resistance and deployment manageability.

The parameters for the following simulations are the same as recorded in Table 13.

**FIGURE 57: AVERAGE DECLINATION**

The declinations are the same for both volumes of SSB, with both sitting at 0.38 degrees. This shows that both a 15L and 30L SSB contribute to a stable system and fulfill the criteria for declination, however the 30L SSB is able to maintain this declination value whilst also tackling a more aggressive current, as seen earlier.



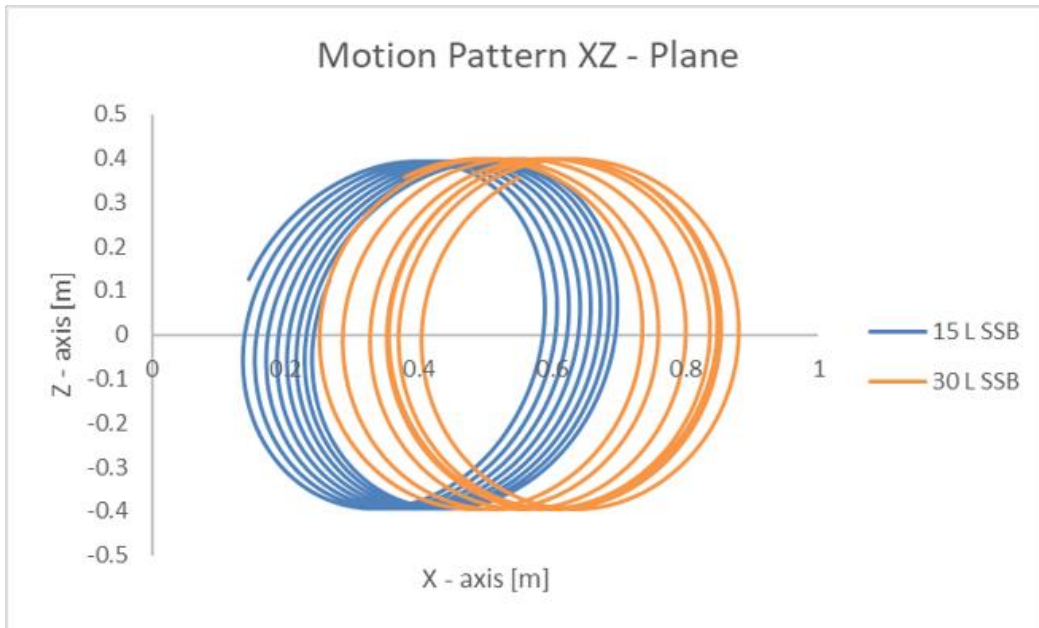


FIGURE 58: MOTION PATTERN XZ-PLANE

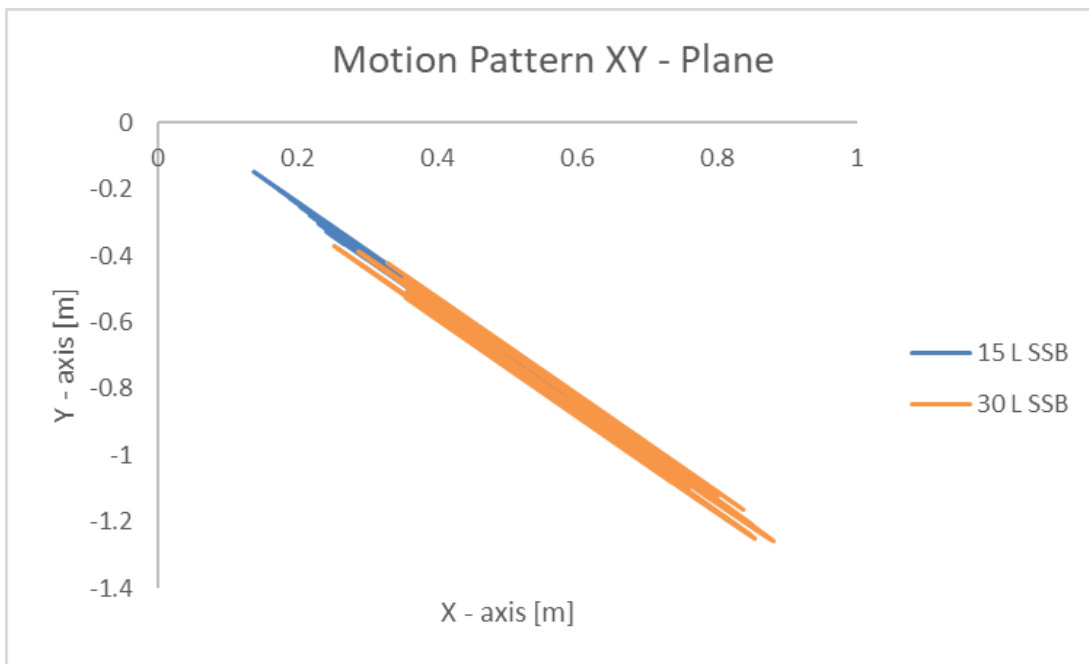


FIGURE 59: MOTION PATTERN XY-PLANE

We also observe very similar motion patterns, again showing us that both systems are stable up to the maximum current value they can withstand in the water column. The XZ plane movement for both systems are as we would expect. The profiler oscillates and adopts the movement of the current during the simulation, meaning that both systems allow the profiler

to move without diving under the sea surface whilst not being displaced from the point of deployment.

	Profiler	Line	Total [kN]
Weight [kN]	0.196	0.458	0.654
Buoyancy [kN]	0.225	0.541 (15L SSB)	0.766 (15L SSB)
		0.692 (30L SSB)	0.917 (30L SSB)

TABLE 18: WEIGHT AND BUOYANCY

	Maximum Morisons force, $M_f$ [kN/m]	Maximum tensile stress [kN]
15L SSB	0.000329	0.01059
30L SSB	0.000334	0.00559

TABLE 19: MORISONS FORCE AND TENSILE STRESS

As similarly displayed in the preliminary simulation stage, the tables above show the most relevant values obtained for the systems. We observe a larger buoyancy force when using a larger SSB, despite the Morison's force remaining at a similar value for both systems. We also observe that the tensile stress is almost halved when using a larger SSB.

By using Equation 14 that compares the buoyancy of the system and the hydrodynamic forces and weight to each other,

(EQUATION 14)

$$F_b > f_m L + G$$

We can mathematically confirm that both systems will stay afloat and therefore concur with the results and simulated versions.

For the system with a 15L SSB we obtain:

$$F_b > f_m L + G$$

$$0.766 \text{ kN} > 0.000329 \frac{\text{kN}}{\text{m}} * 220 \text{ m} + 0.654 \text{ kN}$$

$$0.766 \text{ kN} > 0.726 \text{ kN}, \text{ ok}$$

For the system with a 30L SSB we obtain:

$$F_b > f_m L + G$$

$$0.917 \text{ kN} > 0.000334 \frac{\text{kN}}{\text{m}} * 220 \text{ m} + 0.654 \text{ kN}$$

$$0.917 \text{ kN} > 0.727 \text{ kN}, \text{ ok}$$

For the system with a 15L SSB we can see that the net difference between the system buoyancy and the hydrodynamic forces and weight is just 0.04kN. This value indicates that although the system float at the given current, the system has a lower resistance to further current, hence why the system failed after shortly after 0.18m/s of current. For the 30L system we can see that the net difference in the equality is much larger, sitting at 0.19kN. This allowed for a slightly larger dry length and a larger current resistance, as shown in the previous graphs, due to a larger buoyancy value in the system overall. The combination of these factors allows to deduce that a larger SSB volume is advantageous. A larger subsurface buoy also reduced the tensile stress and therefore the system would have a theoretical longer life cycle and deployment period, due to the ability to withstand more cyclic loading.

While increasing the size of the subsurface buoy greatly increases the systems stability, other options to increase current resistance were explored, as increasing the size of the buoy decreases the practicality of the system.

The next graph shows a comparison between the initial design and a design where both current resistance parameters were implemented, namely slack and SSB volume.

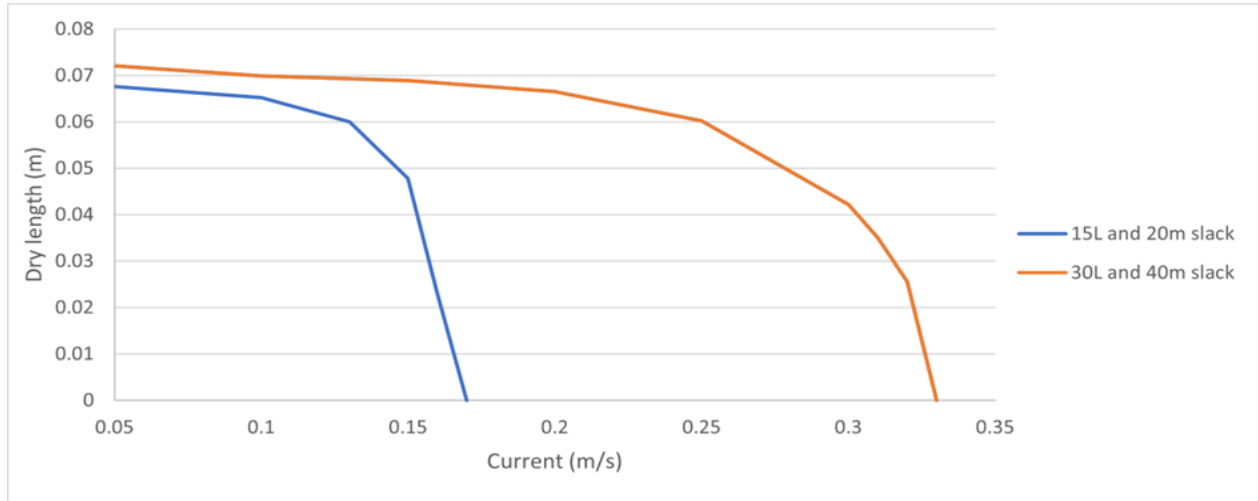


FIGURE 60: COMBINATION OF A LARGER VOLUMED SSB AND A LONGER LINE

The graph in Figure 60 illustrates how the combination of a larger volumed SSB, and a longer line substantially increases a mooring systems resistance to current.

By using the same equality,

$$F_b > f_m L + G \quad (\text{EQUATION 14})$$

We would be able to confirm the systems' buoyancy and therefore confirm the resistance increase in each of the described systems above. A 240m line length would also have a longer life cycle due to less tensile stress in the line. The combination of a larger SSB and a longer line would allow for an even longer life cycle, as it would have a larger resistance to cyclic loading and other failure factors such as fish bite. The combination of the two factors would also achieve a higher current resistance result, therefore meaning a system with a larger SSB and a longer line would have a longer life cycle whilst also having the ability to be deployed in more aggressive environments. Ultimately, the proposed final solution based on dry length and current resistance, consisted of a 30L SSB and 240m line.

## 5.2 Scale model

Based on the volume and mass of the components in the simulations from the results section, a 1:20 scale model was created using basic cylinders to represent the profiler and subsurface buoys. The goal for this model was to observe if the simulations would translate into a real-life application, however, the results of the model are only visual observations that concur with the results of the simulations.

The 1:20 scale was primarily based on the volume and mass of each component and the actual dimensions of the components were not to scale as there was so little mass involved with the model. Due to the little mass of the models, the mass moment of inertia can be considered as the same as we experienced in the simulations. The three cylinders that represent the 2 SSBs and the profiler were 3D printed using Polylactic Acid Filament (PLA) with the scaled volumes and corresponding dimensions as follows:

Component	Simulation volume (L)	Model volume (L)	Model mass (g)
Profiler	22.5	1.125	1000
15L SSB	15	0.75	250
30L SSB	30	1.5	250

TABLE 20: SIMULATION AND MODEL VOLUMES

The cylinders were printed using a 100mm diameter by 100mm height cylinder .stl file and scaled accordingly to achieve the correct volumes, as can be seen below in the following figures. The image below shows the preview of the cylinders in the Ultimaker software.

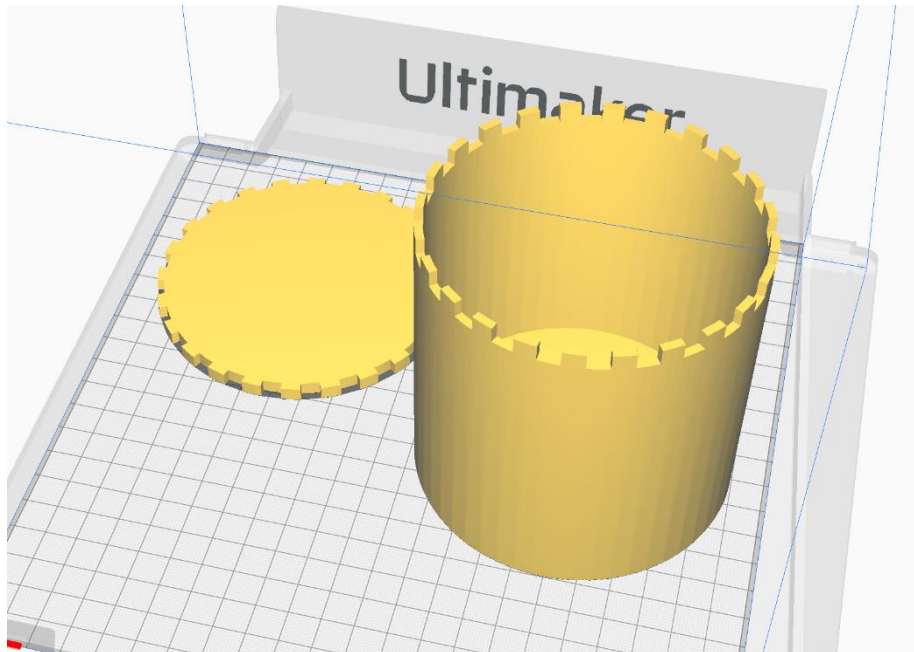


FIGURE 61: PREVIEW OF THE 3D CYLINDER

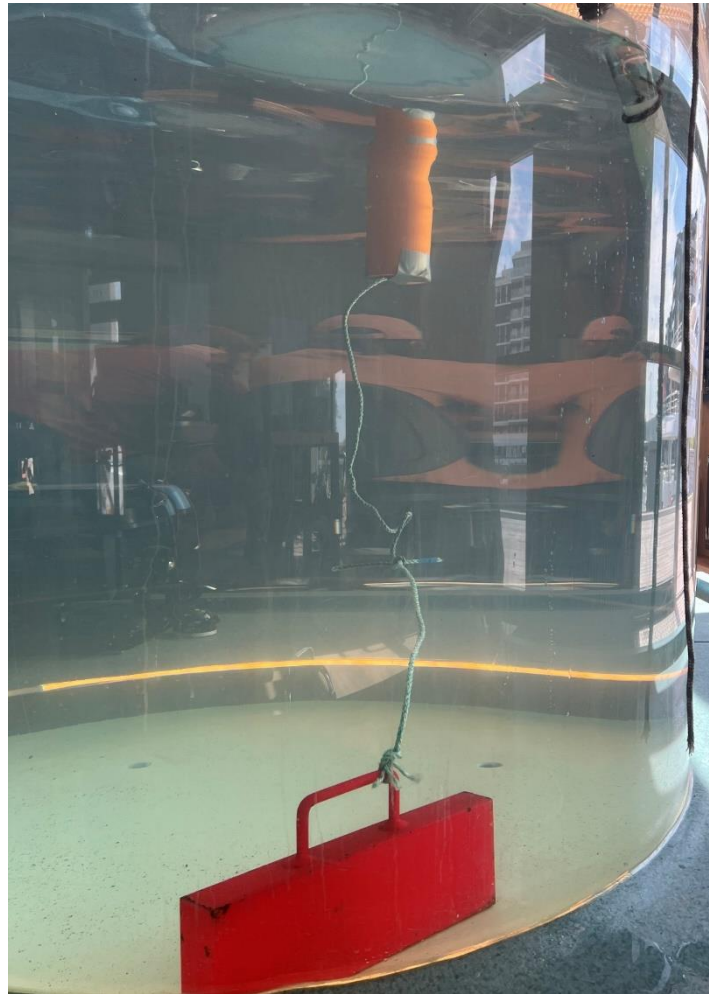
The finished cylinders were then filled with sand to the required mass based on the scale ratio and deployed in a test tank at Oceanlab.



FIGURE 62: 3D PRINTER CYLINDERS WITH MASSES

A 15mm braided nylon was attached to an infinitely weighted anchor and the cylinders were deployed using the same rope as per the simulation's setup. The first deployment only included the profiler to check the behaviour of the profiler in the water. The result shown in

the image below shows that the profiler floats in the same manner as in the simulations when no external forces are acting upon it.



**FIGURE 63: PROFILER FLOATING IN THE SAME MANNER AS IN THE SIMULATIONS**



**FIGURE 64: DRY LENGTH OF MODEL PROFILER**

We can also see that there is sufficient dry length relative to the profiler length which so far concurs with the simulations and physics of the model. The 30L subsurface buoy model was then attached. This buoy was attached to the line below the surface, between the anchor and the profiler and can be seen below.



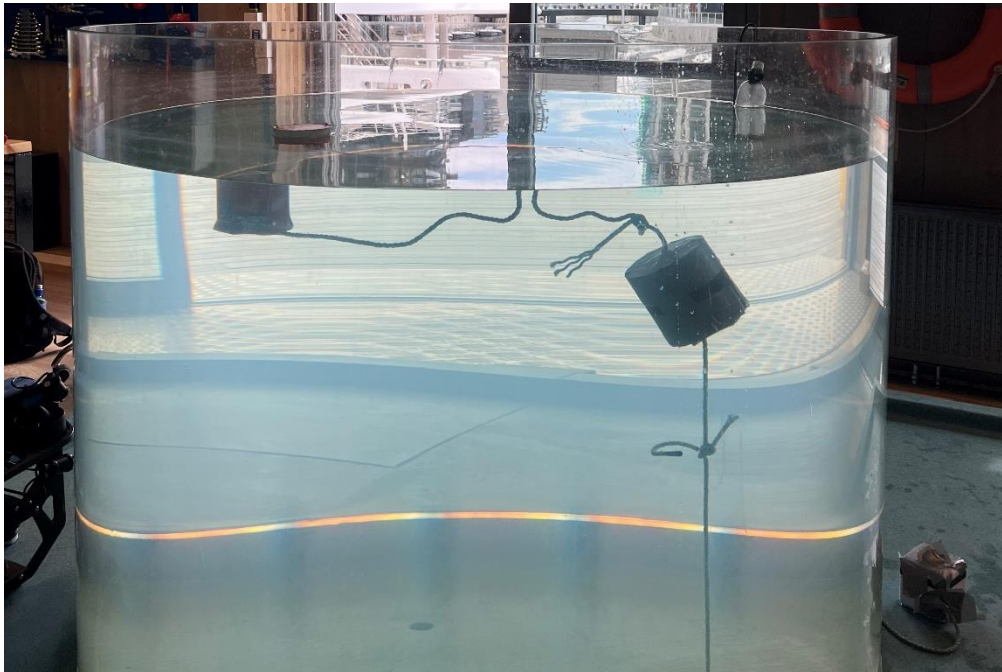


FIGURE 65: WORKING MODEL OF A 30L SYSTEM

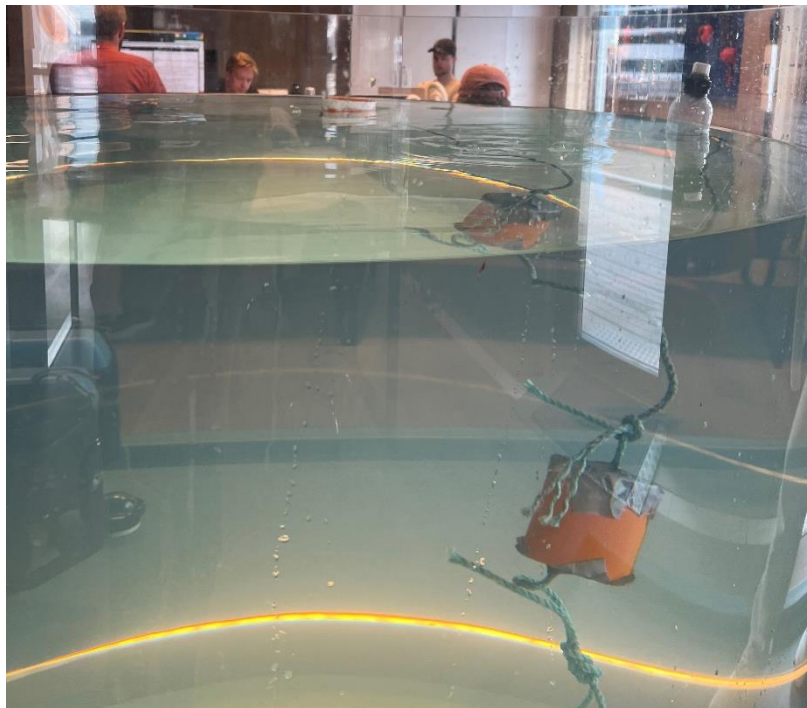
The photo shows the profiler still maintaining a dry length and the subsurface buoy below the surface as the simulation would also display. We can see a taut line down towards the anchor point, which again concurs with the simulation and the requirements of the task brief. We also observe a slight inverse catenary shape in the upper section of the line, between the profiler and the SSB model, which also concurs with the simulations and the theoretical design we opted for. By attempting to simulate a current in the water, we observed the profiler's movement around the tank. The profiler managed to stay afloat and used the same motion as illustrated in the previous graphs, which was the observation we were looking for in the model test.

The test with the smaller 15L model SSB was less successful. The photo below shows how the model with the smaller SSB was setup and appeared in the tank.



**FIGURE 66: MODEL OF 15L SYSTEM IN TANK**

The photo initially shows us that there is considerably less dry length before any movement in the tank was applied. This reinforces the results regarding the 15L vs 30L SSB comparison in the simulation process. After some movement or current was generated in the tank, the whole system ultimately began a slow sinking process, as shown below. Here we can assume that the current generated was larger than the buoyancy force of the system, as previously explained in the results section.



**FIGURE 67: FAILED 15L SYSTEM MODEL**

This observation again confirmed the same results the simulations had also attained and presents strong evidence for the use of larger volume SSBs.

Overall, the scale model was a valuable addition to the project as it allowed us to observe the physical behaviour of a mooring system in a real-life environment, albeit using a simple environment and simple geometry. The model accurately represented the results of the simulations and the larger SSB model also fulfilled the criteria of a system set by Oceanlab and therefore verified the simulation work carried out within OrcaFlex. The models also concurred and reinforced the hydrodynamic theory and mechanics of both systems and their components, which gives us a solid base for recommendations for further research and development.

## 6. Discussion

In this discussion we will aim to reflect and interpret the findings of the research conducted in this project. The section will identify strengths and weaknesses based on the results and observations throughout the duration of the research, in order to draw a relevant conclusion and propose areas of focus for future endeavours in this particular application. The section will also aim to critically identify sources of error and discuss possible solutions to these errors.

The results from the simulations clearly displayed a correlation between having a larger SSB, a longer line with more slack and enhanced stability in more adverse current scenarios. For example, from the graphs in Figures 54, 55 and 56, we can see that the current resistance is closer to 50% higher when using a larger system. The same result can be observed in the photos attained for the model section. The results also demonstrated that the use of an inverse catenary mooring setup was a viable choice for the system.

### 6.1 Consequences of line length

In this type of mooring system, selecting an adequate length for the system to be deployed with greatly effects the behaviour of the profiler. The line length can be both too short or too long and each have varying consequences but often have a common result; the profiler sinking below the surface.

From the simulations, we see that increasing line length positively effects the system's ability to withstand current, with a 100m line boasting a 184% advantage in current resistance versus a 0m line length increase in a 200m depth column.

However, should the line be too long, the profiler may drift too far from its intended location, leaving it vulnerable to strong winds and currents, whilst also changing the data collection location. This can cause damage to the profiler as it is supposed to be secured by the mooring system. In addition to this, the system may become tangled or snagged on underwater obstructions, causing further damage or even leading to the complete loss of the profiler [27].

Furthermore, there is also evidence to support that there is a point at which a longer line no longer contributes to stability as substantially as expected. For example, Figure 55 shows that after 40m of extra line length, there is negligible change in current resistance. Any extra line after this point would only reduce user-friendliness and increase the probability of the failure states mentioned earlier.

If the rope is too short, the profiler may be unable to move with tides and currents, causing it to be pulled too close to shore or other obstructions. This can cause significant damage to the profiler or other structures in the area. This factor also increases the likelihood of failure due to cyclic loading or fish bite, leading to the loss of the profiler [27]. A too short line also limits the profiler's flexibility in violent weather conditions, therefore delivering a negative dry length value as a result of this, or the failure of the system.

To be able to ensure the effectiveness and safety of the mooring system, it is crucial to ensure that the line is the appropriate length for the profiler and the specific conditions of the mooring location, considering factors such as tide and wind conditions, water depth, and the weight and size of the profiler. An appropriate length will reduce the drag effects on the system to a desired level as a longer line will increase drag, but a shorter line will be less resilient to hydrodynamic forces. The manageability of the system should also be considered in order to more accurately deduce the sizes of the components and line lengths. Regular inspection and maintenance of the mooring system is essential to ensure its effectiveness and safety and a relevantly sized system would accommodate for simpler maintenance routines.

## 6.2 System mass

Compared to typical mooring systems, the final design is relatively compact and manageable. The profiler and subsurface buoy in this project weigh just a fraction of a typical mooring system, at 20kg with a volume of 22.5L for the profiler and 5kg with a volume of 30L for the SSB. Based on the data attained in the results, we have concluded that so little mass in the system decreases its ability to withstand more violent currents as seen in Figure 54. When compared to traditional mooring systems, the system is substantially smaller in size than

those deployed and described in the literature review. However, the small mass and dimensions of our model ensure that the mooring system is manageable for one person, in line with the task brief.

### 6.3 Effects of subsurface buoys

When deploying a mooring system of this type, the design of the system must focus on the use of SSBs. The subsurface buoy is a component that by convention stabilises the system and ensures that the system remains in the desired deployment location.

Firstly, we can conclude that increasing the volume of the subsurface buoy in an inverse catenary mooring system directly provides increased stability in the system. For example, as shown in Figure 54, the larger the subsurface buoy the more current the system was able to withstand, with a 30L SSB providing 482% more current resistance than a 6L buoy.

Secondly, based on findings in the preliminary simulation section, a systems stability is greatly increased by employing the use of two sub surfaces buoys rather than one. Here we can see that from the preliminary simulation results, the system with two SSBs was able to withstand almost 0.2m/s faster current than a system with just one SSB. This factor however created some conflict with the task brief, as Oceanlab wished for the system to be deployed with one SSB. Moreover, an extra SSB would also contribute to increased maintenance routines and a less manageable system for an individual to handle.

### 6.4 Line diameter

A key factor in reducing the overall drag of the system and consequently the forces that effect the buoyancy of the system is the line diameter.

The tests performed indicate that the smaller the diameter a system uses, the more current resistance it possesses, for example, Figure 56 shows that the smallest diameter line was able to withstand 0.129m/s more current than that of a larger diameter line. In the case of the system in this project, this was a positive factor as it reduced drag and therefore contributed

to increased stability. This is largely due to the little mass in the system. A drawback to this current resistance method is that if larger masses were involved, the diameter of the line would have to increase to accommodate for this, therefore increasing the resultant drag forces on the line that lower the current resistance value.

Despite the results showing that diameter does directly increase current resistance, only one type of material was investigated in the simulations after the design process, which does limit our ability to directly confirm that the diameter is a major factor in increasing current resistance.

### 6.5 Line length vs SSB volume

As current resistance increases with both line length and SSB volume, limiting factors such as handleability, drift and line entanglement should be considered. Drift and line entanglement is only affected by the line length, while handleability is affected by both line length and SSB volume. Therefore, in scenarios where higher current resistance is needed, one should consider increasing the SSB volume before the line length. If more current resistance is needed after reaching the maximum SSB volume that can be handled by a single operator, line length should be increased. Line length has the greatest potential for increasing current resistance within the allowable parameters for handleability.

To maintain the required dry length in low currents up to  $0.17m/s$ , a very compact design with a line length 1.1 times the depth of the water-column and a 15L SSB placed 10m below the surface can be used. If stronger currents are expected the volume of the SSB should be increased within tolerance for handleability. With the same line length and a 30L SSB, the system should be able to withstand currents up to  $0.5m/s$ .

### 6.6 Current resistance

As the speed of the current increases, it displaces the vertical profiler away from its origin directly above the anchor. As the angle between the profiler and anchor increases to the

maximum allowed value given by the length of the mooring line, a vertical force is exerted on the profiler. The balance between this vertical force and the net buoyancy of the whole system determines the dry length of the profiler.

From our simulations we have found the three main factors involved in the systems current resistance to be stability, line length and drag.

### 6.7 Stability due to tension

As the profiler is displaced along the x axis the total distance to the anchor increases according to:

(EQUATION 16)

$$L_t = \sqrt{z^2 + x^2}$$

Where  $L_t$  is the total line length from the profiler to the anchor,  $z$  is a constant describing depth of the water column and  $x$  is the profiler's horizontal displacement from the origin. Here we define stability as the systems resistance to displacement along the x axis.

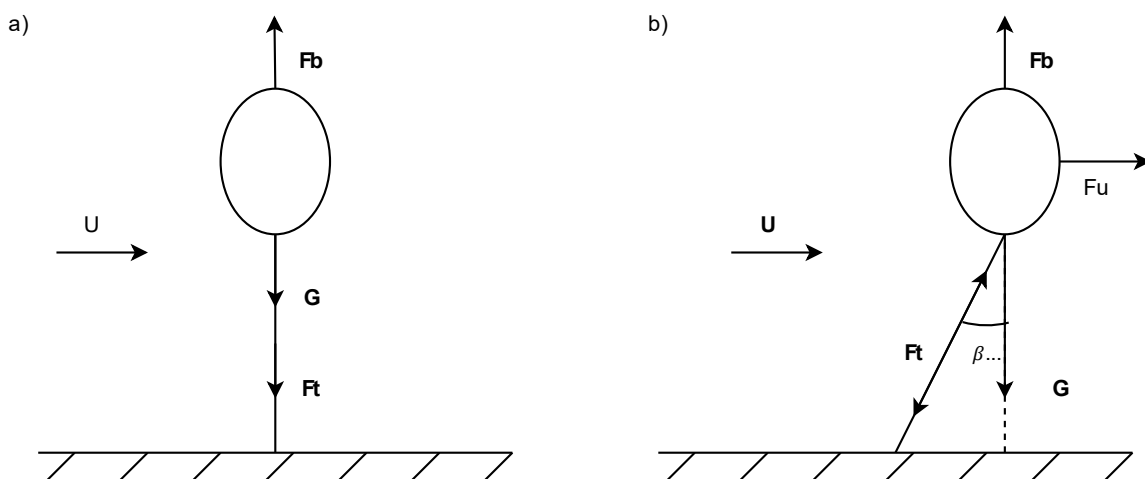


FIGURE 68: SSB FREE BODY DIAGRAM



(EQUATION 17)

$$\sum F_x = 0 \Rightarrow F_u = \Delta F_t \sin \beta$$

$$\sum F_z = 0 \Rightarrow F_b = G + \Delta F_t \cos \beta$$

There is a balance between the drag force from the current  $F_u$  and the horizontal part of the line tension  $F_t$ . From Equation (17) there is a clear correlation between line tension and current resistance. With a higher line tension, more force is required to change the buoys position in the water column. Increasing the buoyancy of the subsurface buoy will increase the line tension between the SSB and the anchor, in turn improving the systems stability.

## 6.8 Recommendations for future research

Based on the results and the discussion of the results, we conclude that there are three major areas for further research in order to establish a more successful mooring system. The three factors are line material, system mass and SSBs.

Firstly, line material is an extremely dynamic factor in a mooring system's stability. According to research in this thesis, Dyneema line is an extremely versatile material for use in mooring lines. However, this type of line can also tackle much heavier loads as its Ultimate Tensile Strength is very high and this value was never reached in the simulations performed. We recommend further research into the different type of elastic lines, or lines more suited to less mass, and their properties. This factor could potentially present a more viable material that in turn increases a system's resistance to current whilst also remaining manageable for one person.

Secondly, the use of higher mass in the system can arguably increase the viability of such a simple mooring system in more violent weather conditions. We recommend investigating the possibility of using heavier SSBs that are not as easily influenced by strong currents in order to improve this type of system's ability to withstand current and remain deployed in the desired location.

Similar to the second factor discussed above, we highly recommend the use of two SSBs in order to stabilise the system to an adequate degree. The use of two SSBs can also be a viable solution in order to balance out the small mass of the system, as there is an added stability point in the system. We believe that despite adding another SSB that this would not affect the ease-of-use aspect of the system required by the task brief.

## 7. Conclusion

To conclude, this thesis has examined the design and analysis of mooring systems using existing literature and studies to arrive at a proposed design that coincides with the project brief and parameters.

Firstly, the research discovered that varying line length, diameter, and SSB volume has great impact on the overall viability of a proposed mooring system. These factors allowed us to carefully select and adjust the relevant masses and volumes in our system in order for the design to be successful. These designs were also represented through a scale model and verified mathematically using relevant theorems.

Furthermore, the parameters and objectives of the project has enabled us to widen our understanding of this engineering application through the use of theory and research conducted using the recommended software, OrcaFlex.

It is also important to note that to maximise a system's handleability and effectiveness when deployed, it is imperative to have a deep understanding of the environmental conditions in the chosen deployment area. Failing to understand the subject location can result in miscalculated system dimensions which ultimately would lead to an ineffective system. The recommended final design, consisting of a 4mm line, one 30L SSB attached 10m below the surface and a line length of 240m, proved to be resistant to strong winds and waves up to 0.5m, but struggled in more aggressive currents.

Based on the combination of the research conducted and the limitations deduced in the thesis, we recommend further research into the line material and SSB volume and placement

in order to expand the knowledge of low mass mooring systems in varying depth and weather aggressive deployment locations.

Finally, this thesis has ultimately provided valuable insights into this particular field by utilising dynamic analysis and relevant testing of a variety of systems to arrive at viable solutions and conclusions that aim to lay foundations for future endeavours in this application. We hope that the insights provided in this thesis based on the knowledge gained, will help shape future innovations and revolutions in this exciting area of engineering.


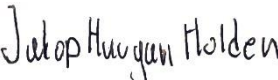
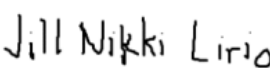

## 8. Reference List

- [1] OsloMet Oceanlab. "OsloMet Oceanlab coordinates research, innovation, and public outreach activities related to ocean technology and sustainability."  
<https://uni.oslomet.no/oceanlab/> (accessed 09.03.2023).
- [2] R. Costanza, "The ecological, economic, and social importance of the oceans," *Ecological Economics*, vol. 31, no. 2, pp. 199-213, 1999/11/01/ 1999, doi:  
[https://doi.org/10.1016/S0921-8009\(99\)00079-8](https://doi.org/10.1016/S0921-8009(99)00079-8).
- [3] K.-T. Ma, Y. Luo, T. Kwan, and Y. Wu, *Mooring System Engineering for Offshore Structures*, 1. ed. Cambridge: Gulf Professional Publishing, 2019.
- [4] Syrenna. "We open the ocean space to everyone." <https://www.syrenna.com/> (accessed 27.03.2023).
- [5] Orcina. "OrcaFlex – World-leading software that goes beyond expectation."  
<https://www.orcina.com/orcaflex/> (accessed 09.03.2023).
- [6] K. Manghani, "Quality assurance: Importance of systems and standard operating procedures," (in eng), *Perspect Clin Res*, vol. 2, no. 1, pp. 34-7, Jan 2011, doi: 10.4103/2229-3485.76288.
- [7] D. Qiao, R. Haider, J. Yan, D. Ning, and B. Li, "Review of Wave Energy Converter and Design of Mooring System," *Sustainability*, vol. 12, no. 19, p. 8251, 2020. [Online]. Available: <https://www.mdpi.com/2071-1050/12/19/8251>.
- [8] N. O. a. A. Administration. "Moorings."  
<https://www.pmel.noaa.gov/ocs/moorings#:~:text=The%20ratio%20of%20the%20mooring,not%20have%20much%20vertical%20movement> (accessed 09.05.2023).
- [9] C.-C. T. Brett Taft, "Low Load Compliant Mooring," Science Applications International Corporation (SAIC)-National Data Buoy Center Stennis Space Center, Stennis MS 39529, 2009.
- [10] B. Prindle, *Factors correlated with incidence of fishbite on deep-sea mooring lines*. 1981.
- [11] R. Balzola, "Mooring line damping in very large water depths," 1999.
- [12] J. M. J. Journée and W. W. Massie, *Offshore Hydromechanics First Edition*. Delft: Delft University of Technology, 2001.
- [13] R. Nicoll. "Why it's hard to distinguish between the effects of buoy and line drag on mooring knockdown." <https://dsaocean.com/buoy-and-mooring-drag/> (accessed 09.05.2023).
- [14] A. Martini, P. Jansen, and A. Marouchos, "Mooring Lightweight Wave Buoys – A Flexible Design Approach for a Wide Range of Coastal Conditions," in *OCEANS 2021: San Diego – Porto*, 20-23 Sept. 2021 2021, pp. 1-5, doi: 10.23919/OCEANS44145.2021.9706040.
- [15] F. Ding, L. Qiang, W. Peng, Z. Hong, and Y. Cheng, "The research for the stationkeeping system and the mooring system for deep-water drilling device," in *2011 Second International Conference on Mechanic Automation and Control*

- Engineering*, 15-17 July 2011 2011, pp. 1793-1796, doi: 10.1109/MACE.2011.5987308.
- [16] M. D. Hamidreza Ghafari. (2018, April 1) Parametric study of catenary mooring system on the dynamic response of the semi-submersible platform. *Ocean Engineering*. 319-332.
- [17] A. L. Luff, Sheehan, E.V., Parry, M. et al., "A simple mooring modification reduces impacts on seagrass meadows," *Scientific Reports*, 2019.
- [18] J. Yu, Zhang, S., Yang, W., Xin, Y., & Gao, H., "Design and Application of Buoy Single Point Mooring System with Electro-Optical-Mechanical (EOM) Cable," *Journal of Marine Science and Engineering*, 2020.
- [19] J. Reimer. "Underwater drone technology can enhance port maintenance." <https://www.here.com/learn/blog/underwater-drone-technology> (accessed 12.05.2023).
- [20] S. Xu, S. Wang, and C. G. Soares, "Review of mooring design for floating wave energy converters," *Renewable and Sustainable Energy Reviews*, vol. 111, pp. 595-621, 2019.
- [21] S. Xu, S. Wang, and C. G. Soares, "Experimental study of the influence of the rope material on mooring fatigue damage and point absorber response," *Ocean Engineering*, vol. 232, p. 108667, 2021.
- [22] H.-D. Pham, P. Cartraud, F. Schoefs, T. Soulard, and C. Berhault, "Dynamic modeling of nylon mooring lines for a floating wind turbine," *Applied Ocean Research*, vol. 87, pp. 1-8, 2019.
- [23] D. Ocean. "Oceanographic moorings can have dozens or even hundred of parts." <https://dsaocean.com/proteusds/oceanographic/> (accessed 12.05.2023).
- [24] M. Stewart, "10 - Pipe expansion and flexibility," in *Surface Production Operations*, M. Stewart Ed. Boston: Gulf Professional Publishing, 2016, pp. 731-812.
- [25] T. E. ToolBox. "Young's Modulus, Tensile Strength and Yield Strength Values for some Materials." [https://www.engineeringtoolbox.com/young-modulus-d\\_417.html](https://www.engineeringtoolbox.com/young-modulus-d_417.html) (accessed 12.05.2023).
- [26] Certex. "SK-78 Dyneema Rope." <https://www.certex.no/en/products/fibre-ropes-slings-and-lashing/fibre-ropes/dyneema/sk-78-dyneema-rope-p42307> (accessed 24.05.2023).
- [27] C. Scott. "How to Make Mooring Lines." Conservation Diver. <https://conservationdiver.com/how-to-make-mooring-lines/> (accessed 11.04.2023).

## 9. Appendix

## BIDRAGSSKJERMA FOR GRUPPEARBIED

STUDENTENS NAVN	SIGNATUR	BESKRIVELSE AV BIDRAG
Emma Josefine Junge		Bidrag inkluderer å lære programmet OrcaFlex, kjøre simuleringer, samle og bearbeide innhentet data, gjøre utregninger, definere dimensjonen på endelig profiler, analysere resultater og rapportskrivning.
Jakop Haugan Holden		Bidrag inkluderer rapportskrivning, bruk av OrcaFlex til å samle og analysere data, design av fortøyningssystemer, samle og bruke data fra relevant forskning samt å gjøre utregninger.
Jill Nikki Jeciel Lirio		Bidrag inkluderer rapportskrivning i teoridelen og literature review samt andre seksjoner i rapporten, fiksing av rapport format og ulike lister i rapporten, diskusjon av resultater fra OrcaFlex, hjelp til med gjennomføring av scale model.
Louis Robert Crosbie		Bidrag inkluderer oppsett av OrcaFlex server og program, bruk av OrcaFlex til simuleringer. Rapport skrivning i alle seksjoner og rettskriving for hele rapporten, matematiske utregninger i forhold til balansen av systemet og laging og design av scale model.